

**2D- SEISMIC REFLECTION DATA
INTERPRETATION OF SINJHORO BLOCK
SANGARH AREA, SINDH, PAKISTAN**



By

SADIA SADIQ

SABA JAMSHED

SABA AFROZ

Faculty of Earth and Environmental Sciences

Bahria University, Islamabad

2009

ACKNOWLEDGMENT

All adoration and veneration to THE ALLMIGHTY ALLAH. We thank our ALLAH for HIS endless blessings HE bestowed upon us. We thank HIM for making us complete this dissertation. It is THE ALLMIGHTY ALLAH'S help that made our frail effort a success.

We would like to thank our parents for their help and support. They were continuously backing us up during the completion of this dissertation. They always came up as a hope in our forlorn and restless nights.

We express our heartfelt and cordial indebtedness to our supervisor **Mr. Akbar Ali Asif**. His benevolent and benignant help made the completion of this dissertation a reality. He satisfied our agogness with his bent of the subject. Without his assistance this dissertation would never have been the same.

We would like to thank **Mr. Mohsin Muneer** who overviewed our exposition and gave ideas to improve it a lot.

TABLE OF ABBREVIATIONS

ABBREVIATION	STANDS FOR
AGC	Automatic Gain Control
CDP	Common Depth Point
DGPC	Directorate General of Petroleum Concessions
EL	Exploration Lease
FFID	Field File Identification Number
K/T	Cretaceous / Tertiary
LMKR	Landmark Resources
NMO	Normal Move Out
OGDCL	Oil and Gas Development Corporation
PPIS	Pakistan Petroleum Information System
SGR	Sanghar
SP	Shot Point
TLG	Top of Lower Goru
TWT	Two Way Time
VSP	Vertical Seismic Profiling
3D	Three Dimensional

ABSTRACT

This dissertation contains the study of 2D seismic reflection data interpretation of selected seismic lines of Sinjhor Exploration Lease (E.L.), Southern Indus Basin, Pakistan, for delineation of subsurface structures favorable for hydrocarbon accumulation. This Exploration Lease is situated in the Sanghar district of Sindh province and is licensed to Oil and Gas Development Corporation Limited (OGDCL). The seismic data for this dissertation was provided by the Land Mark Resources (LMKR) by the permission of Directorate General of Petroleum Concessions (DGPC). The data comprised ten seismic lines, base map, and VSP of well Chak 7A – 01. The lines which were used are:

(886-SGR-347, 896-SGR-389, 896-SGR-350, 947-SGR-283N, 947-SGR-278N, 936-SGR-122, 896-SGR-393, 896-SGR-394, 886-SGR-391, and 866-SGR-86).

Five prominent reflectors (green, red, yellow, pink, and blue) were marked on the basis of their reflection, which represent Chiltan, Basal Sands (one of the sand shale packages of Lower Goru), Top Lower Goru (TLG), Upper Goru, and Parh limestone formations respectively. Two-way time (TWT) from the seismic sections and average velocities were used to create TWT and Depth Contour maps and 3D Time and Depth Surfaces of Basal sands and TLG. In the end, by the examination of the maps and surface models, leads were identified and well locations were proposed.

1.1 PETROLEUM PLAY

The Lower Cretaceous Shale of Sember Formation is proven source for oil and gas discovered in the Lower Indus basin because of its organic richness, oil prone kerogen type and thermal maturity, and same is the case with Sinjhoru E.L. The lower part of Lower Goru Formation is moderately rich in organic shale having fair to good genetic potential. The Basal and Massive Sands of the Lower Goru Formation are the main reservoir rocks in this area. Thick sequence of shale and marl of the Upper Goru Formation as well as shale within the Lower Goru Formation serves as cap rock for the underline sandstone reservoirs.

1.2 PREVIOUS SEISMIC STUDY

Seismic data acquisition was carried out in 1980s and 1990s in this area by OGDCL, using dynamite mostly, as source of energy. As this area is very producing, the lines are still being reprocessed. Khadro (Deccan Basalts), top Lower Goru, Basal Sand (lower Goru) and top of Chiltan Formation are the most prominent reflectors.

1.3 OBJECTIVES OF RESEARCH

The main objective of this research work is to carried out interpretative study of the available seismic lines. This study contains the demarcation and delineations of structural and regional fault trends in the area and to mark the different stratigraphic horizons. This will lead towards the hydrocarbon prospects, generation and accumulation in the study area. This whole research gives an approach to locate the favorable spots for hydrocarbon accumulation.

1.4 DATA OBTAINED FOR STUDY

For the above mentioned purpose, ten Seismic lines having 48 – fold 2D data were obtained from Land Mark Resources (LMKR) by the permission of Directorate General of Petroleum Concessions (DGPC). Out of these ten lines, eight are dip lines and remaining two are strike lines. Lines (886-SGR-347, 896-SGR-389, 896-SGR-350, 947-SGR-283N, 947-SGR-278N, 936-SGR-122, 896-SGR-393, 896-SGR-394) are dip lines, and lines (886-SGR-391, 866-SGR-86) are strike lines. The dip lines are oriented in Southwest-Northeast direction. And the strike lines are oriented In North-South direction.

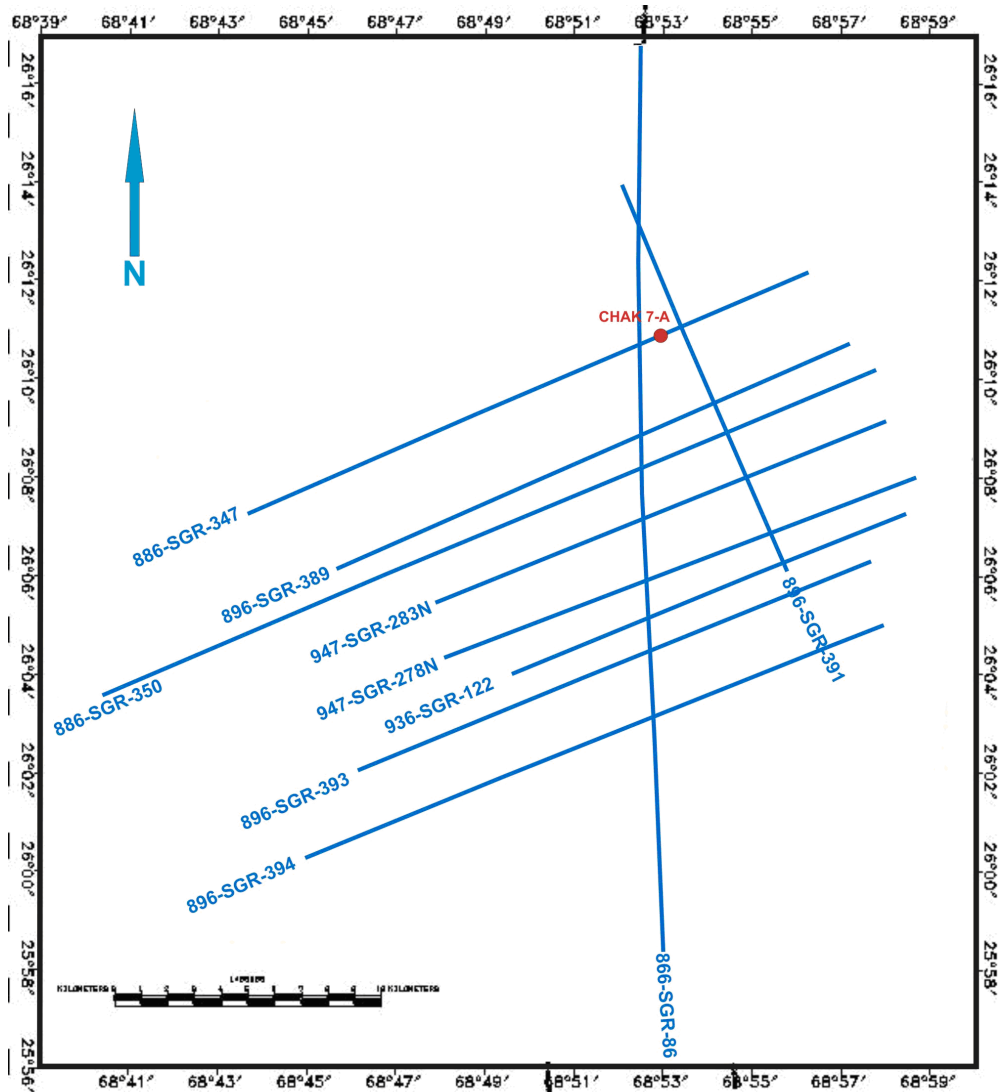


Figure 2: Showing selected lines on the base map of Sanghar Area

2 GENERAL GEOLOGY OF SOUTHERN INDUS BASIN

BASIN

In this chapter the general geology of southern Indus basin with special emphasis on Sember and Lower Goru Formations of cretaceous age, as they are our horizons of interest for hydrocarbon exploration is discussed.

2.1 MAIN UNITS OF SOUTHERN INDUS BASIN

This basin (Figure 3) is located just south of Sukkur Rift — a divide between Central and Southern Indus basins. It comprises the following five main units:

1. Thar Platform
2. Karachi Trough
3. Kirthar Foredeep
4. Kirthar Fold Belt
5. Offshore Indus

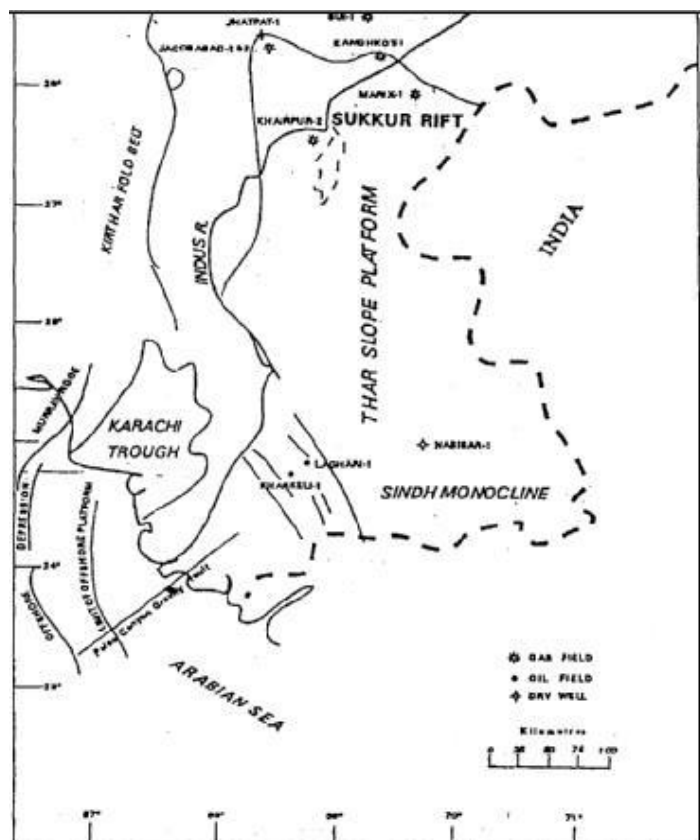


Figure 3: Structural setting of Southern Indus basin (modified after Qadri & Shuaib, 1986)

As is evident from (Figure 3), the platform and trough extend into the offshore Indus. The Southern Indus Basin is bounded by the Indian Shield - to the east and the marginal zone of Indian plate to the west. Its southward extension is confined by off-shore Murray Ridge—Oven Fracture plate boundary (Qadri, 1994).

2.1.1 Thar Platform

Thar platform (Figure 3) is a gently sloping monocline analogous to Punjab Platform controlled by basement topography. The sedimentary wedge thins towards the Indian Shield whose surface expressions are present in the form of Nagar Parkar High. It differs from the Punjab Platform in that it depicts the buried structures formed due to extensional tectonics resulting from the latest counter-clockwise movement of the Indian Plate (Qadri, 1994).

The platform marks very good development of Cretaceous sands (Goru) which are reservoirs for oil/gas fields (Qadri, 1994).

2.1.2 Karachi Trough

The Trough is characterized by thick Early Cretaceous sediments and also marks the last stages of marine sedimentation. It contains a large number of narrow anticlines in series some of which contain gas reservoir (Sari, Hundi & Kothar). The Early, Middle and Late Cretaceous rocks are well preserved in the area. It has been a -trough throughout the geological—history. The most interesting feature is the continued deposition across the Cretaceous/Tertiary (K/T) boundary (Qadri, 1994).

2.1.3 Kirthar Foredeep

Kirthar Foredeep trends north-south and has received the sediments aggregating a thickness of over 15,000 meters. It has a faulted eastern boundary with Thar Platform (Figure 3). Upper Cretaceous time is missing but Paleocene deposition is well developed. This area has great potential for maturation of source rock (Qadri, 1994).

2.1.4 Kirthar Fold Belt

This north-south trending tectonic feature (Figure 4) is similar to Suleiman fold belt in structural style and Stratigraphic equivalence. Rocks from Triassic to Recent were deposited in this region. The configuration of the Kirthar fold belt also marks the closing of Oligocene—Miocene seas (Qadri, 1994).

2.1.5 Offshore Indus

This area forms the part of passive continental margin and appears to have gone through two distinct phases of geological history (Cretaceous-Eocene and Oligocene-Recent). Sedimentation in offshore Indus region started from Cretaceous time (Qadri, 1994).

2.2 STRUCTURAL SETTINGS

The entire southern Indus basin exhibits extensional tectonics and as a consequence, Normal faults are generated showing Horst and Graben structure with former being of great exploratory importance.

Offshore Indus is divided into Platform and Depression along a Hinge Line in close proximity and parallel to 67°E Longitude (Figure 4). Offshore Platform is divided into

Karachi Trough and the Thar Platform's deltaic area by a line which divides Karachi Trough from Thar Slope onshore (Figure 4).

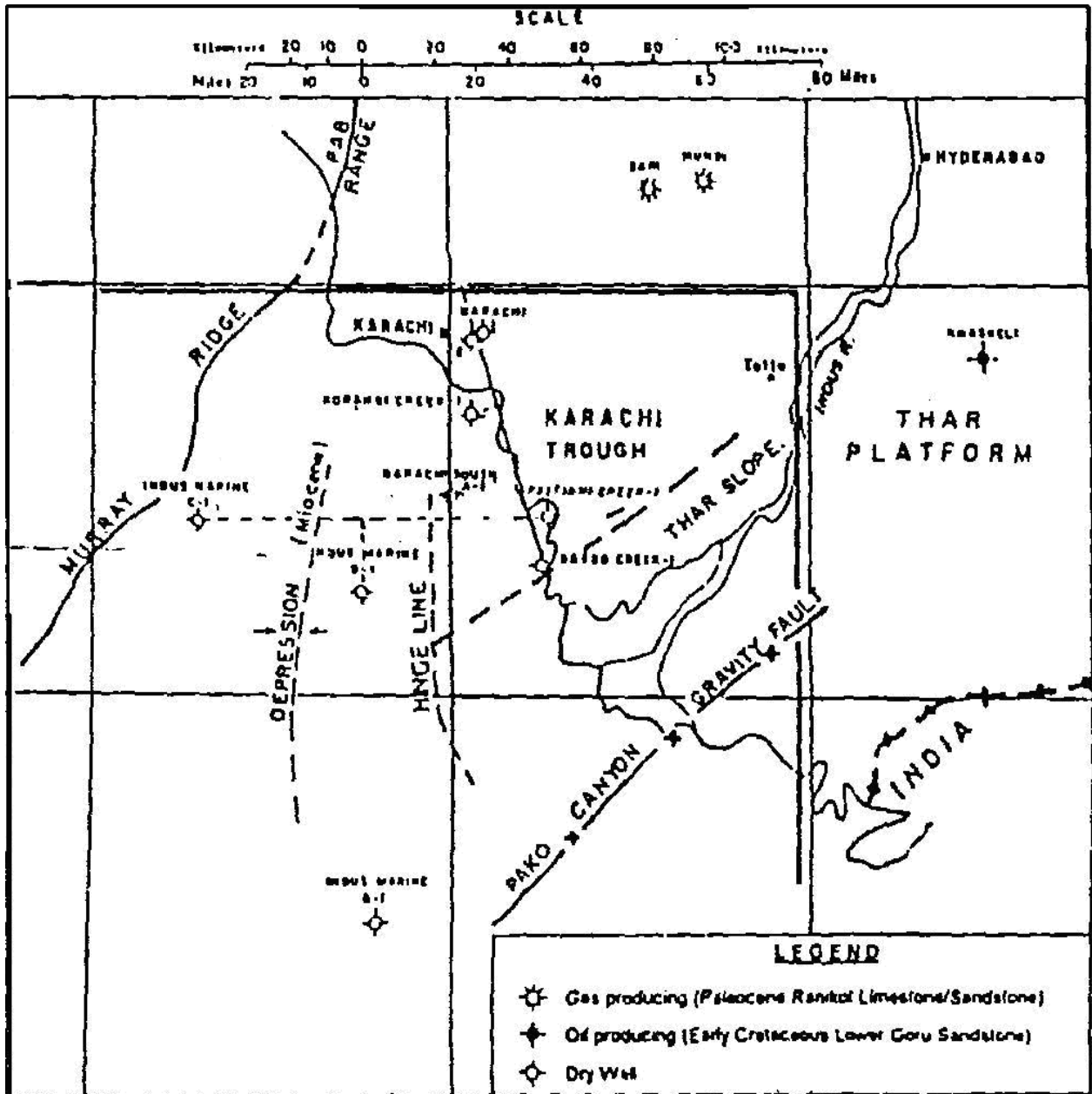


Figure 4: Structural Setting of Southern Indus Basin & offshore area (after Quadri, 1980)

2.3 STRATIGRAPHY

A Summary of Stratigraphic sequence of Southern Indus basin is given below (Table 1).

Table 1: Generalized Stratigraphic sequence of Southern Indus Basin (Qadri, 1994)

AGE	GROUP	FORMATION	LITHOLOGY
Miocene		Gaj Formation	Shale
Oligocene		Nari Formation	Shale, sandstone
Eocene	Kirthar Group	Kirthar Formation	Interbeds of limestone, shale
		Laki Formation	Limestone, shale, laterite
		Sui main limestone	Limestone
Paleocene	Ranikot Group	Lakhra Formation	Limestone, sandstone
		Bara Formation	Sandstone, shale
		Khadro Formation	Sandstone, basaltic flows
C R T A C E O U S		Pab sandstone	Sandstone
		Fort Monro Formation	Limestone, shale
		MughalKot Formation	Mudstone, shale
		Parh limestone	Limestone, marl, shale
		Goru Formation	Sandstone, shale
		Sember Formation	Shale, limestone
Jurassic		Chiltan Formation	Limestone, chert
		Shirinab Formation	Interbeds of shale, lst
NOT EXPOSED			

2.3.1 Jurassic Sequence in Southern Indus basin

The advent of Jurassic is marked by the break in deposition. Rifting and break-up of Gondwana continued during the Jurassic. In southern Indus basin, the submergence of platform produced deep water sedimentation of Shirinab and Chiltan Formations (Qadri, 1994).

2.3.1.1 Shirinab Formation

This is widely developed in Kirthar and Suleiman province. As mentioned in (Table 1), it consists of inter-bedded limestone and shale which grade into low lying Wulgai (Triassic) Formation. The Formation is divided into three members (Spingwar, Loralai, Anjira) based on level of shale. Limestone is generally medium to thin bedded (Qadri, 1994).

2.3.1.2 Chiltan Formation

It is massive, thick bedded, dark limestone. It contains pisolitic limestone beds locally. Upper contact with Mazar dirk is gradational. At places it is organic rich and seems to have generated hydrocarbons. There are some indications of the development of porosity (10%-12%) (Qadri, 1994).

2.3.2 Cretaceous Sequence in Southern Indus basin

The greater India broke up from eastern Gondwanaland some 120 Ma years ago at the time when Sember and Goru Formations were being deposited. The whole cretaceous therefore, represents shallow seas while northern floor of the southern arm of the Tethys was subducting beneath Iran-Afghanistan micro-continent (Qadri, 1994).

2.3.2.1 Sember Formation

The Sember is composed mainly of clastic rocks, primarily shales, sandstones and siltstones with minor limestone. Characteristically, the Formation in outcrop consists of black silty shale with nodular black siltstone and limestone beds (Qadri, 1994).

Sember Formation thins eastwards against the Indian shield and the catch positive areas (Figure 5). Possibly most of thinning is due to erosional truncation. It is suspected that thinning due to onlap may also have occurred.

Numerous good source rock determinations as well as gas and oil shows have been reported from the Sember. Sember is believed to be the source of hydrocarbons in Badin platform fields (Figure 6). Potential reservoirs occur within the sandstones of the Formation. The chances of Sember-sourced oil migration into the underlying Jurassic Formations against faults also appear to be relatively favorable (Qadri, 1994).

The thickest sediments of Sember are deposited in Suleiman lobe area (1000 m) (Qadri, 1994). In Karachi embayment the Sember is over 760 meters in thickness while in Badin platform, thickness is around 650 meters (Figure 7).

2.3.2.2 Goru Formation

The sands of Goru are the most important entity in the southern Indus basin from the petroleum reservoir point of view. The thickest Goru sedimentation occurs within the Karachi Embayment. On the wells west of Badin platform, Goru is partially penetrated about 2,360 meters (Qadri, 1994). Based on its lithological content, Goru Formation has been divided into upper and lower portions, with sand being rarer in upper portion. Upper portion is predominantly shale while the lower portion is the sandy member. This lower portion (lower Goru) is the most important reservoir in southern Indus basin. It contains all the hydrocarbons in Sindh Monocline (Qadri, 1994).

The wells drilled in Badin area exhibit a lateral facies change from east to west, from producible sand/shale sequence in Lower Goru to non-reservoir sand/shale facies, which in turn is entirely represented by shales further west (Qadri, 1994).

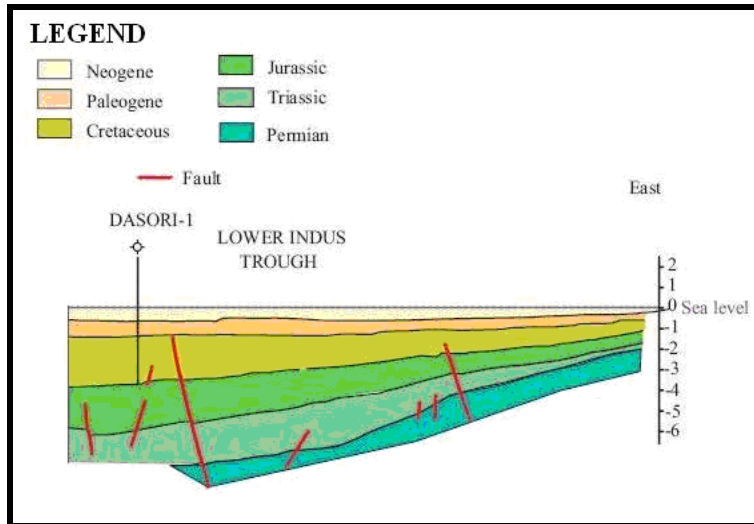


Figure 5: Generalized cross sections showing eastward thinning of Cretaceous rocks (modified from Quadri and Shuaib, 1986; Malik and others, 1988; Kadri, 1995; and OGDC, 1995)

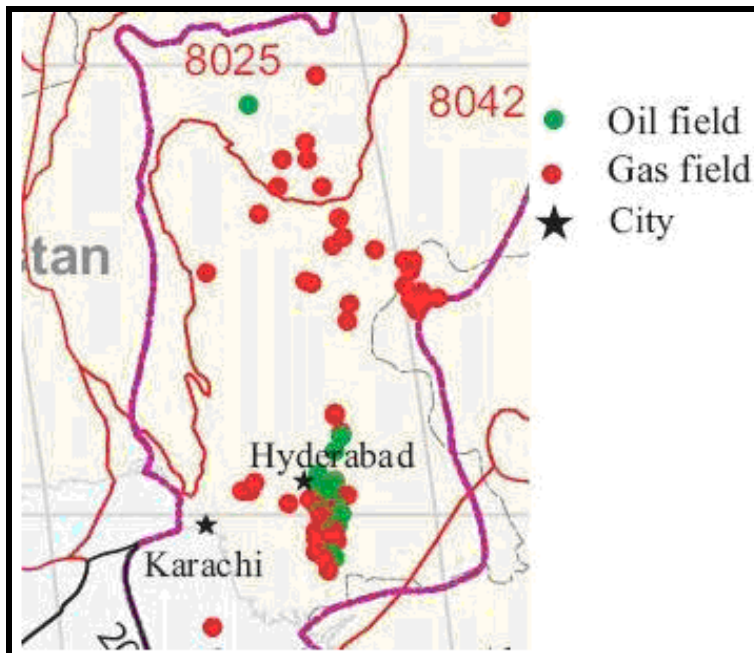


Figure 6: Map showing producing wells in Southern Indus basin with Sember as a source rock (Wandrey and Law, 1999)

CRETACEOUS BADIN PLATFORM, SOUTH INDUS BASIN

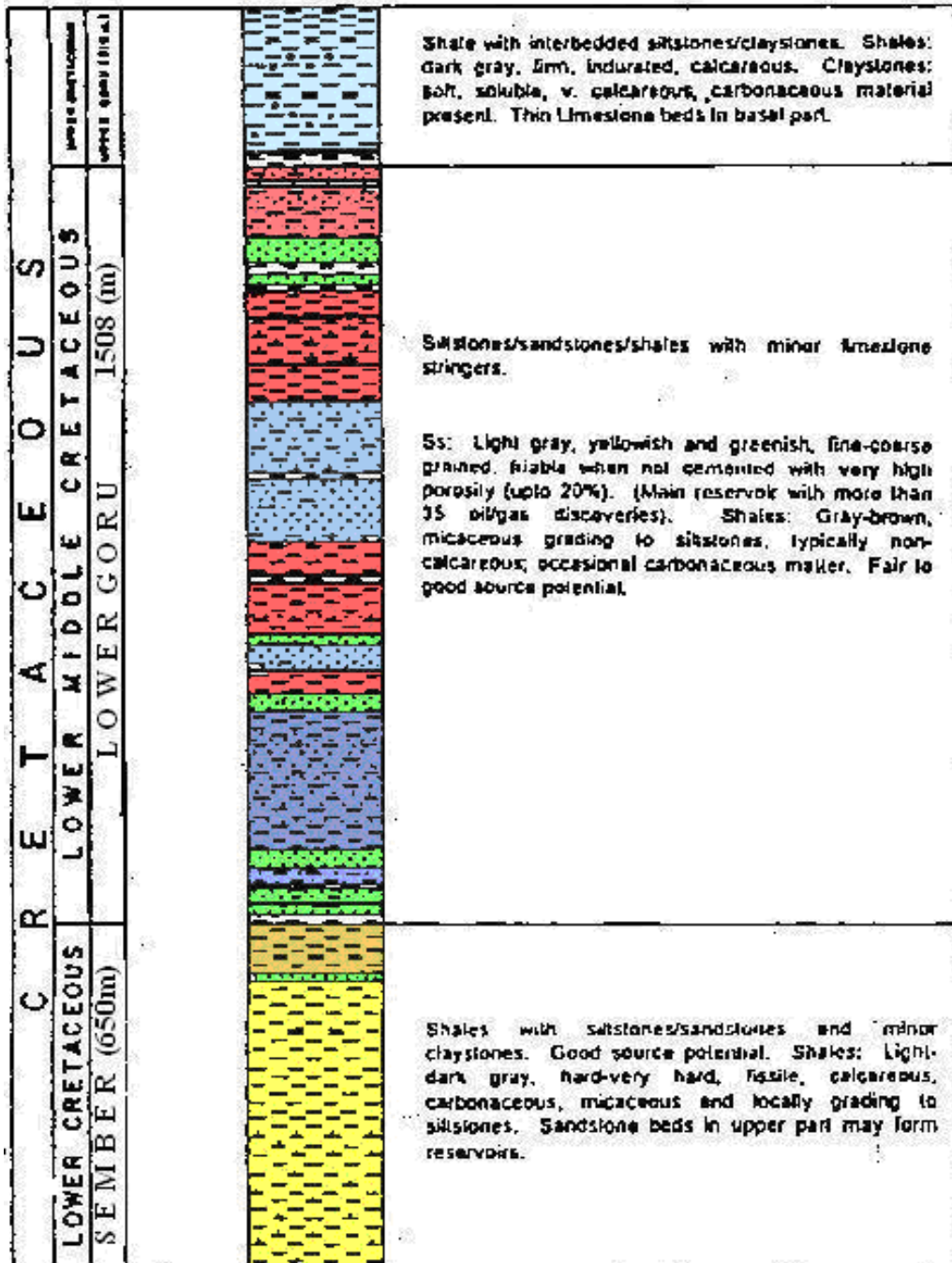
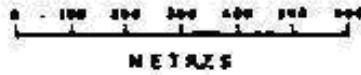


Figure 7: Lithostratigraphic column of Lower Cretaceous in Badin Platform (Qadri, 1994)

2.3.2.3 Parh Limestone

Although Parh limestone occurs widely throughout the Indus Basin, erosional truncation has limited the Formation distribution to an area lesser than Goru and Sember Formations (Qadri, 1994). Like in Badin platform area it is only present in southern portion and that too in the form of thin layer (Figure 7). No oil or gas shows have been found in the Parh limestone in the subsurface and no surface seeps are known (Qadri, 1994).

2.3.2.4 Pab Sandstone

It is light grey to light tan to brown, quartzose, fine to coarse grained, hard to soft sandstone. It is occasionally conglomeratic and generally cross-bedded. It is considered to be deposited under shallow water environment characteristic of the MughalKot deposition. In the MughalKot seepage area, most of oil seeps are from Pab. It also forms petroleum reservoirs at Pirkoh, Loti, Dhodak and Rodho fields. It is considered to have no source potential (Qadri, 1994).

2.3.3 Cretaceous – Tertiary Unconformity

The end of Mesozoic is marked by regression of sea in most of Pakistan. But in Central and southern Indus basins, there are numerous indications which suggest very little gap, if any, between Cretaceous and Paleocene sedimentation.

2.3.4 Paleocene sequence in Southern Indus Basin

The end of Cretaceous and the advent of Tertiary is marked by northward journey of Indian plate which accelerated (16cm/yr., Powell 1979) during Paleocene. The collision of Indian and Eurasian plates resulted in emergence of numerous local areas in lower

Indus basin. This basin is therefore marked by various phases of transgression and regression. Early Paleocene transgression deposited Khadro in negative areas while other areas did not receive Danian sediments. Therefore, in Southern Indus basin the rocks of Paleocene age are almost entirely of marine origin (Qadri, 1994).

In early Paleocene, as a result of east-west compression and north-south tension and counter clockwise rotation of Indian plate, tholeiitic basalts extruded and covered the older weathered Formations. Evidence of this is found in base of Khadro Formation which contains basaltic inflows. This phenomenon is restricted to southern Kirthar region and Badin platform (Qadri, 1994).

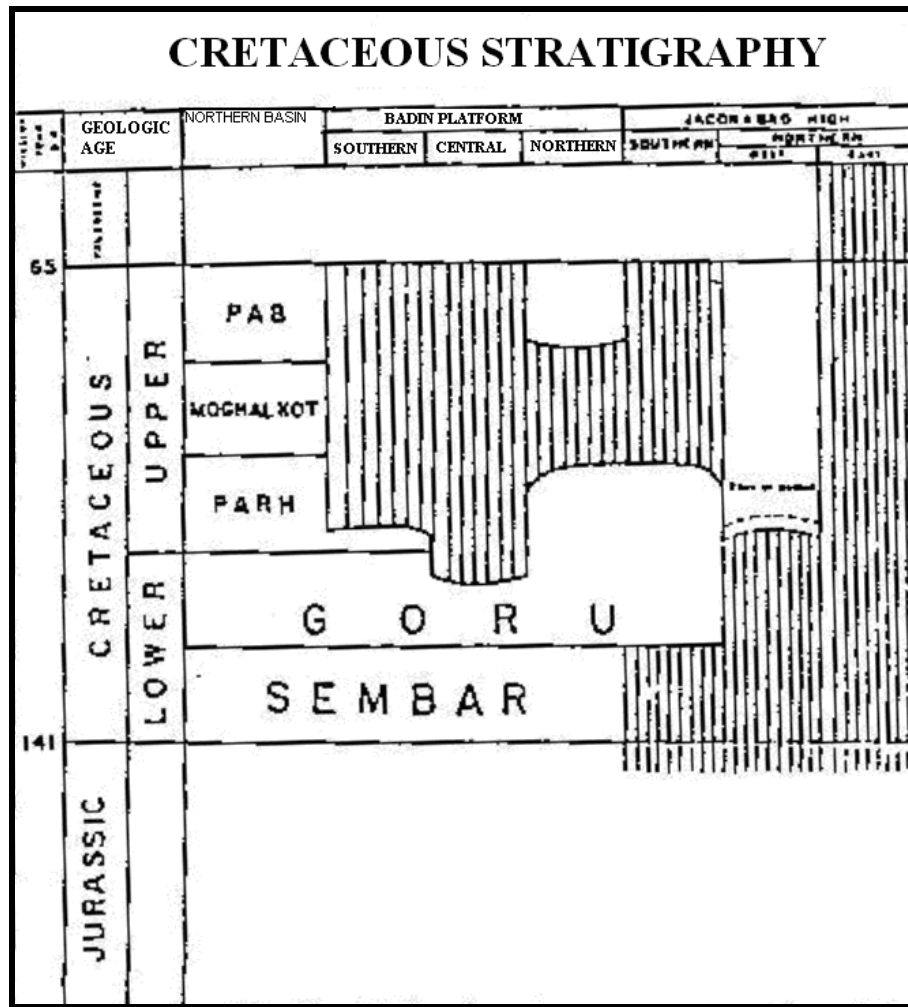


Figure 8: Section showing thickness of Cretaceous Formations in Badin platform (Qadri, 1994)

3 PARTICULAR GEOLOGY OF SINJHORO BLOCK

3.1 TECTONICS

Sinjhoru E.L is a part of Thar Slope Platform area of Southern Indus Basin. It is bounded in the east by Indian Shield and in the west by Kirthar and Karachi Trough and in the north by Mari-Bugti Inner Folded Zone. During the drift of the Indian plate towards the North-North East, which started in the Triassic, sedimentation took place along the leading edge of the plate in a marginal sag basin. Although several sedimentary cycles can be recognized within this phase, no major tectonic activity occurred until well encounter Cretaceous. In the lower Indus region, a depositional environment during the Paleocene resembled the pattern of the Mesozoic. However, later during the Eocene, the first organic pulse exercised its influence on the sedimentation by that time, the paleogeographic changed completely with the emergence of a volcanic island arc, North West of present day Pakistan. The sediments derived from the arc entered marine environments towards South East and independent depocenters developed in various parts of the Pakistan.

Full-scale collision in the Oligocene resulted in the second orogenic pulse and caused the uplift of many areas in the East and South. The marine sediments became restricted to a narrow but rapidly subsiding trough in the Kirthar Area. A large influx of clastic material from the North forced the sea to retreat to the South during the Late Cenozoic. The clastic supply from the rising Himalayas and from the local positive regions of the axial belt was so abundant that a spectacularly thick sequence of molasses sediments reaches more than 7,000m. Towards the end of the Paleocene, the Indus Basin was filled with sediments and must have resembled a vast flood plain with braided stream, the only elevation being the hills of the folded belts.

The part of Lower Indus Basin represents progradational Mesozoic sequences on a westward inclined gentle slope. Every prograding time unit represents lateral facies variations from continental and shallow marine in the East to dominantly basinal to the West. In Thar Slope Area, all Mesozoic sediments are regionally plunging to the west and are truncated by unconformable volcanics (Basalt of the Khadro Formation) and sediments of Paleocene Age.

3.2 STRUCTURE

Chak-7A Structure is located at a distance of about 3 kms North East of Chak-66 and 3.12 kms South West of Chak-2 structures where OGDCL discovered condensate/oil and gas from Basal sands. The eastern and western closures are formed by NW-SE running faults; where as the northern and southern closures are provided by dips. The structural closure is against major eastern fault, having a throw of 100m. Chak-7A structure is well defined by 2-D seismic coverage. Time contour map prepared at the Top of Basal Sands of the Lower Goru level gives the closure area of about 1.9 km² with a vertical closure of about 58m.

The vertical seismic section on line No. 886-SGR-347, showing Chak-7A prospect and location of Chak-7A Well No. 01 at shot point 786.

3.3 PETROLEUM PROSPECTS

3.3.1 Source Rocks

The Lower Cretaceous Shale of Sember Formation is proven source for oil and gas discovered in the Lower Indus Basin because of its organic richness, oil prone kerogen type and thermal maturity. The lower part of Lower Goru Formation is moderately rich in organic shale having fair to good genetic potential.

On litho-stratigraphic correlation between Chak-5 Dim Well No. 1 and Shahdadpur Well No. 01, shale below Massive sands is sufficiently well developed in the prospect area. The shales were geochemically analyzed at Shahdadpur Well No. 01. The studies based on Vitrinite Reflectance infer that the kerogen is immature to the depth of 3345m in Lower Goru Formation, where amorphous organic matter (rich in oil prone kerogen) dominates and can be regarded as “potential source rock”. The results of Pyrolysis Analysis of Shahdadpur Well No. 01 indicate a zone of maturity transition from oil and wet gas generation to dry gas generation in the Lower Goru Formation.

3.3.2 Reservoir Rocks

The Basal and Massive Sands of the Lower Goru Formation were the main objective in this well. The Basal Sands are proven producers in Chak-5 Dim, Mithrao, Chak-66, Resham, Chak-2, Bobi and Jakhro oil and gas fields, while Massive Sands are producers in Chak-63 Well No. 01 and Hakeem Daho Well No. 01.

The Basal Sands with shale having hydrocarbon were encountered at 2817m at Chak-7A Well No. 01. The Massive Sands were encountered at 2915m with fair shows and porosities. The average porosity for these sands ranges between 13-25 % in the Chak-7A Prospect.

3.3.3 Cap Rocks

Thick sequence of shale and marl of the Upper Goru Formation as well as shale within the Lower Goru serves as cap rock for the underlying sandstone reservoirs.

3.4 STRATIGRAPHY

Chak-7A Well No. 01 was drilled from surface down to 3050m (Logger`s T.D. 3052M) in the formations of Post Eocene, Eocene, Paleocene and Cretaceous ages. One unconformity exists between the Alluvium and Laki, second unconformity exists between Laki and Ranikot and third unconformity exists between Ranikot and Parh Formations. Although little variation in thickness was noticed, more or less the encountered stratigraphic sequences remained same as mentioned in prognosis. The top of Lower Goru Formation, anticipated at 2034m, was actually encountered at 2120, i.e. 68m deeper than the prognosed depth.

The stratigraphic succession drilled at Chak-7A Well No. 01 was re-established after assimilating available data from well site and wireline logs and is summarized in (Table 2 & 3). The stratigraphic correlation with the surrounding wells is given in (Table 2 & 3). The lithology as evidenced by flush cuttings and related drilling and mud parameters are plotted on 1:500 scale on Master Log. The formation tops are corrected from wireline logs.

Age	Formation	Lithology	Description	Top (MSL) m	Thickness m	Contact	
Post Eocene	Alluvium		Sandstone with interbeds of clay/claystone, conglomerate and minor traces of coal.	0.0	604	Lower contact unconformable	
Eocene	Laki		Limestone with interbedded marl and shale.	604	541	Upper and lower contact unconformable	
Paleocene	Ranikot		Sandstone, shale with streaks of clay/claystone and thin bands of limestone	1145	497	Upper and lower unconformable	
Cretaceous	Parh		Limestone with subordinate Chalk	1642	99	Upper unconformable	
	Upper Goru		Marl	1741	361	Both conformable	
	Lower Goru	Upper Shales Sand		Shale with intercalations of marl and streaks of sandstone	2102	715	Both conformable
		Basal Sands		Sandstone with few laminations of shale	2817	28	Both conformable
		Talhar Sands		Shale	2847	70	Both conformable
		Massive Sands		Argillaceous Sandstone with subordinate Shale	2915	135	Both conformable
		Sember		Shale			Both conformable
Jurassic	Chilton		Massive Limestone			Both conformable	

Figure 9: Stratigraphic Sequence observed in well Chak 7A 01

Table 2: Showing Stratigraphic Succession of Chak-7A Well No. 1

STRATIGRAPHIC SUCCESSION						
AGE	FORMATION	FORMATION TOPS (m)			THICKNESS	LITHOLOGY
		ANTICIPATE				
		D	WELLSITE	E. LOG		
Recent	Alluvium	Surface	Surface	Surface	+604	Sandstone with interbeds of clay/claystone, conglomerate and minor
UNCONFORMITY						
Eocene	Laki	610	606	604	541	Limestone with thick interval of shale &
UNCONFORMITY						
Paleocene	Ranikot	1150	1145	1145	497	Dominantly sandstone, shale with streaks of limestone and claystone
REGIONAL UNCONFORMITY						
Cretaceous	Parh	1640	1643	1642	99	Limestone with alterations of chalk
Cretaceous	Upper Goru	1745	1744	1741	361	Marl
Cretaceous	Lower Goru	2034	2101	2102	+950	Shale with sandstone, siltstone & marl
	Upper sands, Shale, marl sequence	2034	2101	2102	715	Shale with intercalations of marl and streaks of sandstone.
	Basal Sands	2784	2816	2817	28	Sandstone with few laminations of shale
	Talhar Shale	-	2843	2845	70	Shale
	Massive Sand	-	2915	2915	+137	Argillaceous sandstone with subordinate shale
T.D		3050	3050	3052	-	K.B Elevation: 33.60 AMSI, G.Elevation: 25.60m AMSI

Table 3: Showing Stratigraphic Succession of Chak-7A Well No. 1

STRATIGRAPHIC SUCCESSION								
FORMATION	CHAK-66 # 01		CHAK-7A # 01		RESHAM # 01		CHAK-2 # 01	
	K.B 31.93 m AMSL		K.B 33.60 m AMSL		K.B 32.55 m AMSL		K.B 33.11 m AMSL	
	<i>INTERVAL</i>	<i>THICKNESS</i>	<i>INTERVAL</i>	<i>THICKNESS</i>	<i>INTERVAL</i>	<i>THICKNESS</i>	<i>INTERVAL</i>	<i>THICKNESS</i>
	<i>(m)</i>	<i>(m)</i>	<i>(m)</i>	<i>(m)</i>	<i>(m)</i>	<i>(m)</i>	<i>(m)</i>	<i>(m)</i>
Alluvium	0000-	612	0000-	604	0000-	626	0000-0603	603
UNCONFORMITY								
Laki	612-1161	549	0604-	541	616-1170	544	0603-	533
UNCONFIRMITY								
Ranikot	1161-	474	1145-	497	1170-	479	1136-	506
	1635		1642		1649		1642	
REGIONAL UNCONFIRMITY								
Parh	1635-	108	1642-	99	1649-1760	111	1642-1736	94
Upper Goru	1743-	280	1741-	361	1760-1994	234	1736-2033	297
Lower Goru	2023-	+1031	2102-	+950	1994-3055	+1061	2033-3057	+1024
Upper sands,	2023-	824	2102-	715	1994-2856	862	2033-2778	745
	2847		2817					
Basal Sands	2847-	23	2817-	28	2856-2876	20	2778-2805	27
	2870		2845					
Talhar Shale	2870-	70	2845-	70	2876-2960	84	2805-2895	90
Massive Sand	2940-	+114	2915-	+137	2960-3055	+95	2895-3057	+162
	3054		3052					
T.D	3054		3052		3055		3057	

4 SEISMIC DATA ACQUISITION

The first step involved in seismic study of an area is the acquisition of seismic data. Acquisition of data means that the procedure through which seismic reflection data is collected, is the very first step in the interpretation of seismic data. Seismic exploration is the primary method of exploring for hydrocarbon deposits, on land, under the sea and in the transition zone (the interface area between the sea and land). Although the technology of exploration activities has improved exponentially in the past 20 years, the basic principles for acquiring seismic data have remained the same.

4.1 BASIC PRINCIPLE

In simple terms and for all of the exploration environments, the general principle is to send sound energy waves (using an energy source like dynamite or Vibroseis) into the Earth, where the different layers within the Earth's crust reflect back this energy. These reflected energy waves are recorded over a predetermined time period (called the record length) by using hydrophones in water and geophones on land. The reflected signals are output onto a storage medium, which is usually magnetic tape.

4.2 COMPONENTS OF SEISMIC ACQUISITION SYSTEM

The entire seismic acquisition system is subdivided into 3 components based upon the operation that they perform. These are:

- 1) Input Devices
- 2) Design of detectors array
- 3) Detection and Recording

4.2.1 Input Devices

Also termed as energy source of seismic data, input devices are used to produce vibration in earth. Different kinds of input sources are used for land and marine survey. These input devices include explosive as well as non-explosive energy sources.

4.2.1.1 Impulsive energy sources

Impulsive energy source make use of explosives which are detonated to produce energy. The most common energy source used from this category is Dynamite.

Dynamite is exploded inside a drilled hole at a depth ranging from few meters to several tens of meters. The amount of charge per shot point depends on whether it is a single hole or a pattern shooting. As a rough estimate the charge weight is 10-50 Kg of dynamite.

Geoflux is another impulsive source which consists of an explosive cord, which is buried in the ground at a shallow depth. It is laid down by a hydraulically operated plough, which is especially designed for the purpose.

4.2.1.2 Non-Impulsive sources

These are the sources which do not use explosive detonation mechanism for generation of energy. They produce seismic energy by vibratory or other mechanisms. They are either used in marine survey or in Urban or populated areas where it is not safe to detonate explosives.

Vibroseis, which is the most commonly used vibratory input device, is based on the use of a mechanical vibrator. This is hydraulically driven to exert a force of an oscillating magnitude. It provides best productivity in shots per hour. The frequency range and strength can be controlled to meet survey requirements.

Hammer can also be used to produce seismic energy by impacting it on the ground. But this energy source is only good for shallow seismic. Geograph method, also known as Thumper, involves dropping a weight of about 3 tons from a height of about 3m on to the ground.

In marine survey, Air gun or water gun is used. Air gun discharges highly compressed air into the water. It comprises a chamber, which is charged with compressed air released by electrical triggering. In case of water gun, Compressed air is used to drive a piston that ejects water jet into the surrounding water. (Robinson, 1988; Kearey and Brooks, 1984).

4.2.2 Field Layouts

For a 2D seismic survey, all source and receiver points must lie in a straight line; this is called straight line shooting. Another type of shooting is called crooked line shooting in which the receivers do not lie in a straight line and it is only done when straight line shooting is impossible due to some construction etc. Numerous receiver-source configurations are used in seismic data acquisition.

These include:

- 1) Split spread
- 2) End –on spread
- 3) Cross – spread
- 4) In – time offset spread
- 5) Split –dip spread with shot gap
- 6) Broad side T spread (Robinson and Coruh, 1988)

In seismic lines under study, 90 channels Symmetric Split spread have been used. Symmetric Split spread means that the geophone groups are kept on for seismic signals, on both the sides of a source point, and are equal in number.

4.2.3 Detection of Reflected Signal

After laying out the proper receiver-shot point configuration (as per need) and using energy source, there comes the stage of detection of seismic waves. Seismic equipment of adequate sensitivity, large dynamic range, and suitable frequency response is the aim of all development programs taking place in the field of seismic detection. Geophone is the most important detecting instrument used (Al-Sadi, 1980).

4.2.3.1 Geophone

The receiver used for the detection of ground vibration is called a geophone or a seismometer. It is used for seismic surveying on land, and it can also be operated on the ocean floor if mounted in a suitable container. Mechanism is that the motion of a coil around a magnet induces electric current to flow in the coil. The strength of that current depends on the speed of the motion.

The response of geophones to vibration of different frequency can be tested with a device called a shake table. The frequency of vibration that stimulates the strongest geophone response is recognized as the natural frequency of the geophone. Geophones commonly have natural periods in the range of 5 to 40 Hz.

4.2.3.2 Hydrophones

A hydrophone is a microphone designed to be used underwater for recording or listening to underwater sound. Most hydrophones are based on a piezoelectric transducer that generates electricity when subjected to a pressure change. Such piezoelectric materials or transducers can convert a sound signal into an electrical signal since sound is a pressure wave in fluids.

Table 4: Receiver parameters for under study seismic lines (adopted from seismic section)

GEPHONE TYPE	L-10
GEPHONE FREQUENCY	20 Hz
GROUP SPACING	50 m
GEPHONES PER GROUP	21
GROUP WIDTH	3 m
GEPHONE INTERVAL	5 m

4.2.4 Recording Stage

All registration of signal from geophone is then recorded. There are two systems, which record the geophone signal:

- 1) The Analogue Recording System
- 2) The Digital Recording System

4.2.4.1 Analogue Recording System

This is the earliest system used to record seismic data on magnetic tapes. The analogue recording system is made up of an assembly of electronic units normally housed in a specially adapted truck called the recording station. It involves two steps. First the signal coming from Geophone is amplified and is then recorded.

4.2.4.2 The Digital Recording System

A digital station is equipped with the facility to convert a continuous signal into a digital form. The sample value is expressed in terms of binary digits. This type of recording system amplifies the signal coming by geophone which is followed by Analogue to Digital conversion (A/D conversion) and is then recorded.

Table 5: Recording parameters (adopted from seismic section)

INSTRUMENTS	SN-338-HR
TAPE FORMAT	SEG-B
FIELD RECORD LENGTH	5000 msec
SAMPLE RATE	2 msec
FIELD FILTER	Notch filter out
POLARITY	Normal

4.3 THE CDP METHOD

CDP method was introduced by Mayne in 1963. The CDP offers some cancellation of noise, i.e., multiples and random noise. In this method the signals associated with a given reflection point (Common depth point) but recorded at different shot and geophone positions are defined. The seismic data acquisition is done such that CDP method yields greater number of shot points per unit distance along the line causing repetition of reflection point at an interface. It means, if a reflecting point is repeated twice during shooting, there would be two seismic traces corresponding to that point, so it admits 2-fold acquisition or it can be designated as 200% data. The data fold can be evaluated from the following relation:

$$F = \frac{N\Delta y}{2\Delta x}$$

Where

N = Number of recording channels

Δy = Group Interval

Δx = Shot point interval

Our current data is 48 fold meaning 4800%.

5 SEISMIC DATA PROCESSING

Once seismic data has been acquired on field, the second step is the processing data. Data Processing involves sequence of operations, which are carried out according to a pre-defined program to extract useful information from a set of raw data (Al-Sadi, 1980). The main purpose of processing is to convert seismic data recorded in the field into a coherent cross section, indicating significant geological horizons into the earth subsurface, related to hydrocarbon detection and seismic Stratigraphy (Hatton et al., 1986, Dobrin and Savit 1988).

Seismic data processing consist of applying a sequence of computer programs, each designed to achieve one step along the path from field tape to record section. From ten to twenty programs are usually used in a processing sequence, and these are selected from a library of several hundred programs. Each company's library is unique, although many programs are will be almost identical with those of another company. In each company's library there may be several programs designed to produce the same effect by different approaches. For example one program may operate in time domain while another works in frequency domain, yet they may yield similar results (Zia-ur-rehman, 1989).

Successful exploration and exploitation programs require the best possible “picture” of the subsurface. Seismic migration is one of the four basic steps that give us the best “picture”. These four primary data processing steps are; in their usual order of application

1. Demultiplexing
2. Deconvolution
3. Stacking
4. Migration

5.1 DEMULTIPLEXING

Demultiplexing is the reorganization of recorded data to common depth point gathers. The outcome of a geophone group during field recording is a continuously varying electrical voltage. Since seismic data are processed in digital computers, the continuous geophone output voltage must be converted to digital format by sampling.

Sampling occurs in the field or in the processing centre in an analog to digital converter (A/D). Consider four geophone arrays, whose outputs are brought to four terminals arranged in a circular pattern, and an arm, pivoted at the circle's center rotating counterclockwise and making with momentary contact with the four terminals in succession. The instantaneous voltage at each terminal is recorded each time the rotating arm sweeps over it, yielding an array of samples. If each sample is identified by its geophone group sources (A, B, C, D) and by its chronological sequence in that group (1, 2, 3...) then the output of the A/D converter is:

A1,B1,C1,D1,A2,B2,C2,D2,C3,B3,C3,D3,.....

This scrambled sequence is referred to as a “multiplexed” array. However, it is more convenient to process seismic data in trace sequential array:

A1,A2,A3,...., B1,B2,B3,...., C1,C2,C3,...., D1,D2,D3,....

Unscrambling a multiplexed array into a trace sequential array is called “demultiplexing”. It is accomplished by a simple computer sorting program and it is the first step in any data processing sequence (Zia-ur-rehman, 1989).

5.2 PREPROCESSOR

5.2.1 Geometry definition

In geometry definition the geometry of the traces is made. It consists of the information which is associated by the trace. It has information such as the File number on which the terrace is present, the Field File Identification Number (FFID), the first live channel, the last live channel, the Picket interval, total number of traces per shot, source and receiver information, fist receiver point, last receiver point, the number of misfires, deep holes, pattern shots, pop shots, etc (personnel communication).

5.2.2 Editing

Raw seismic data inevitably contains some unwanted noise and perhaps some dead traces. If obviously useless information is to be removed from the processing stream, it must first be identified and then blanked or muted by assigning zero values to all samples in the affected time interval. Unwanted data are usually identified by visual examination of raw field traces, although obvious cases (dead traces, strong noise bursts, etc) can be detected and edited automatically. The raw field traces used in this editing procedure can be obtained from field monitor records or from one of the trace gathers previously described (Zia-ur-rehman, 1989).

5.3 TRACE BALANCING – AGC

The AGC function does not employ a gain to the whole trace, but employs a gain to a certain time sample within a time gate. A disadvantage is that when the AGC gain is applied, it is not possible to reconstruct the original signal again. Therefore, the AGC is only used for display and printing purposes (Yilmaz, 2001).

5.4 CDP SORT

Each trace to be included in a common depth point stack comes from a different digital seismogram. A large number of digital seismograms can be sorted in computer memory after they had been prepared by demultiplexing. the process of selecting a set of traces to be stacked is called CDP Sort (Robinson and Coruh, 1988).

5.5 DECONVOLUTION

Deconvolution is the analytical process of removing the effects of some previously filtering operation (convolution). Inverse filters are designed to deconvolve seismic traces by removing the adverse filtering effects associated with the propagation of the seismic pulses through a layered ground or through a recording system (Kearey, Brooks and Hill, 2003). Deconvolution is a filtering process whereby the undesirable complexities in the source wavelet and reverberation multiples are reduced or, better yet, eliminated.

5.6 VELOCITY ANALYSIS

Velocity in seismic processing is an important parameter, which controls the stacking quality. Thus the proper velocity value gives the optimum dynamic correction, which leads to efficient stacking process. The seismic traces of a common depth point gather are basis for each velocity analysis. Before velocity Analysis- suitable static correction and data enhancement procedures are applied to the data.

5.7 RESIDUAL STATICS

Elevation static corrections are well known and important elements in the processing of seismic data. For these corrections many methods are used, more advanced methods of computing statics are occasionally used, such as multi layered weathering computations

based on refraction and uphole data, or first arrival time usage for statics calculations. But, whatever the method, there are certain assumptions and extrapolations that are to be made, and they are called as residual statics. These residual static corrections are important part of data refinement and are derived in various ways (Zia-ur-rehman, 1989).

5.8 MUTE

Muting means Zeroing of data or turning it down. It is a technique used in Seismic data processing for the removal of noise and unwanted traces from the seismic data that is obtained by acquisition. This noise or unwanted data includes Airwaves and direct arrivals.

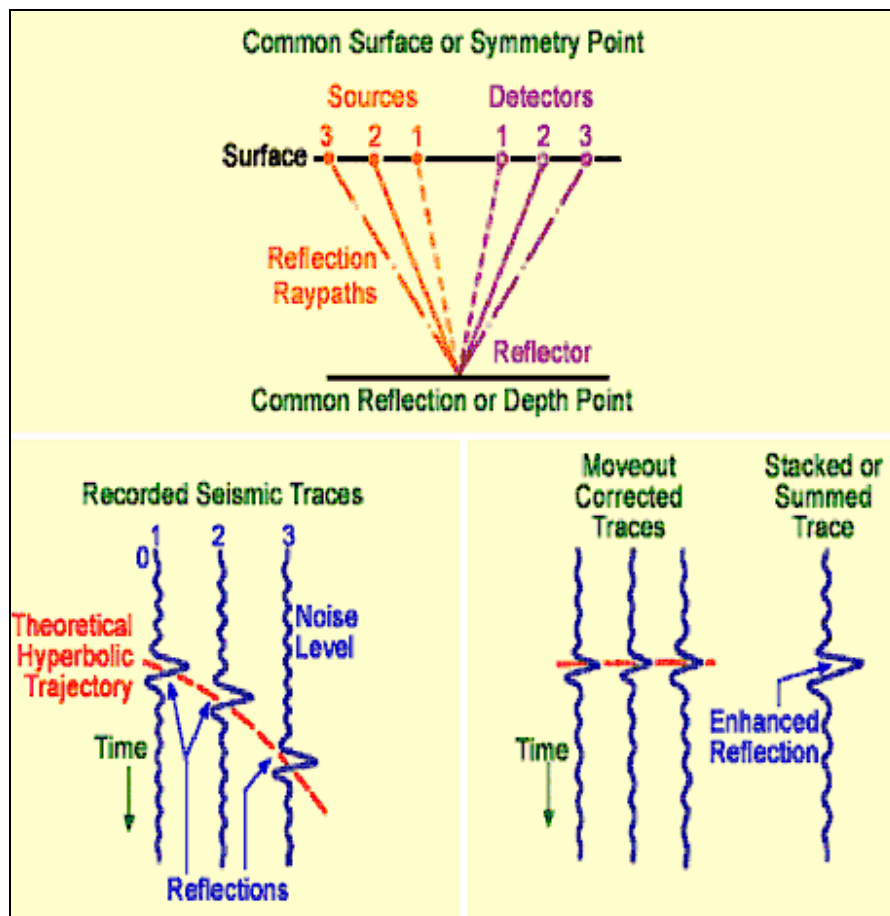


Figure 10: Reflection hyperbola of a horizontal reflection surface corrected by NMO followed by Stacking

5.9 NMO CORRECTION

Normal move out correction is related more with non-dipping interfaces. On the other hand Dip move out correction is related to the dipping reflectors. For a single constant velocity horizontal layer, the travel time curve as a function of offset is a hyperbola (Figure 13). The time difference between travel time at a given offset and a zero offset is called Normal move out (NMO) or dynamic correction. The velocity required to correct for normal move out is called the normal move out velocity (Yilmaz, 1987).

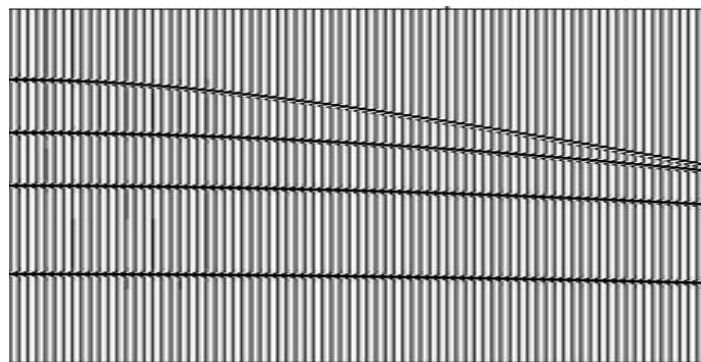


Figure 11: Reflection hyperbolas before NMO correction

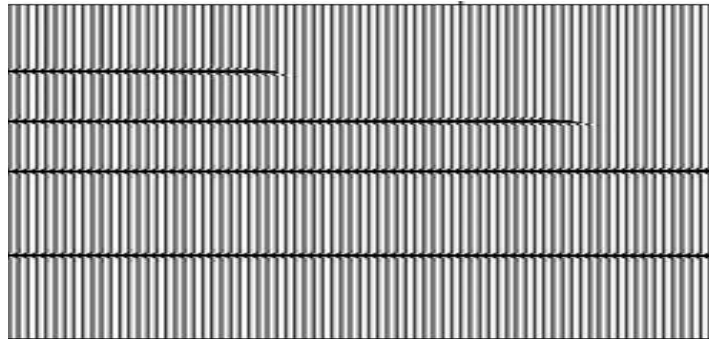


Figure 12: Reflection hyperbolas after NMO Correction

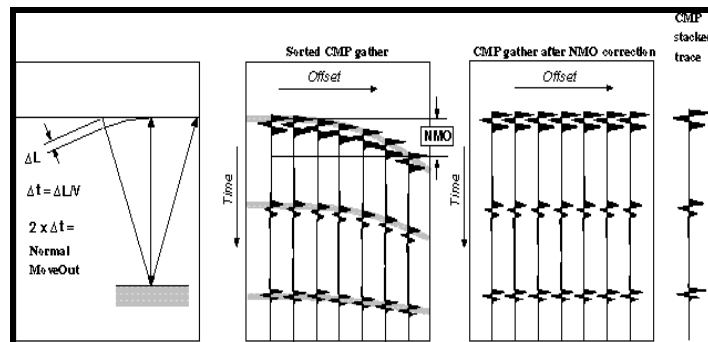


Figure 13: NMO process

(www.gsj.go.jp/.../seismic/seismic.method.html)

5.10 DATUM CORRECTION

Datum corrections, also known as Elevation corrections are used to nullify the effect of topographic variations in the area. Aim of datum correction is to adjust the seismic traces in such a way that the sources and receivers are present at horizontal level. To achieve this, the travel times of the separate traces are corrected. The whole trace is corrected with the same shift.

5.11 STACK

Stacking with its associated velocity analysis enhances real data while minimizing noise. Once necessary corrections have been applied, the data may be stacked. The traces are gathered into depth point order (both statics and dynamics applied, and the traces muted). All that remains to stack the data is to sum all the traces in each depth point, resulting in a single, stacked trace being output for each depth point (Zia-ur-rehman, 1989).

5.12 MIGRATION

Seismic migration corrects for geometric displacement of data from a dipping reflector and/or lateral velocity changes and places them in their true spatial position rather than at an assumed point in depth between the source and the receiver. The goal of seismic process is to make subsurface reflection data appear like a vertical slice or geological cross-section of the earth along the plane of seismic array. The goals of migration process are two-fold—first, to ensure that those reflections are in their correct subsurface locations, and second to eliminate the signal interference caused by point diffractors (Siraki, 1985).

5.13 FINITE DIFFERENCE MIGRATION

This method involves a solution of the two – dimensional scalar wave equation. The logic of the finite difference migration is similar to that of ray tracing. Ray tracing projects raypaths back to the subsurface. The finite difference migration method projects emerging wavefronts backward into the subsurface. Both procedures are based on Huygens's principle.

5.14 BAND PASS FILTER

A band-pass filter is a device that passes frequencies within a certain range and rejects (attenuates) frequencies outside that range. The range of the frequencies is given & we get the data in the required range. It removes all the events outside the upper & lower frequency limits of the signal.

6 INTERPRETATION

Seismic interpretation is the transformation of seismic reflection data into a structural and stratigraphic picture by processing issue, contouring of subsurface horizon in further depth conversion by applying some suitable velocities. The seismic reflection interpretation usually consists of calculating the positions, and identifying geologically, concealed interfaces or sharp transition zones from seismic pulses returned to the ground surface by reflection. The influence of varying geological conditions is eliminated along profile to transform the irregular travel time into acceptable subsurface model. This is very important for confident estimation of the depth and geometry of bedrock or target horizon (Dobrin & Savit 1976).

The major aim of seismic reflection surveying is to reveal as clearly as possible the structure of the subsurface. Geological meaning of seismic reflection is simply an indication of an acoustic boundary where we want to know that whether this boundary makes a fault or a stratigraphic contact with any other boundary. We want to distinguish the features that are not marked by the sharp boundaries. Geologists ordinarily group the sequence of sedimentary rocks into units called “Formations”. These formations can be described in terms of age, thickness and lithology of the constituent layer. To distinguish different formations on the basis of seismic reflections is an important question in interpreting seismic data that may be structural, stratigraphic or lithological (Robinson & Coruh 1988).

There are two main approaches for the interpretation of seismic sections:

- Structural Analysis
- Stratigraphic Analysis

6.1 STRUCTURAL ANALYSIS

It is the study of reflector geometry on the basis of reflection time. The main application of the structural analysis of seismic section is in the search for structural traps containing hydrocarbons. Most structural interpretation uses two way reflection times rather than depth. And time structural maps are constructed to display the geometry of selected reflection events. Seismic sections are analyzed to delineate the structural traps like folds, faults and anticlines. In this modern era of science and technology, much software provides a great help in analyzing the seismic data both structurally and stratigraphically. There is software that provides a great help to interpreters by automatically detecting the fault zones and then marking them on the whole project area. But, for this the seismic data should be high resolution.

In the given project seismic sections have been analyzed structurally as well as stratigraphically. Since no software was available for the interpretation purpose (marking the reflectors and reading the two way times automatically), horizon-marking and time-reading have been done manually.

6.2 STRATIGRAPHIC ANALYSIS

Stratigraphic analysis involves the subdivision of seismic sections into sequence of reflections that are interpreted as a seismic expression of genetically related sedimentary sequences. The principles behind this seismic sequence analysis are of two types:

Firstly, reflections are taken as chronostratigraphical units (deposited at the same time), since the type of rock interface that produce reflections are strata and unconformities, by contrast the boundary of diachronous lithological units tend to be transitional and not to produce reflections.

Secondly, genetically related sedimentary sequences normally comprise the set of concordant strata that exhibit discordant with underlying and overlying strata.

According to Dobrin & Savit, throughout the history of reflection method, its performance in locating hydrocarbons in stratigraphic traps has been much less favorable than in finding structurally entrapped oil and gas.

Stratigraphic oil traps can result from reefs, pinch outs, or other features associated erosional truncation, facies, transition and sand lenses associated with buried channel, lacks, are similar sources. Different software provide help in stratigraphic analysis as well by overlaying different seismic attributes on seismic sections to detect pinch outs, truncations etc.

6.3 INTERPRETATION OF SEISMIC LINES OF STUDY

AREA:

Five seismic lines (hard copies) were provided for the given project. These were:

- **896-SGR-350** **(dip line)**
- **896-SGR-394** **(dip line)**
- **896-SGR-393** **(dip line)**
- **886-SGR-391** **(strike line)**
- **866-SGR-86** **(strike line)**

However, five more lines have been included in the project to have a better control over time and depth contouring. These lines are:

- **886-SGR-347** (dip line)
- **947-SGR-278(N)** (dip line)
- **947-SGR-283 (N)** (dip line)
- **936-SGR-122** (dip line)
- **896-SGR-389** (dip line)

The general dip direction in the project area is NE-SW and hence the lines oriented NW-SE is regarded as strike lines. A base map of lines selected for the project is displayed on the next page (Figure 14).

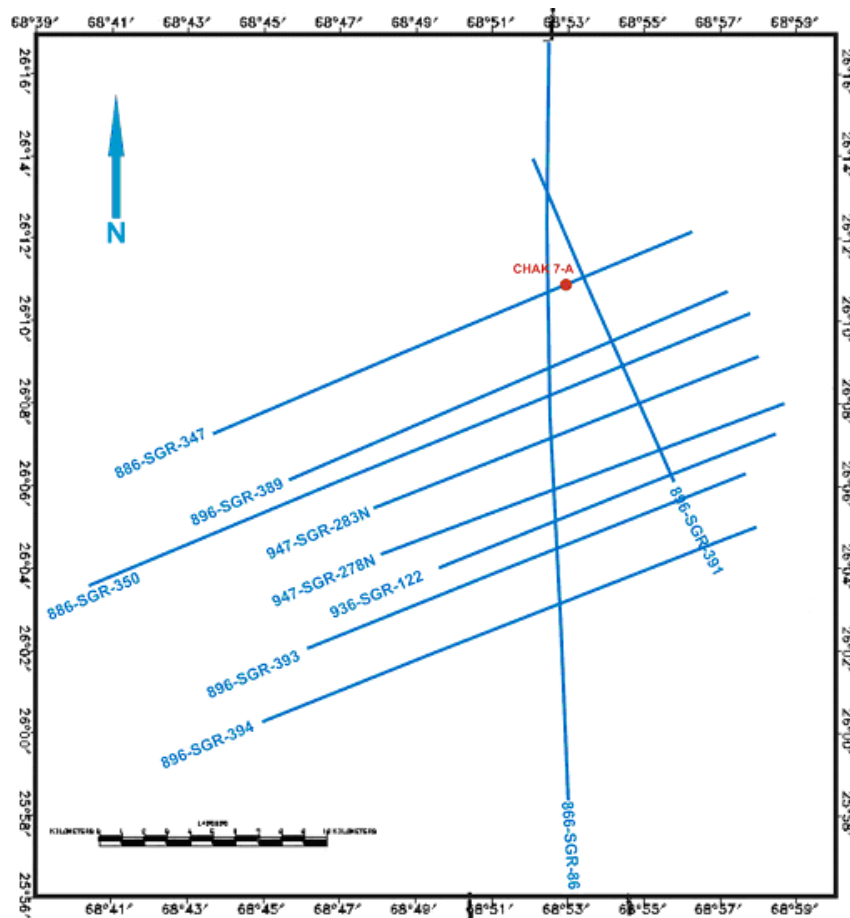


Figure 14: Base map of seismic lines used in the project

6.3.1 Quality of Seismic Data:

For a reliable interpretation of any seismic data it is important that the quality of seismic being acquired is good. It means that data resolution should be good so that the identification of faults and horizon correlation is not a big problem.

The seismic lines for the given project can be regarded as of good quality. Horizons up to 3 sec show good continuity; faults can also be identified easily. Of the five marked horizons, only top basal sands' reflector (red) was a bit difficult to tie on available seismic sections (Figure 15).

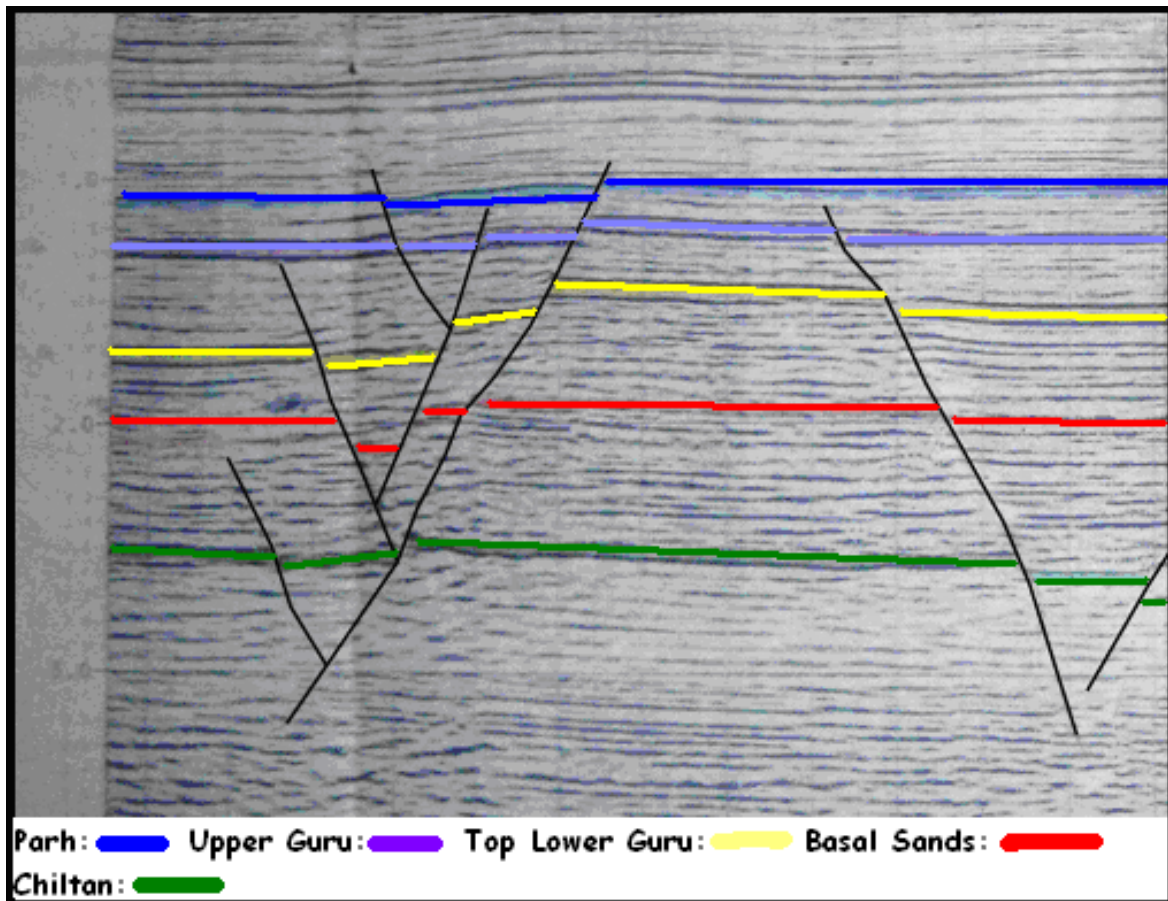


Figure 15: A portion of line 886-SGR-347. All marked horizons and faults have good continuity; only the red horizon doesn't show good continuity

6.3.2 Interpretation Steps Adopted

Following steps are used in interpreting the provided seismic lines:

- Marking of reflectors & their identification
- Identifying the faults, and then posting them on the base map
- Reading the time
- TWT contour mapping
- Depth contour mapping.
- Making of 3D time and depth surfaces
- Preparation of depth models of seismic lines.

6.3.2.1 Marking Of Reflectors And Their Identification:

The first and foremost approach is to mark the reflectors on the seismic section. These are marked on the basis of best coherency and continuity of the amplitude of the seismic traces. Continuity is good where there is a sharp acoustic impedance contrast; Acoustic impedance is the product of velocity and density of the rock layer.

For the given project, five horizons have been marked on ten seismic lines mentioned earlier. Firstly, these horizons were marked on the seismic line 886-SGR-347. Then, they were tied to the other nine lines (Figure 18 & 19).

In order to identify different horizons, and hence to determine their lithology, well data is necessary. A number of wells have been drilled in and around the project area, providing useful information about the subsurface. For the given project, data of Chak 7-A well was used. The marked horizons were identified on the basis of this well data, which was drilled on line 947-SGR-347.

Horizons identified on the basis of well data, from shallow to deep are as follows:

- **Blue Horizon (Top Parh Limestone)**
- **Purple Horizon (Top Upper Goru)**
- **Yellow Horizon (Top Lower Goru)**
- **Red Horizon (Top Basal Sands)**
- **Green Horizon (Top Chiltan Limestone)**

Green Horizon was identified on the basis of character as Chiltan Limestone. Chak 7-A well ended in Basal sands, so Chiltan couldn't be marked on its basis. Figure 20 to 31 shows the marked seismic sections.

6.3.2.2 Identifying the Faults

Fault direction in the project area is NW-SE (Figure 35). Identification of faults is very important considering that they provide traps for hydrocarbons. The faults are typically identified on the basis of break in the continuity of the reflectors. The prominent faults are obvious on the seismic record. As the project area lies in an extensional regime, Horst & Graben structures can be seen on seismic lines. On the available seismic sections, fault identification was not difficult as data quality was good. Marked faults were correlated from section to section and hence their lateral extent was determined in the project area. Heave and throw of fault is defined below (Figure 16). Heave and throw is also shown on actual data (Figure 17).

Dip separation- offset distance measured parallel to dip of the fault

Heave- horizontal component of dip separation

Throw- vertical component of dip separation

Figure 20 to Figure 31 show the marked seismic sections with faults.

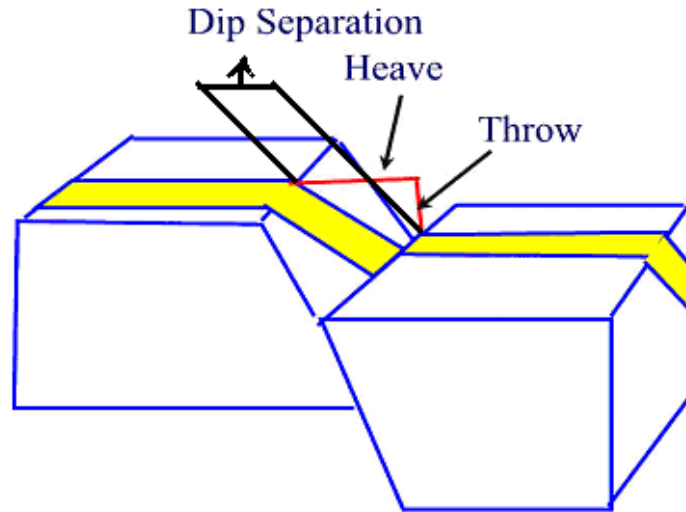


Figure 16: Throw, heave and dip separation

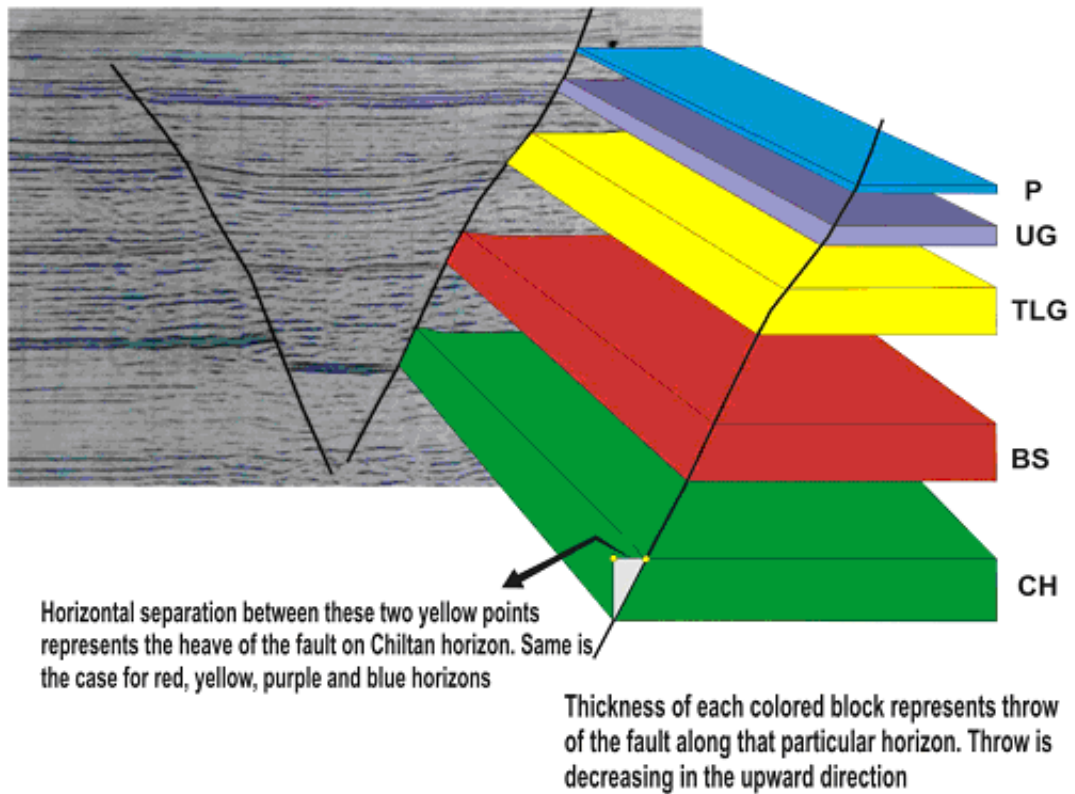


Figure 17: Throw and heave on actual data Portion of LINE: 886-SGR-350
(P – Parh, UG – Upper Goru, TLG – Top Lower Goru, BS – Basal Sands,
CH – Chiltan)

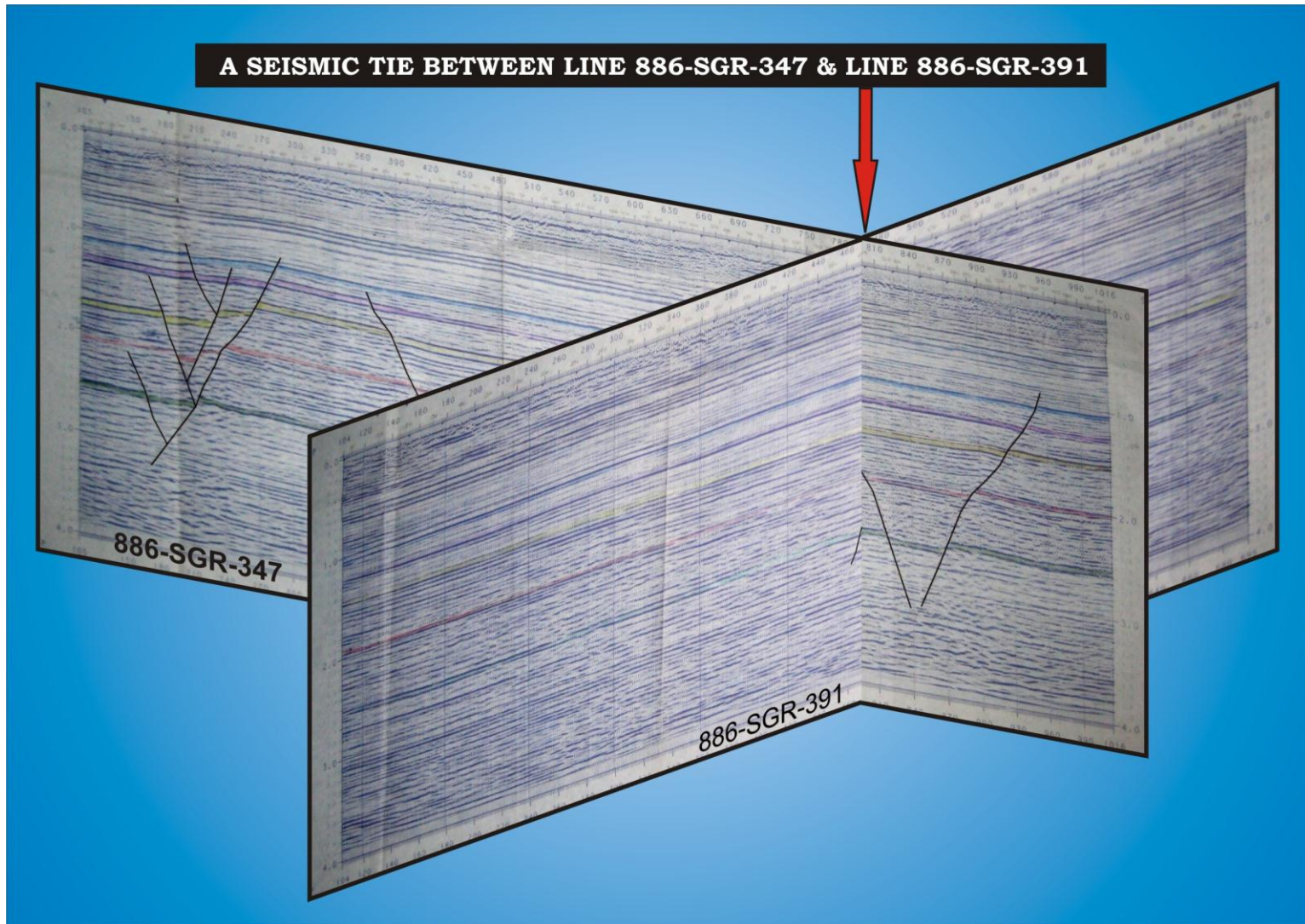


Figure 18: Five horizons were tied from line 886-SGR-347 to line 886-SGR-391

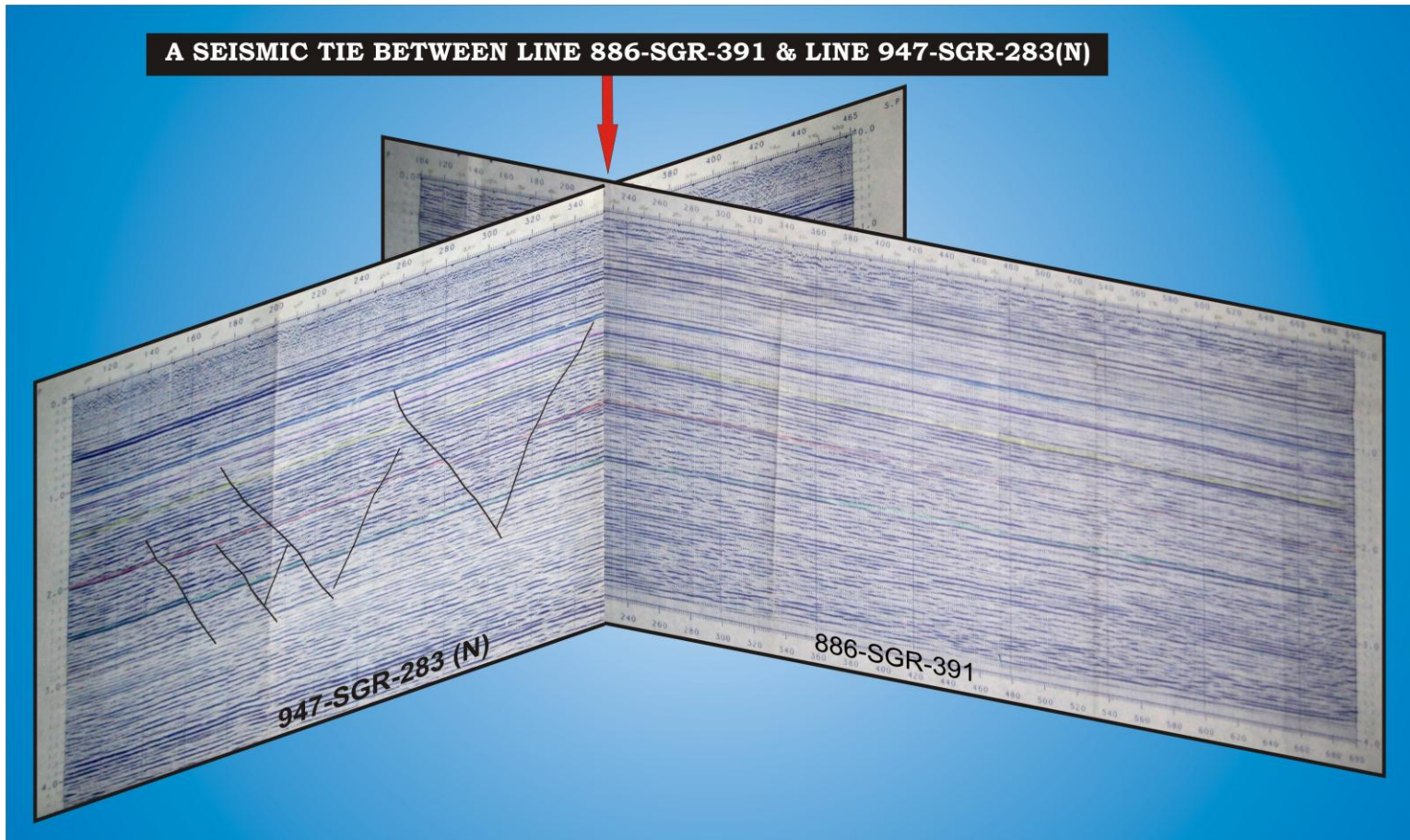


Figure 19: Five horizons were tied from line 886-SGR-391 to line 947-SGR-283 (N)

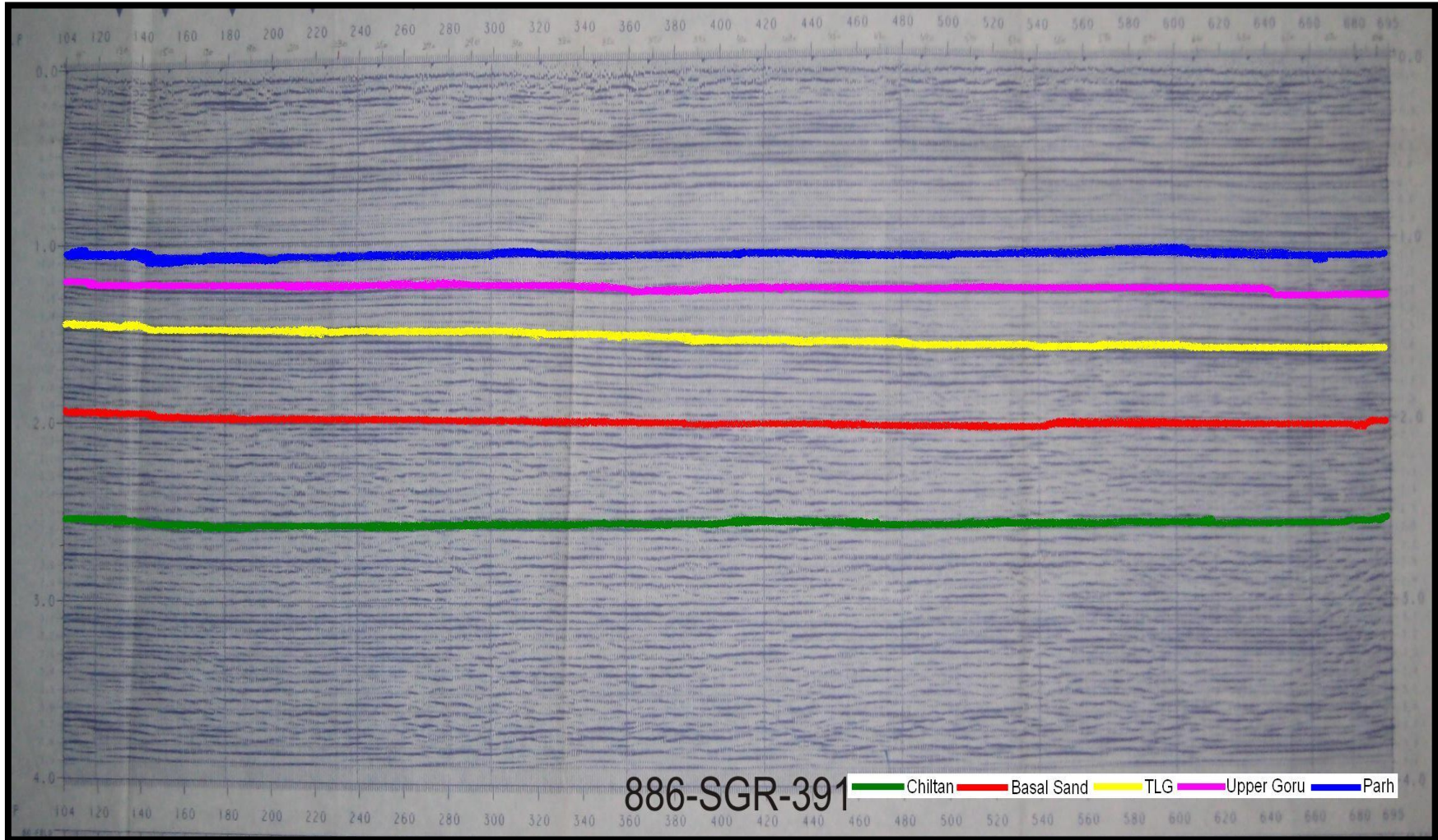


Figure 20: Interpreted seismic strike line 886-SGR-391 (strike line)

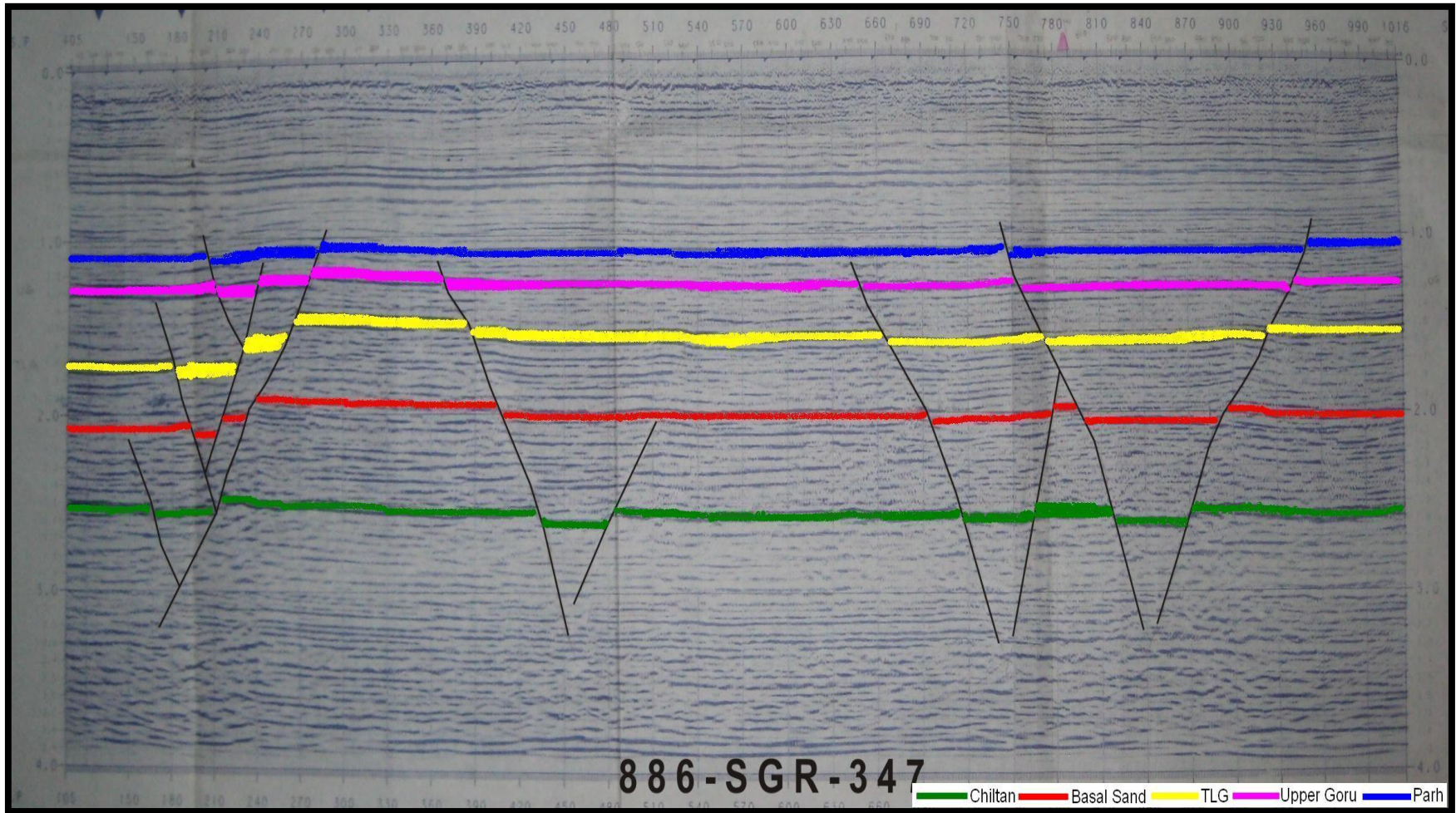


Figure 21: Interpreted seismic dip line 886-SGR-347 (dip line)

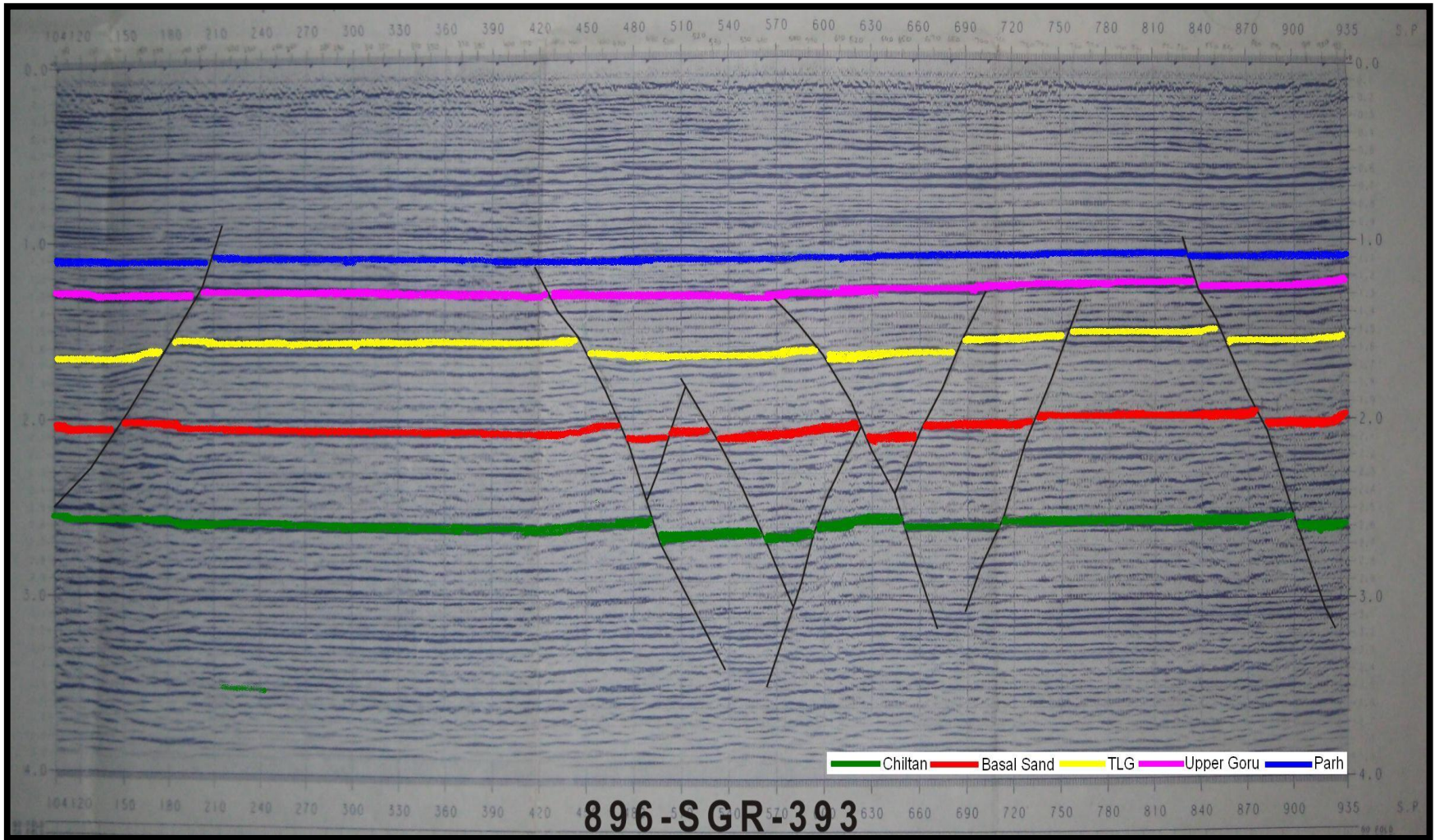


Figure 22: Interpreted seismic dip line 896-SGR-393 (dip line)

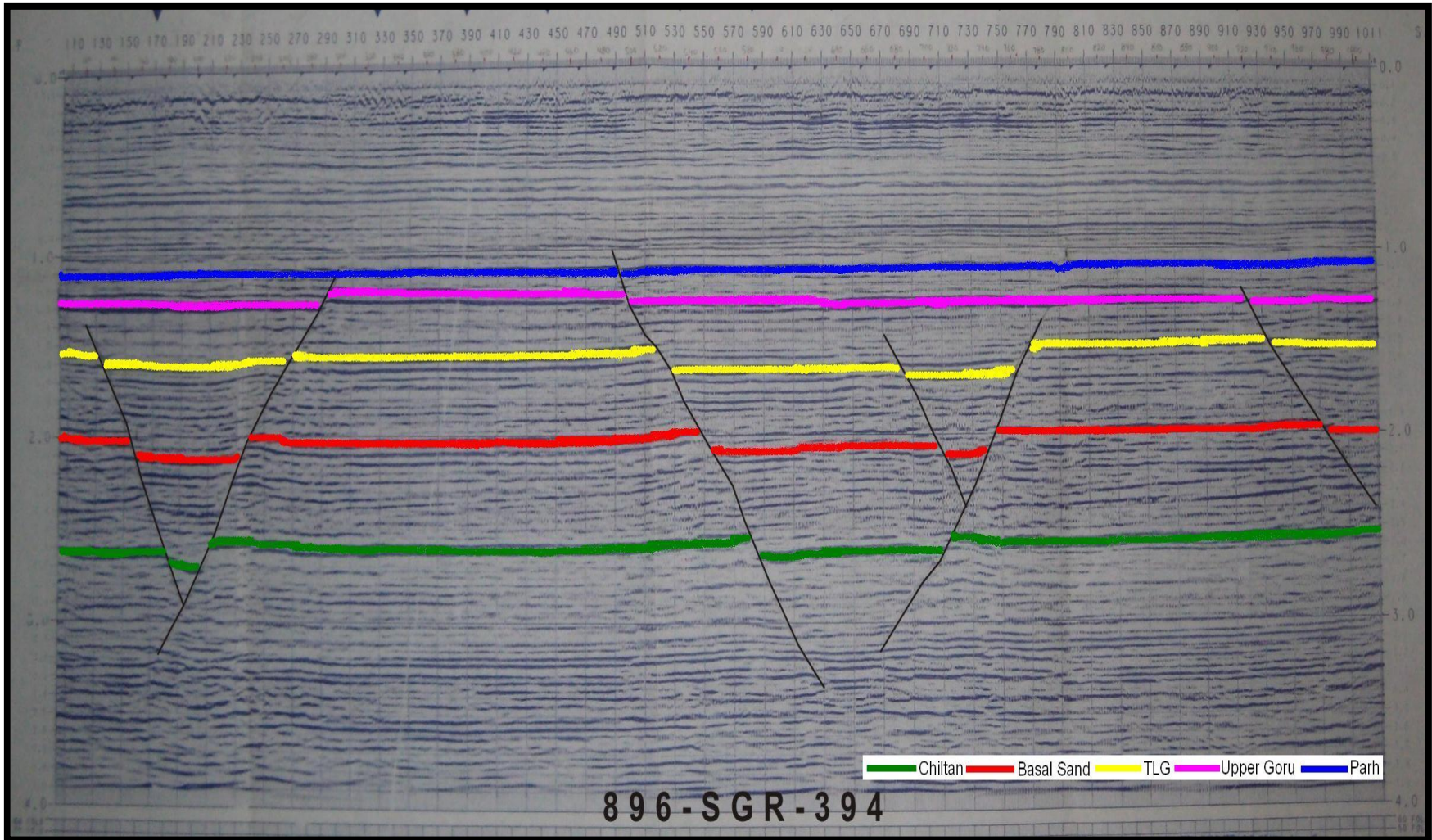


Figure 23: Interpreted seismic dip line 896-SGR-394 (dip line)

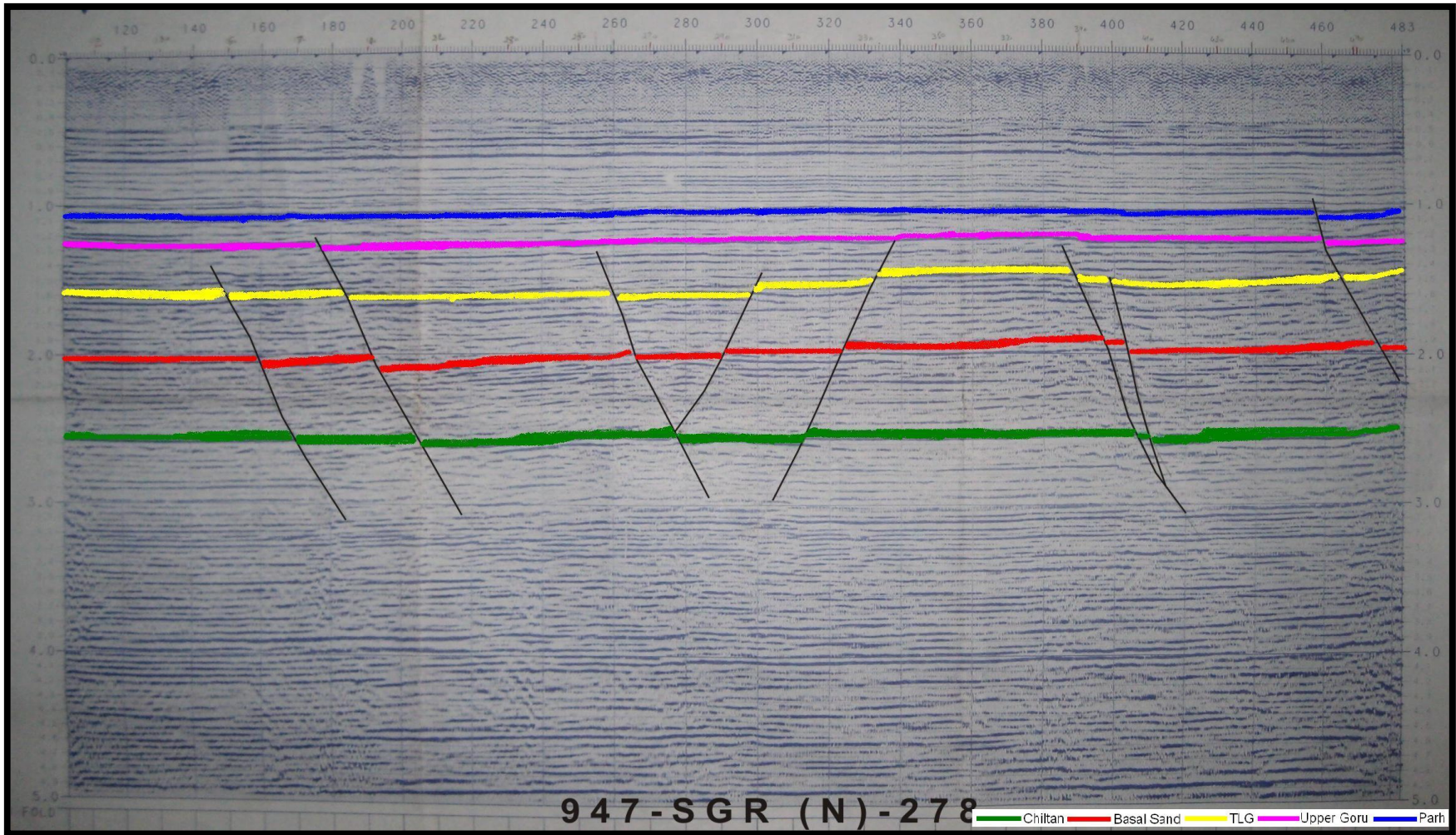


Figure 24: interpreted seismic dip line 947-SGR (N) -278 (dip line)

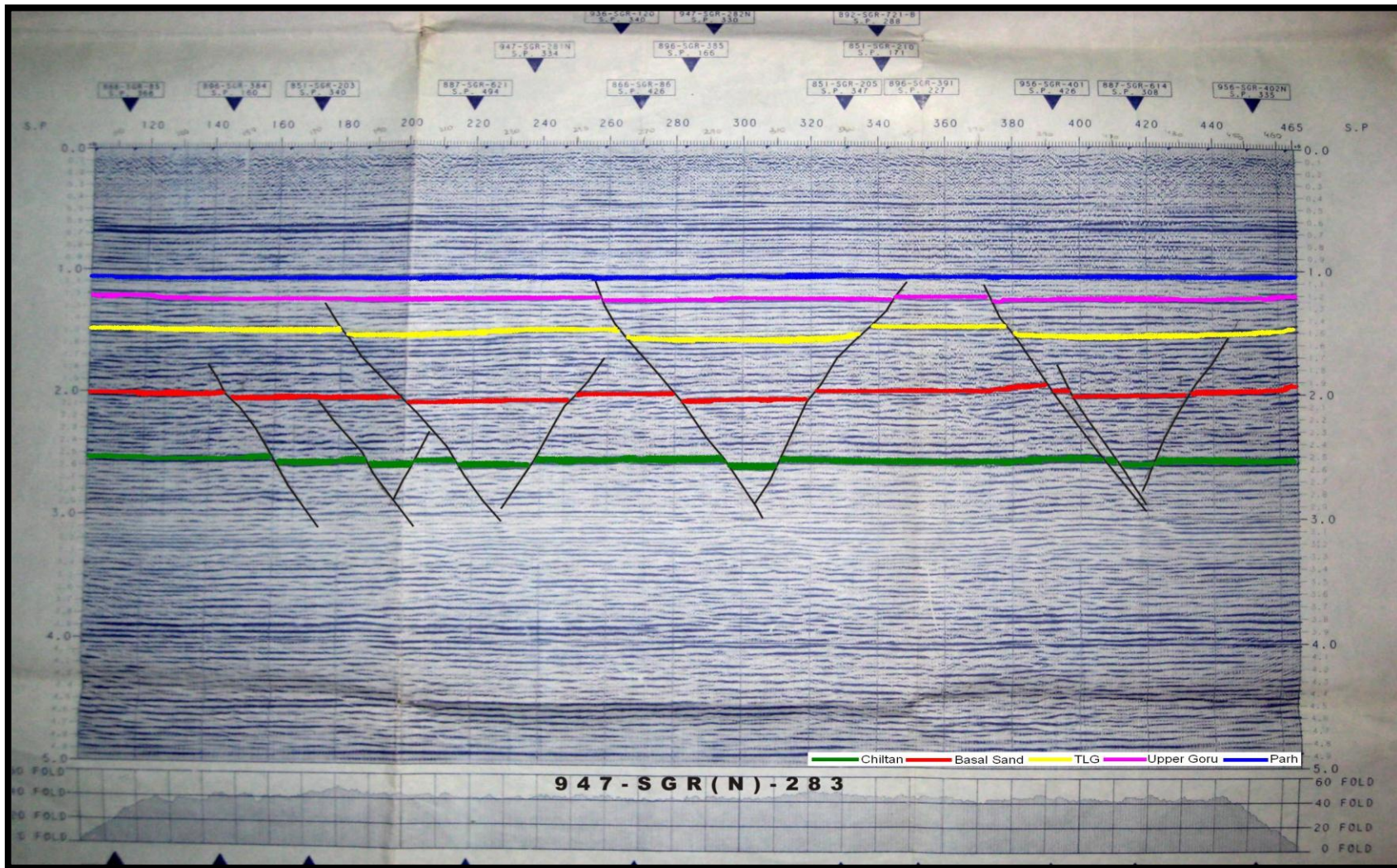


Figure 25: Interpreted seismic dip line 947 - SGR (N) – 283 (dip line)

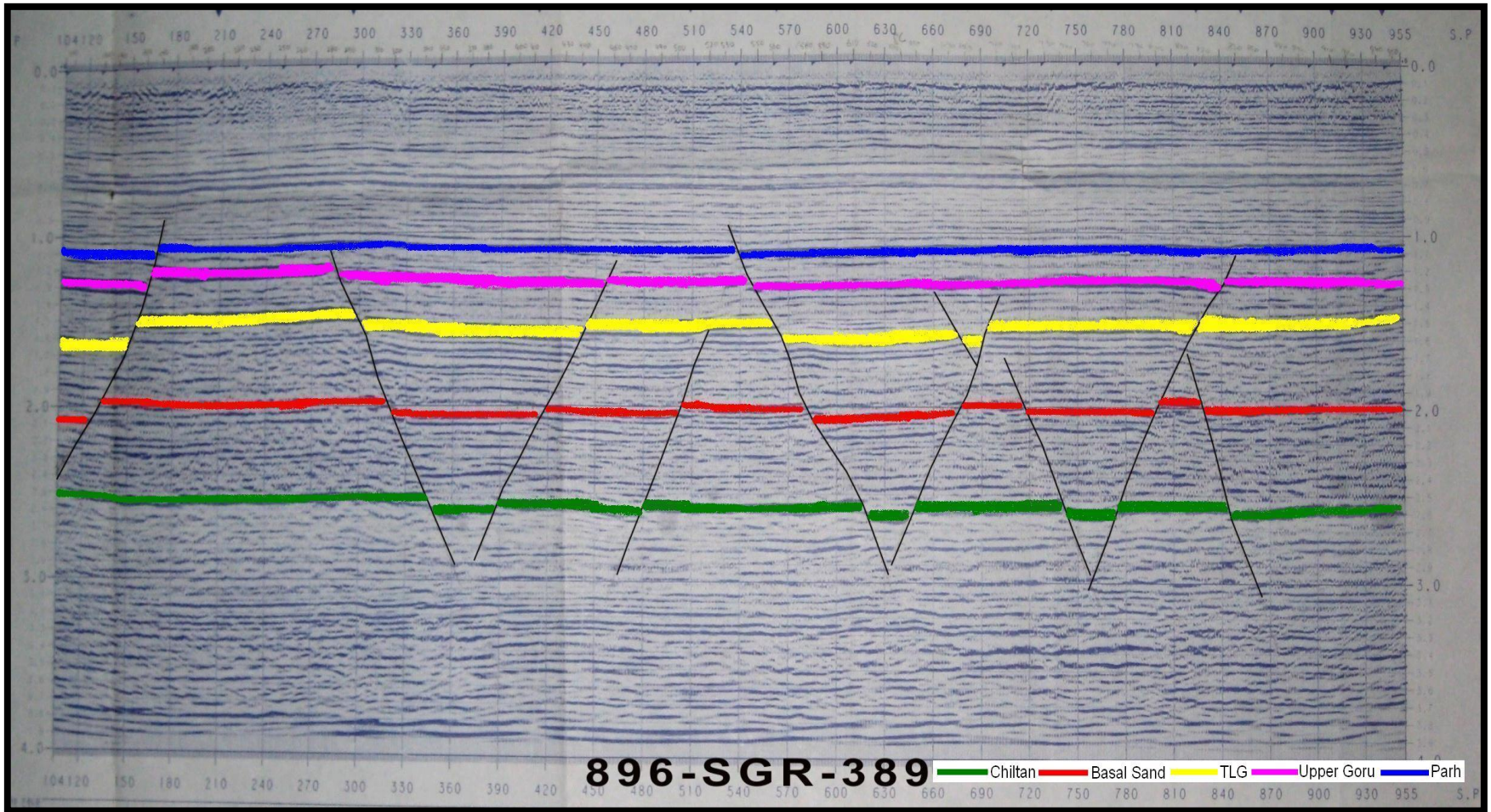


Figure 26: Interpreted seismic dip line 896-SGR-389 (dip line)

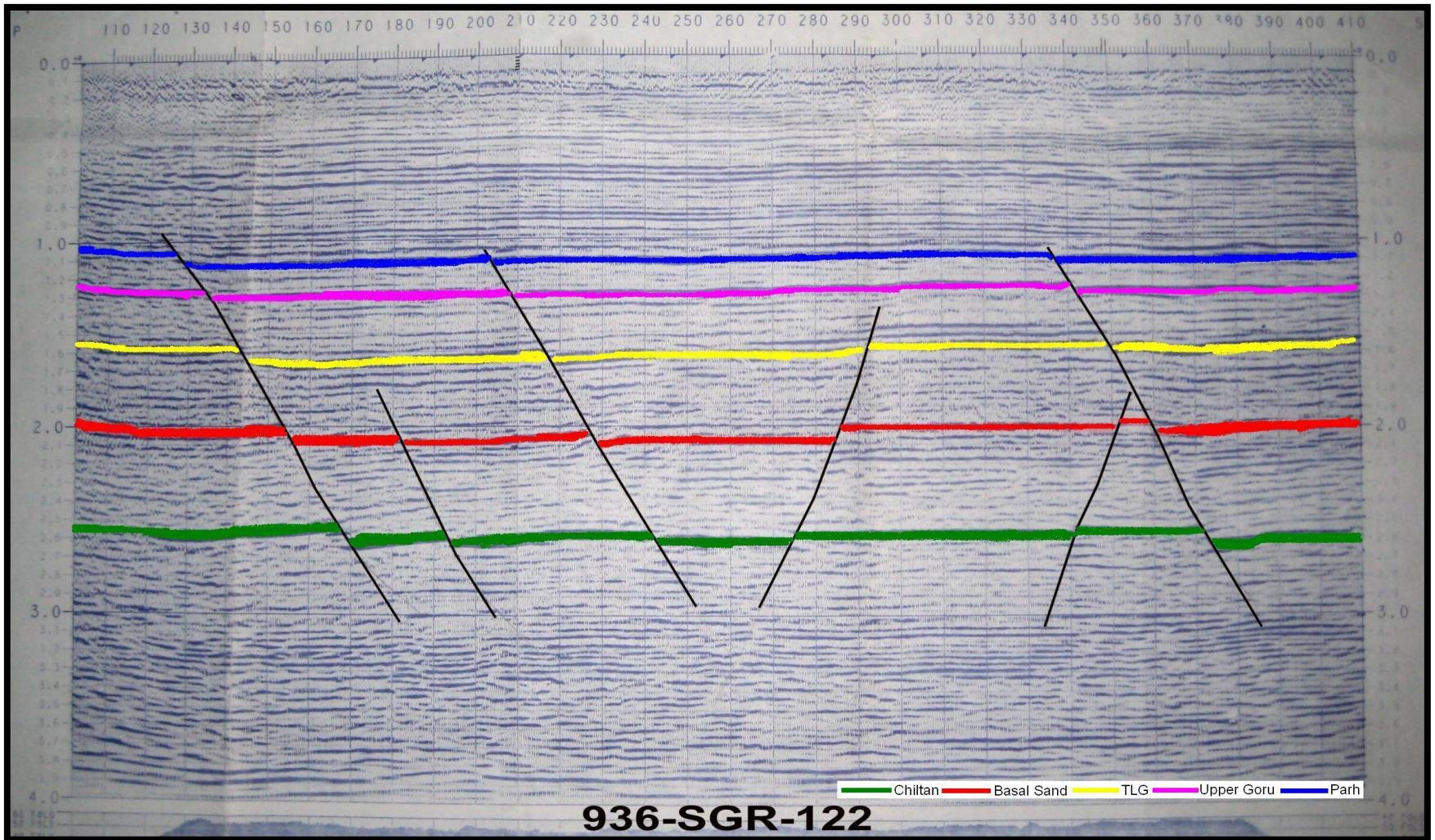


Figure 27: Interpreted seismic dip line 936-SGR-122 (dip line)

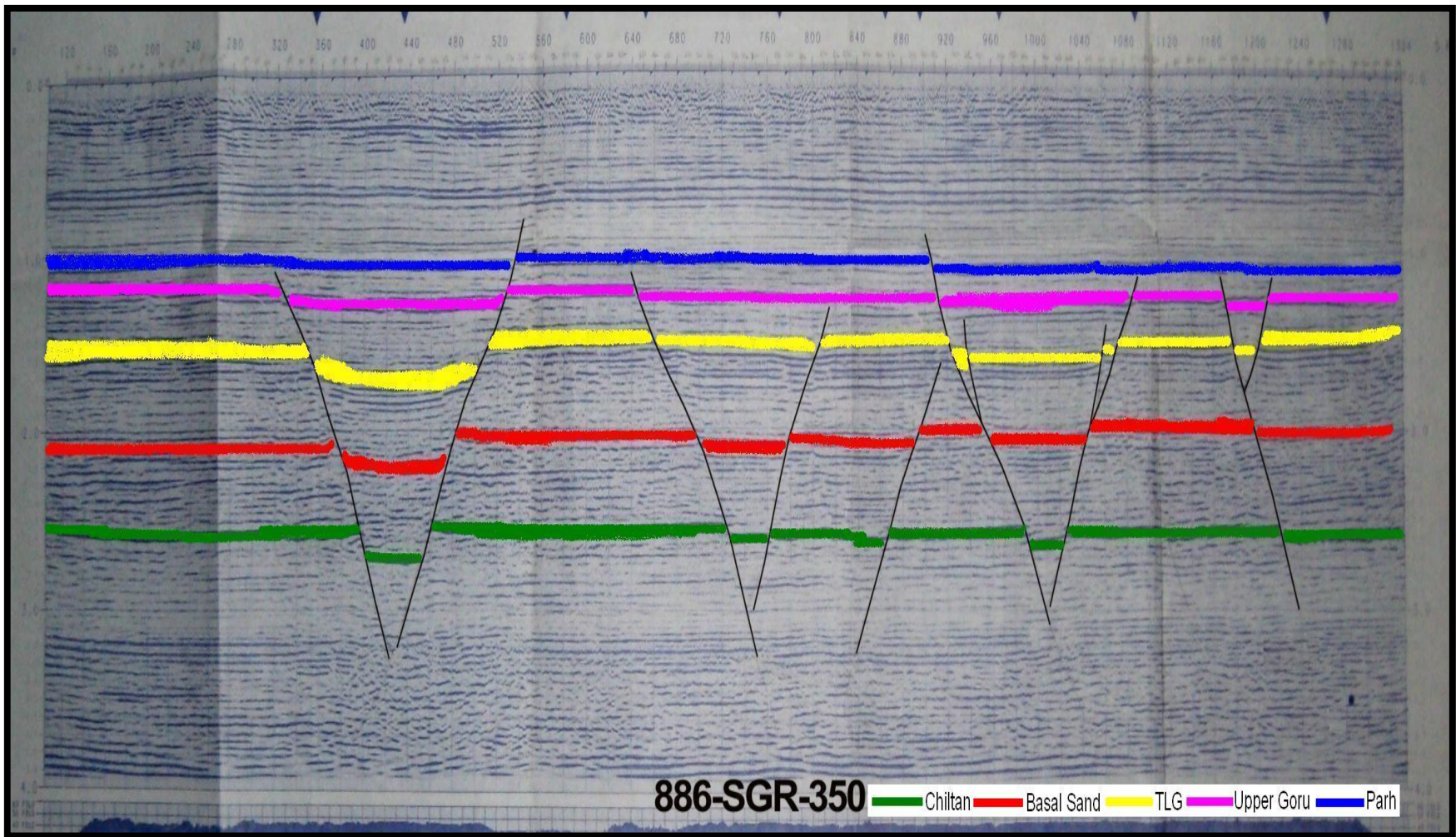


Figure 28: Interpreted Seismic dip line 886-SGR-350 (dip line)

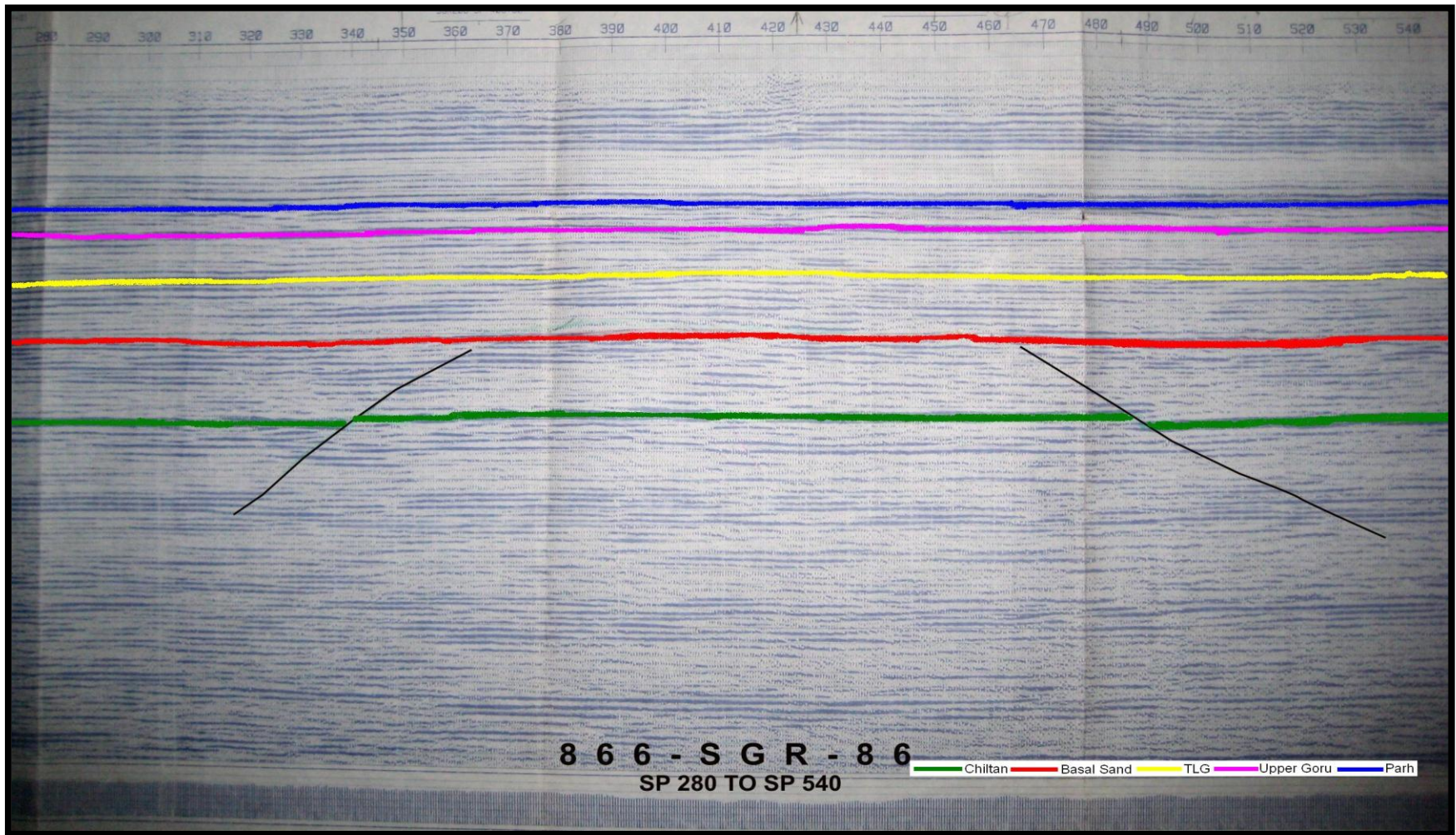


Figure 29: Interpreted seismic strike line 866-SGR-86 (strike line)

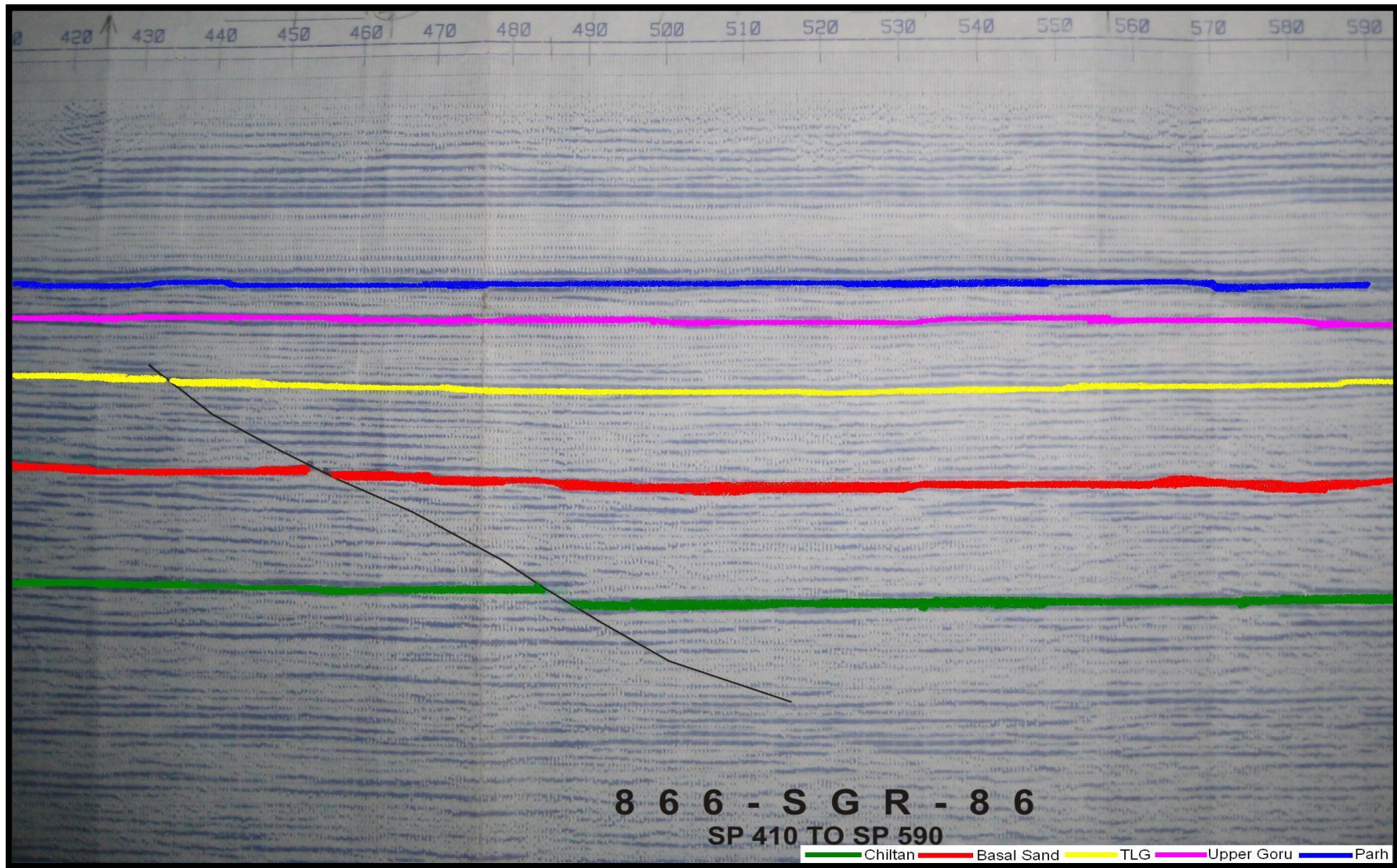


Figure 30: Interpreted seismic strike line 866-SGR-86 (strike line)

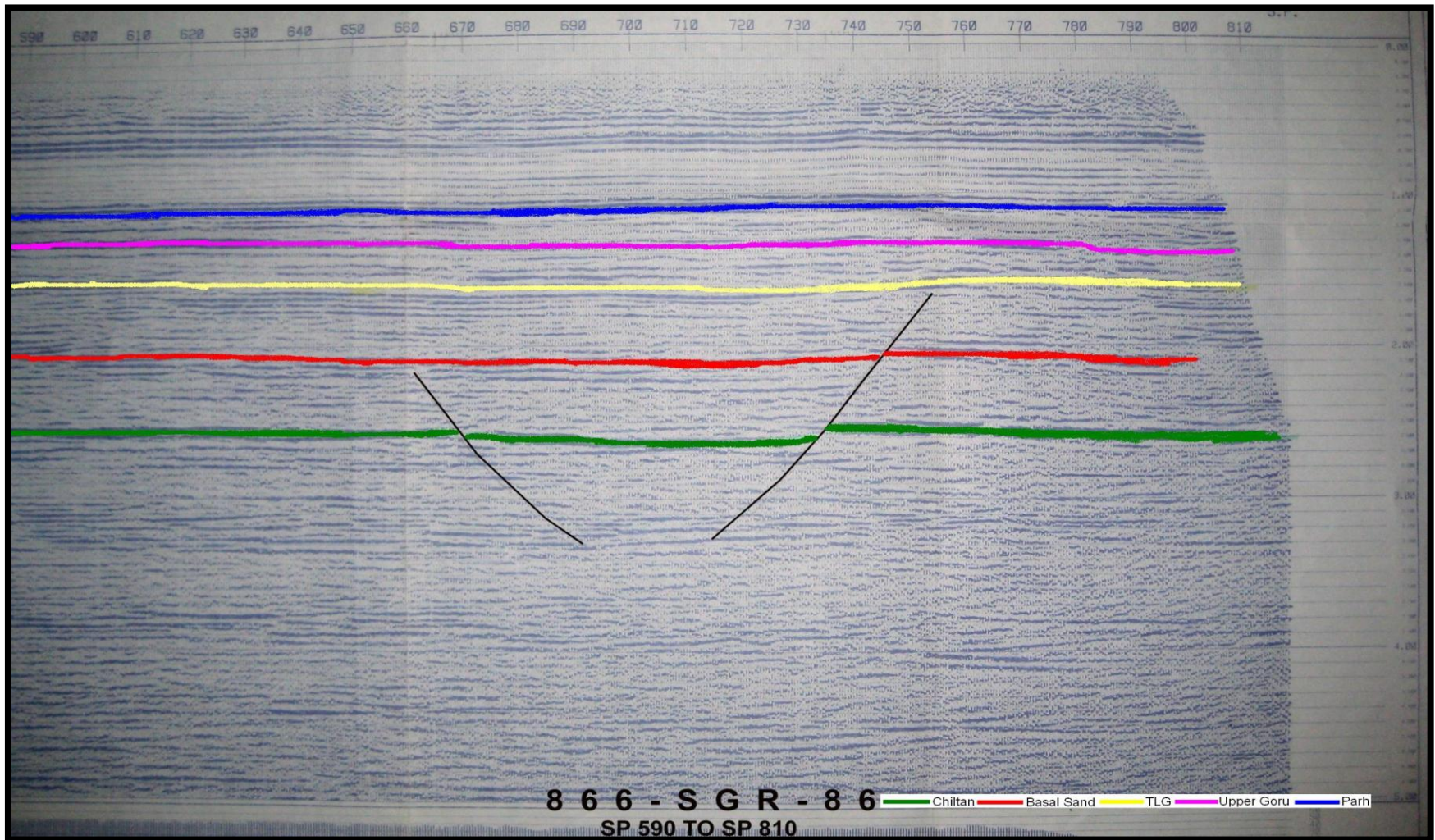


Figure 31: Interpreted seismic strike line 866-SGR-86 (strike line)

With the help of marked horizons and faults, and study of well data, a representative section showing the Petroleum system in the area is displayed as under (Figure 32):

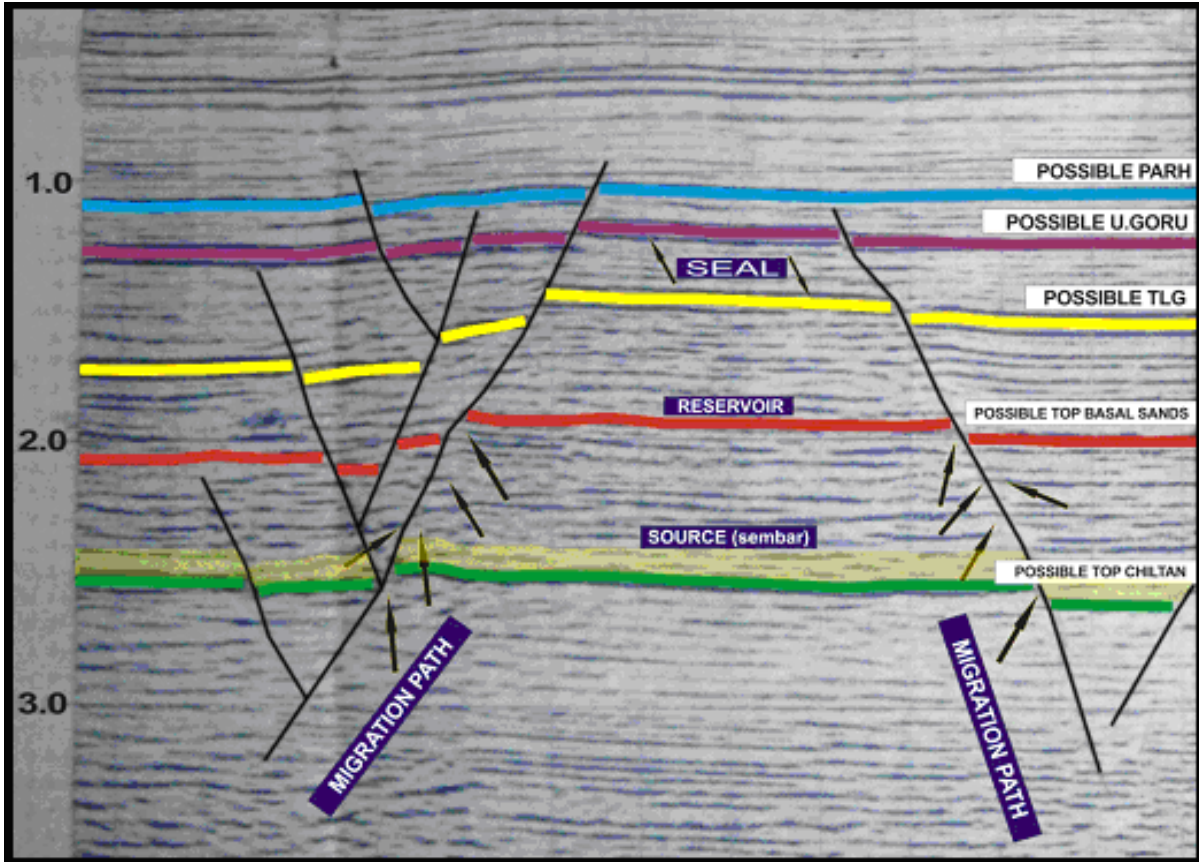


Figure 32: Expected Petroleum system in the study area

6.3.2.3 Reading the Reflector Time:

After marking the five horizons on ten seismic sections, time was read. The marked horizons fell in a time range about of 1 to 2.7 sec (Figure 20 to 31). These time values were saved in MS Excel format (see the attached tables). Time against the fault blocks was read carefully in order to have a reasonable time values for heave and throw of the faults. If there are errors in time reading, they are further represented in the contour maps and hence a somewhat true picture of the sub surface cannot be obtained. Pseudo structures can appear to be present; likewise, real features of interest can be missed.

6.3.2.3.1 Time Sections

Four time sections were generated using *MS Excel* and then edited in *Corel Draw 12*. The reason was to check the accuracy of time-reading. Generated time sections were in perfect match with the actual seismic sections (Figure 33 to 36). They show the structure of the area in a very cut down manner. These time sections show clearly the character of the marked reflectors, and also the faults which are cutting across them.

Following abbreviations were used for marked horizons:

- **Parh Limestone (P)**
- **Upper Goru (UG)**
- **Top Lower Goru (TLG)**
- **Basal Sands (BS)**
- **Chiltan (CH)**

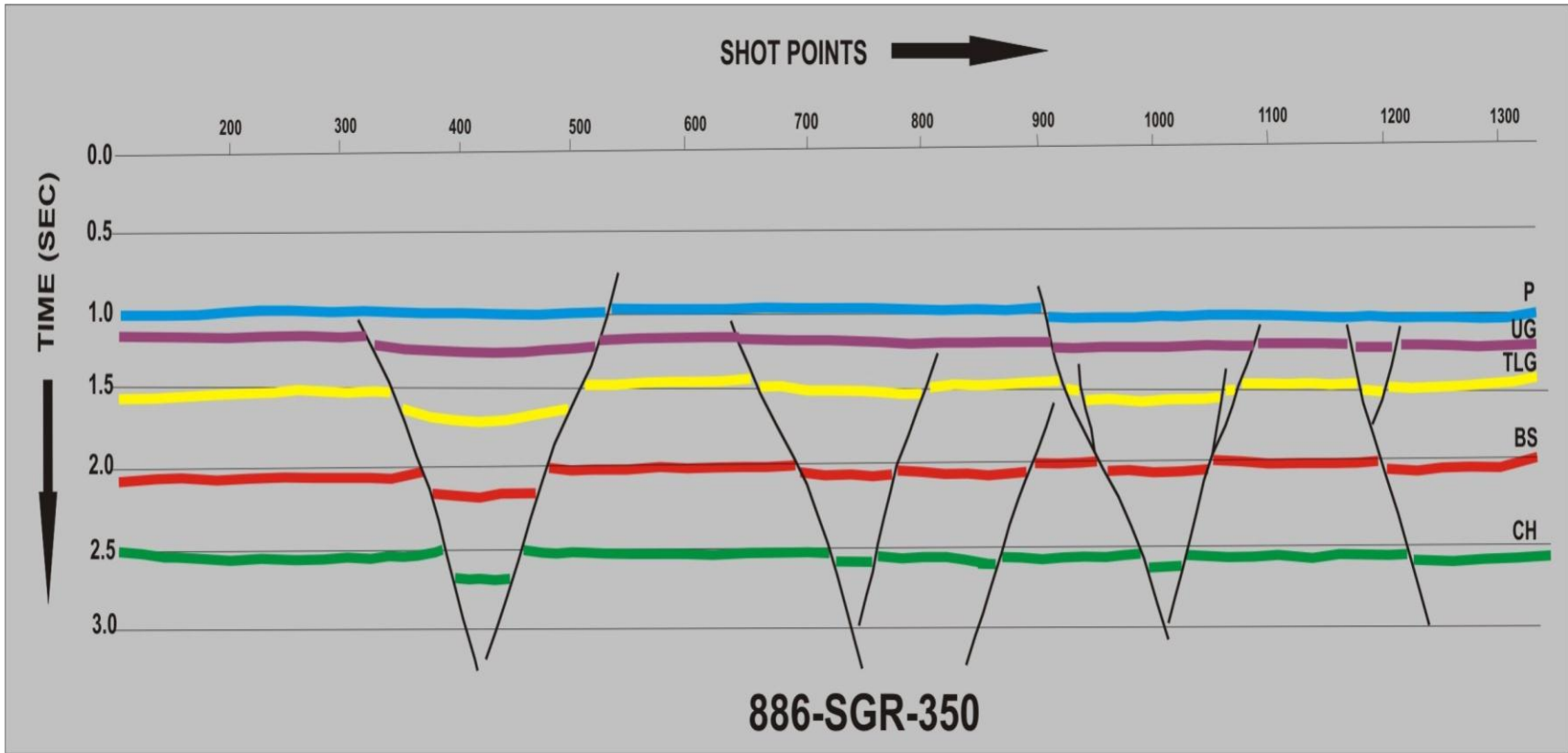


Figure 33: Time section of line 886-SGR-350

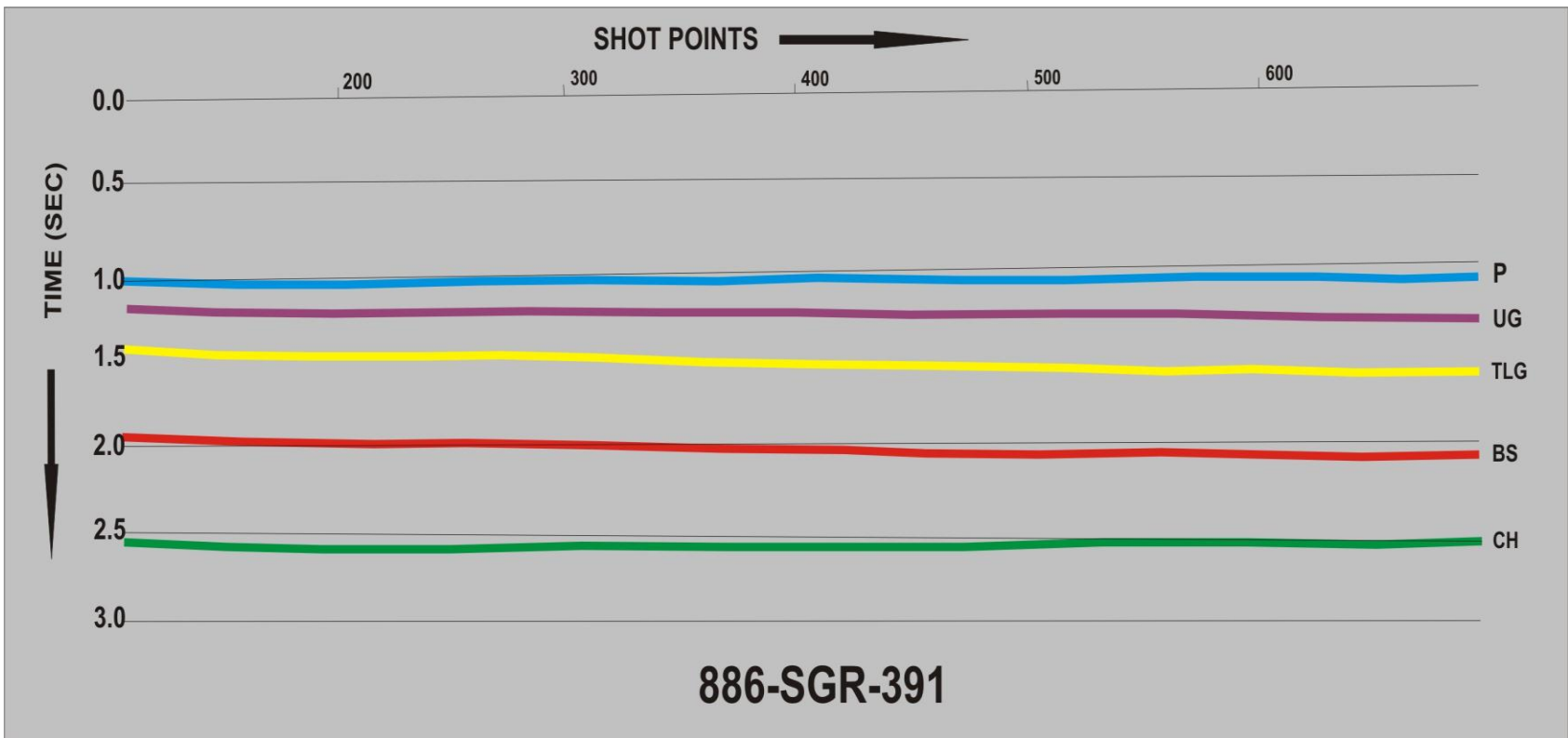


Figure 34: Time section of line 886-SGR-391

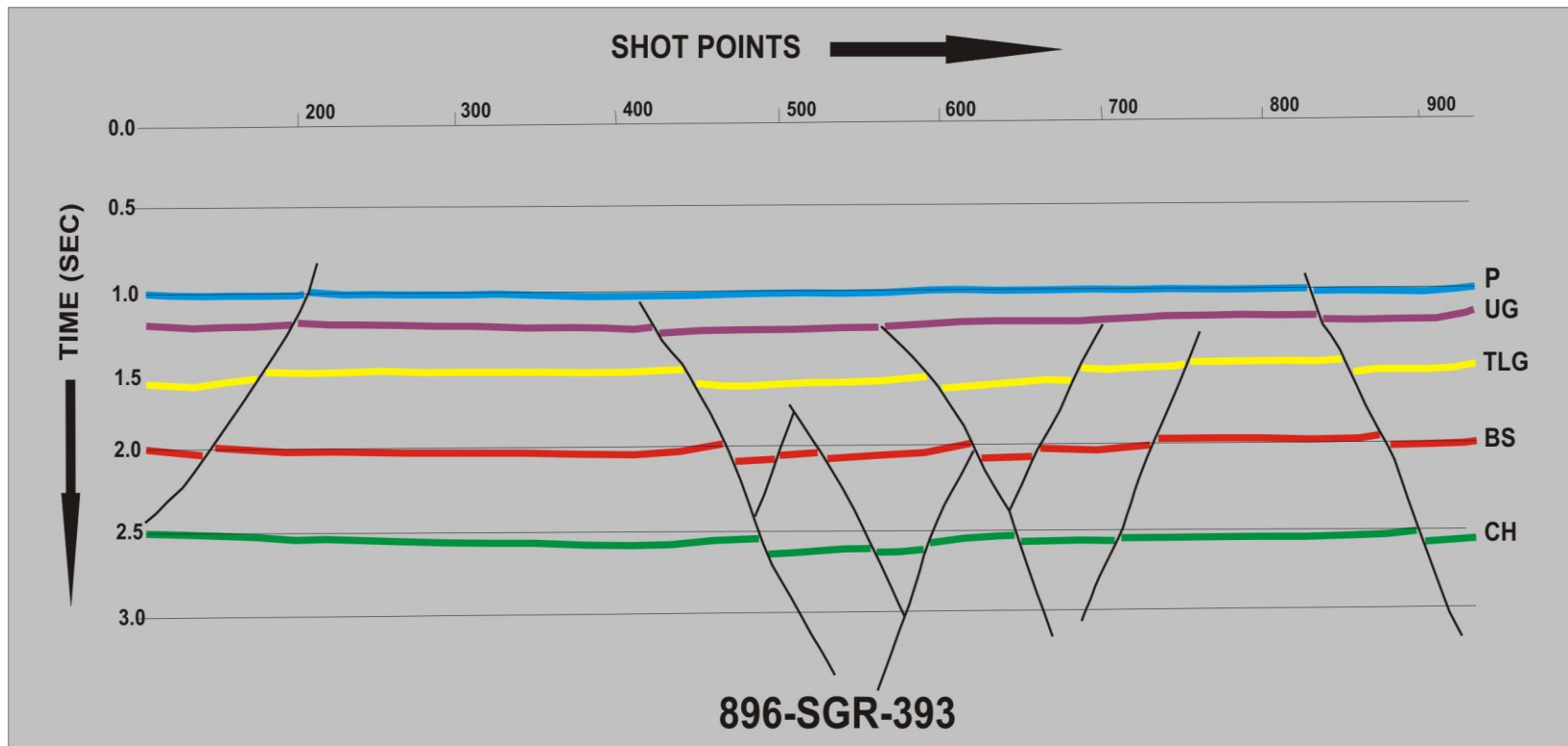


Figure 35: Time section of line 896-SGR-393

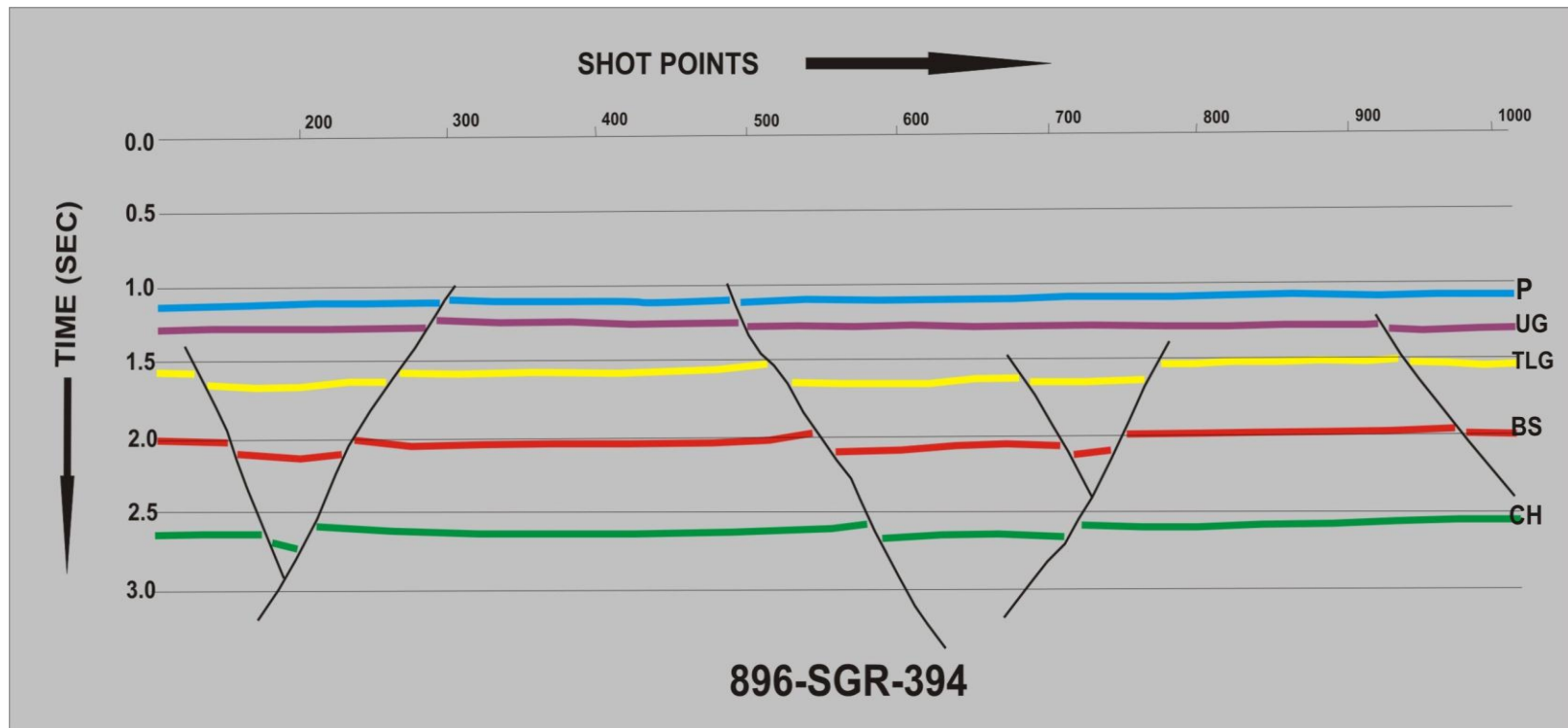


Figure 36: Time section of line 896-SGR-394

6.3.2.4 TWT Contour Maps:

Contour map is that map which is made up of contour lines, and the contour lines are that lines which join points of equal values. So in TWT contour maps, the map is made up of the values of time. This value of time is the time taken by the seismic waves to go into the subsurface, hit an interface, and come back to the surface. The TWT map is made for any formation of interest, so this map shows the position of that formation in time. The highs on the map show the areas which are at shallow level, and they have low values. The lows or depressions show the areas which are at a deeper level, and they have high values.

In this dissertation, the TWT Contour maps of two formations are made, namely, Top Lower Goru (TLG) and Basal Sands. The maps also show the seismic lines and the faults which are present in the area. The faults have their own importance; they make the areas of interest more prominent. For example, when looking for an appropriate position to drill for a well, the closure provided by the faults is given prime importance.

In order to make time contour maps in any mapping software, one needs X Y and Z values. Z values here are the time values. Time contour maps were generated in *Surfer 8.0*, *FieldPro* and then edited in *Corel Draw 12*, where needed.

Faults were first put manually on basemap and then using the software to have a check on their accuracy. Same procedure was adopted for the basal sands' reflector.

To recognize faults as the breaks in the data for the software, fault files were created. While reading time of horizons, time against the same fault blocks was read; same faults were recognized on different seismic sections and hence different fault planes were identified and put on the basemap (Figure 37).

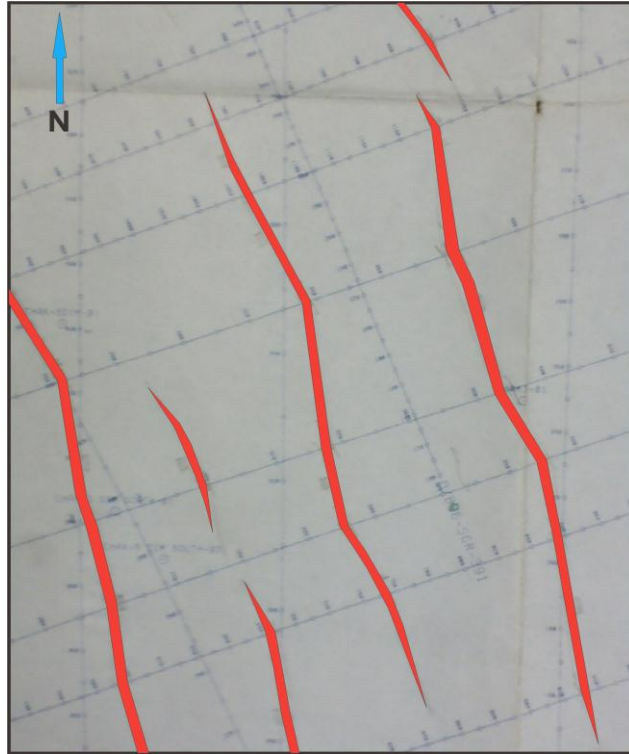


Figure 37: A portion of basemap of project area showing faults on TLG level

6.3.2.4.1 TWT Contour Map on TLG (Top Lower Goru):

Every mapping software creates a data grid prior to contouring. Gridding for TLG was done in *Surfer 8.0*. Different gridding techniques were available. For the given data, “Nearest neighbor” was used because it handled the faults very well. The purpose of grid is to distribute the data through extrapolation or interpolation. While contouring, extrapolation often creates the pseudo contours at the edges of a contour map. To overcome this problem a cut polygon was created to limit the contours inside the project area. Contouring was done in *FieldPro* as it accepts the grid files generated in *Surfer 8.0* (Figure 38). Top Lower Goru (TLG) in the project area has mainly shale and marl with thin layers of sands. So, it can better act as a seal rather than a reservoir.

Contour interval = 10 ms & Fault direction = NW-SE

Minimum contour value = 1390 ms & Maximum contour value = 2000 ms

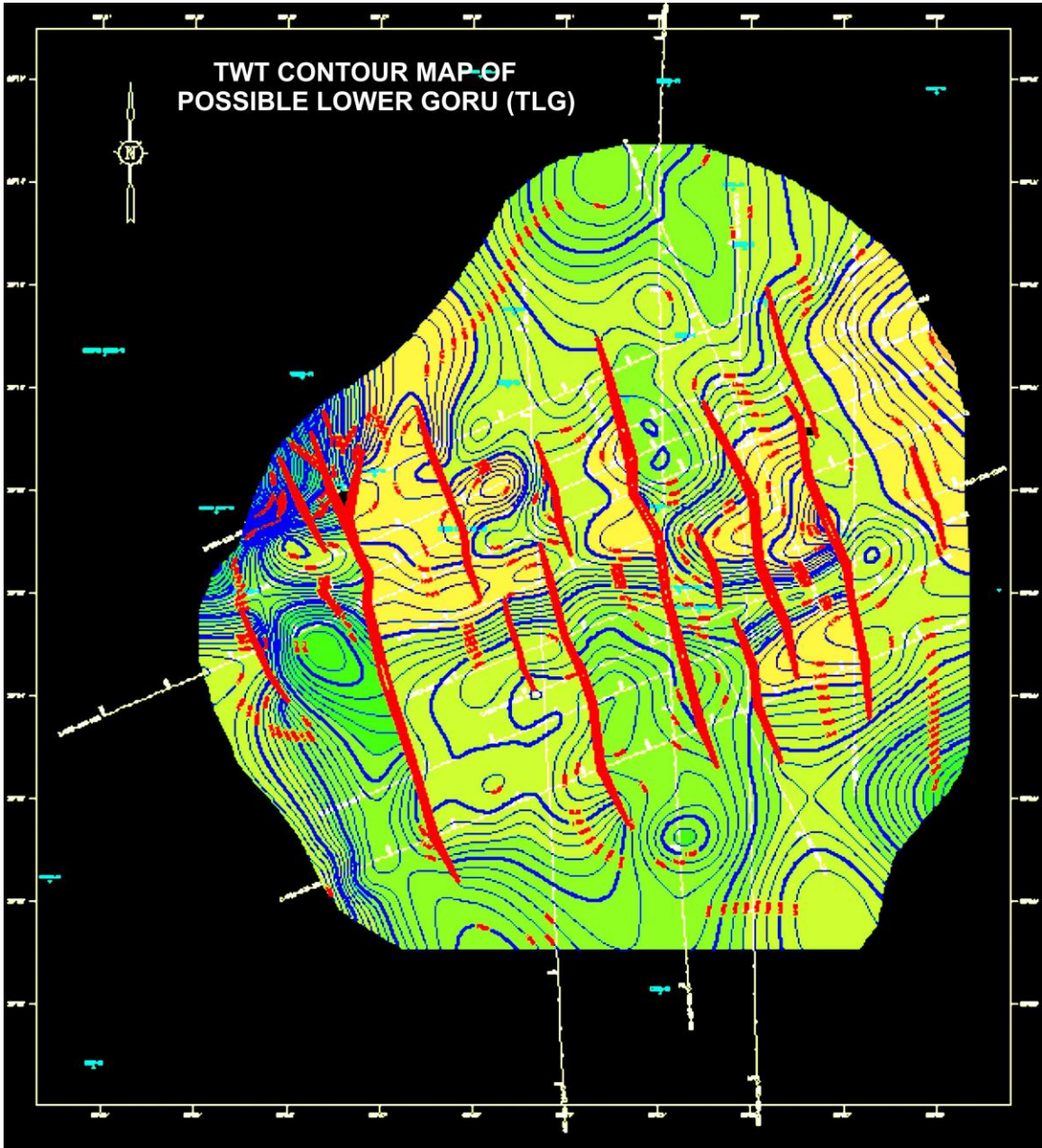


Figure 38: TWT contour map on TLG level

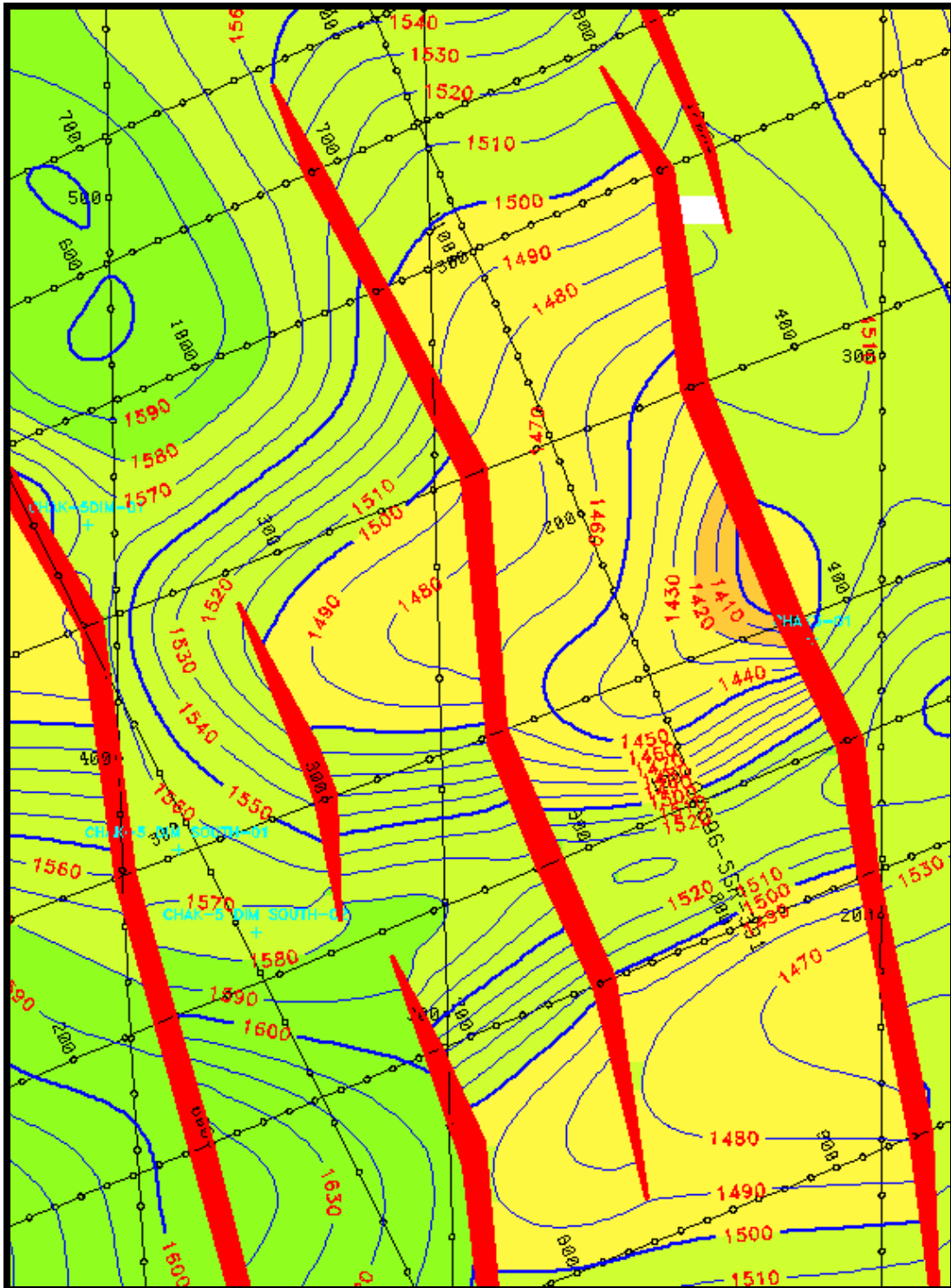


Figure 39: TWT contour map on TLG level (zoomed image)

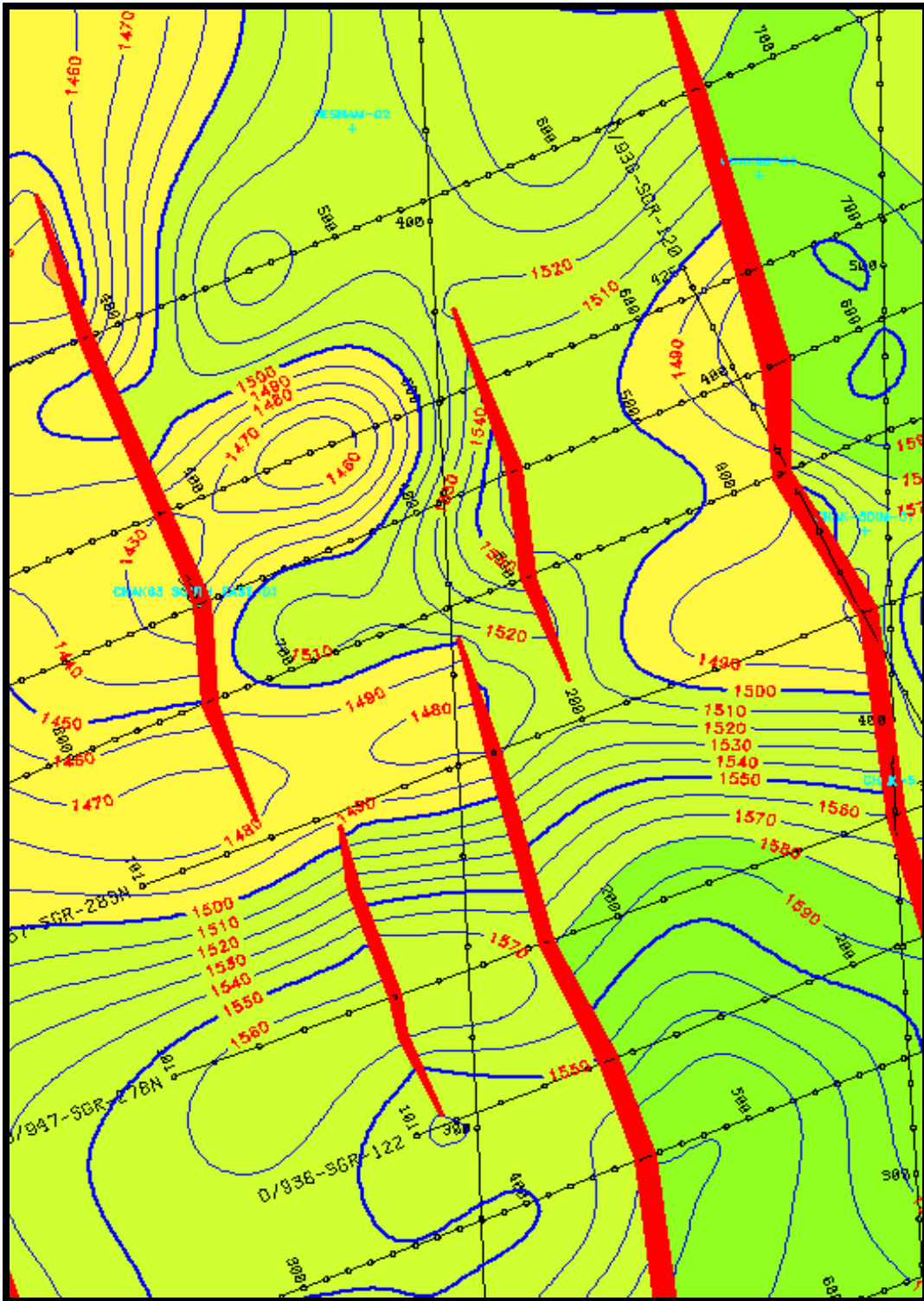


Figure 40: TWT contour map on TLG level (zoomed image)

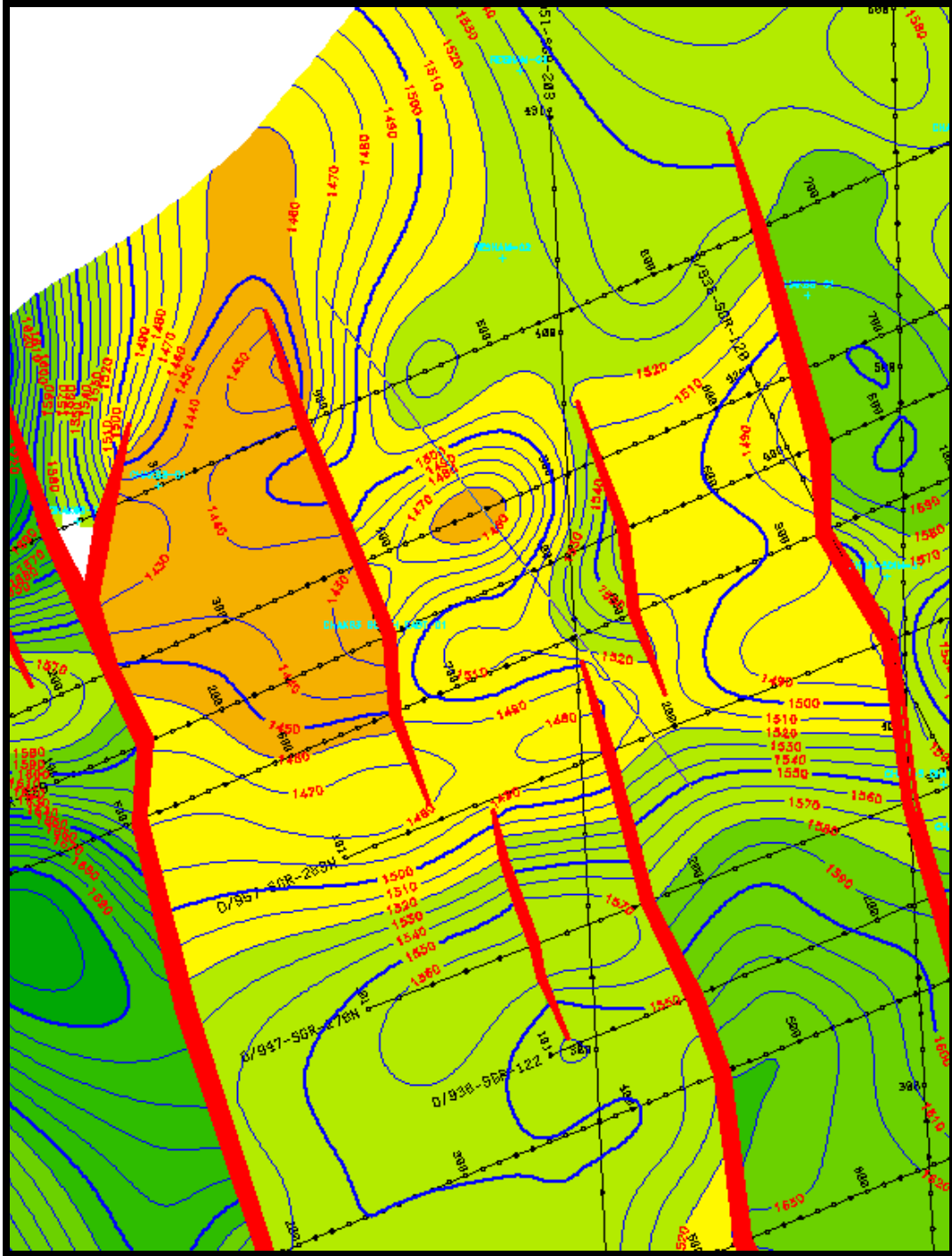


Figure 41: TWT contour map on TLG level (zoomed image)

(Figure 38) and zoomed portion of this image (Figures 39, 40 and 41) show various small closures but considering the lithology of TLG in project area, they don't have prime importance as far as reservoir potential is concerned.

6.3.2.4.2 Time Contour Map on Top Basal Sands:

Top basal sands are the main target horizon in Lower Indus basin. Massive sands are considered as secondary target. Considering the economics, even small closures of 1.5 sq.km can be of importance. Chak 7-A well was drilled on a small closure of 1.9 sq.km; it was a gas/condensate discovery. The well ended in Massive sands at a depth of 3050m.

A TWT contour map was created in *FieldPro*; gridding was done in *Surfer 8.0* (Figure 42, 43, 44 & 45).

Gridding method = Nearest neighbor

Minimum contour value = 1888 msec

Maximum contour value = 2200 msec

Fault direction = NW-SE

Structure type = Closure against faults (Horst Blocks)

A cut polygon was also used in mapping in order to avoid pseudo contouring at the edges of the map (Figure 42).

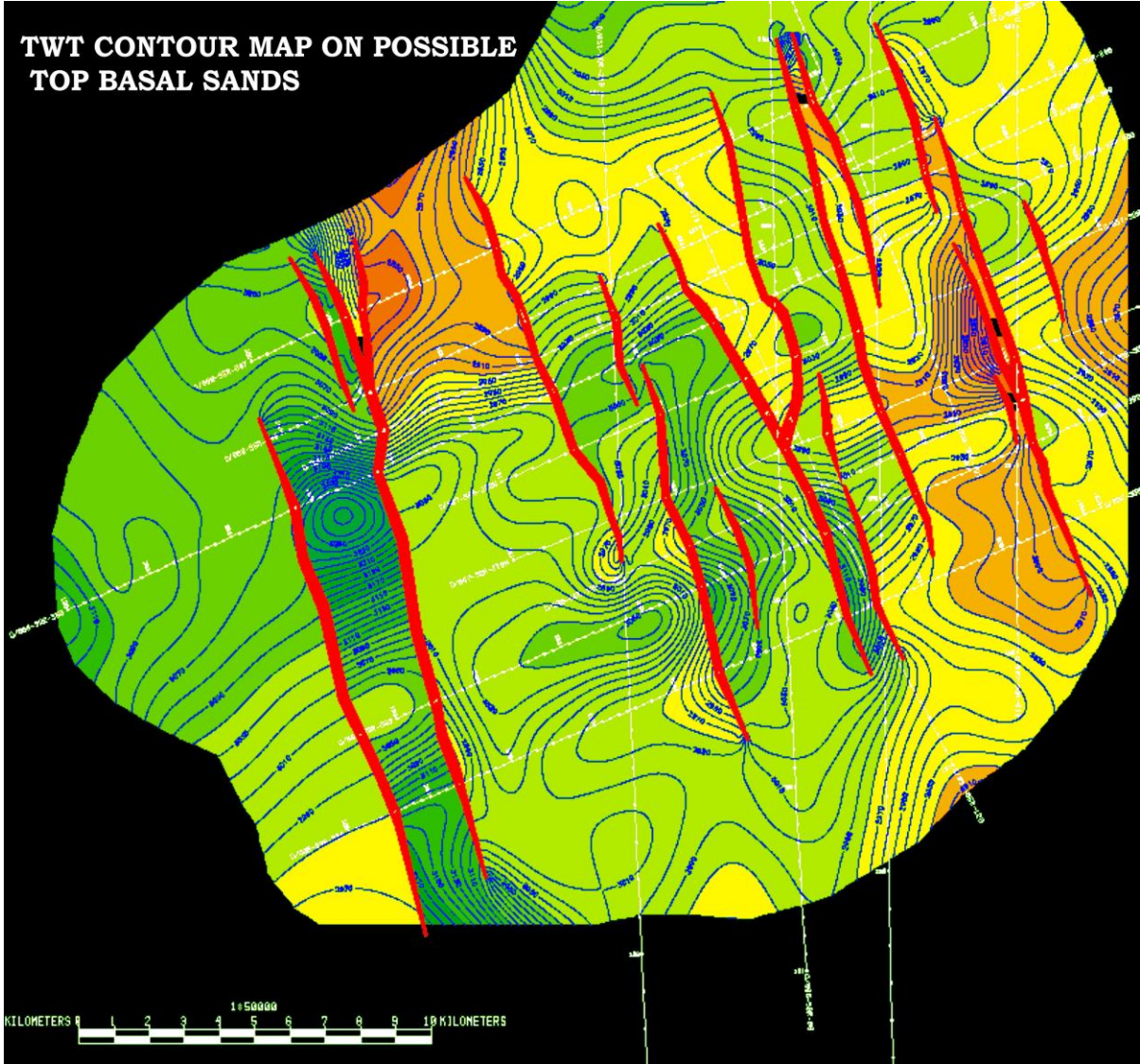


Figure 42: TWT contour map on Top Basal Sands

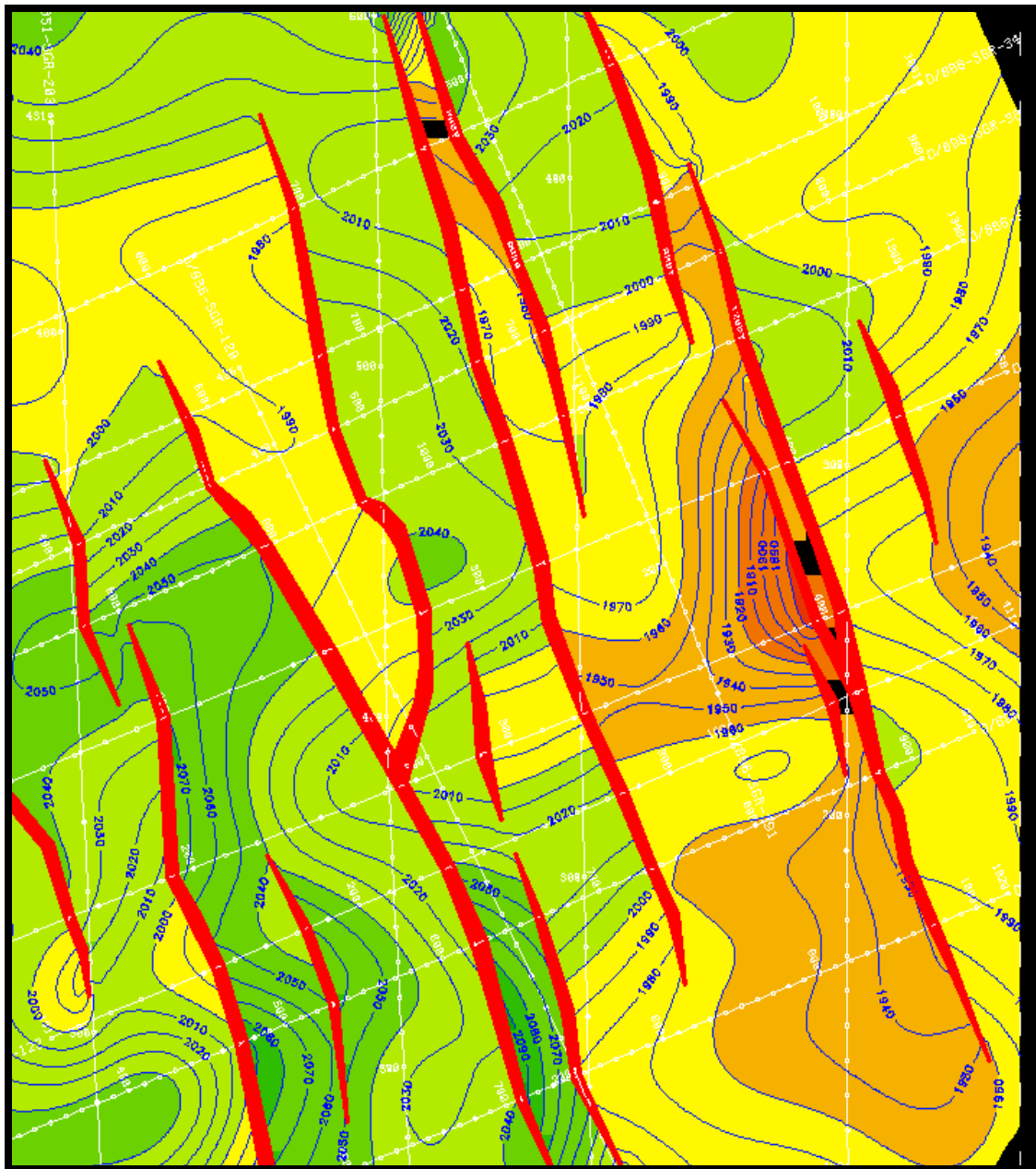


Figure 43: TWT contour map on Top Basal Sands (zoomed image)

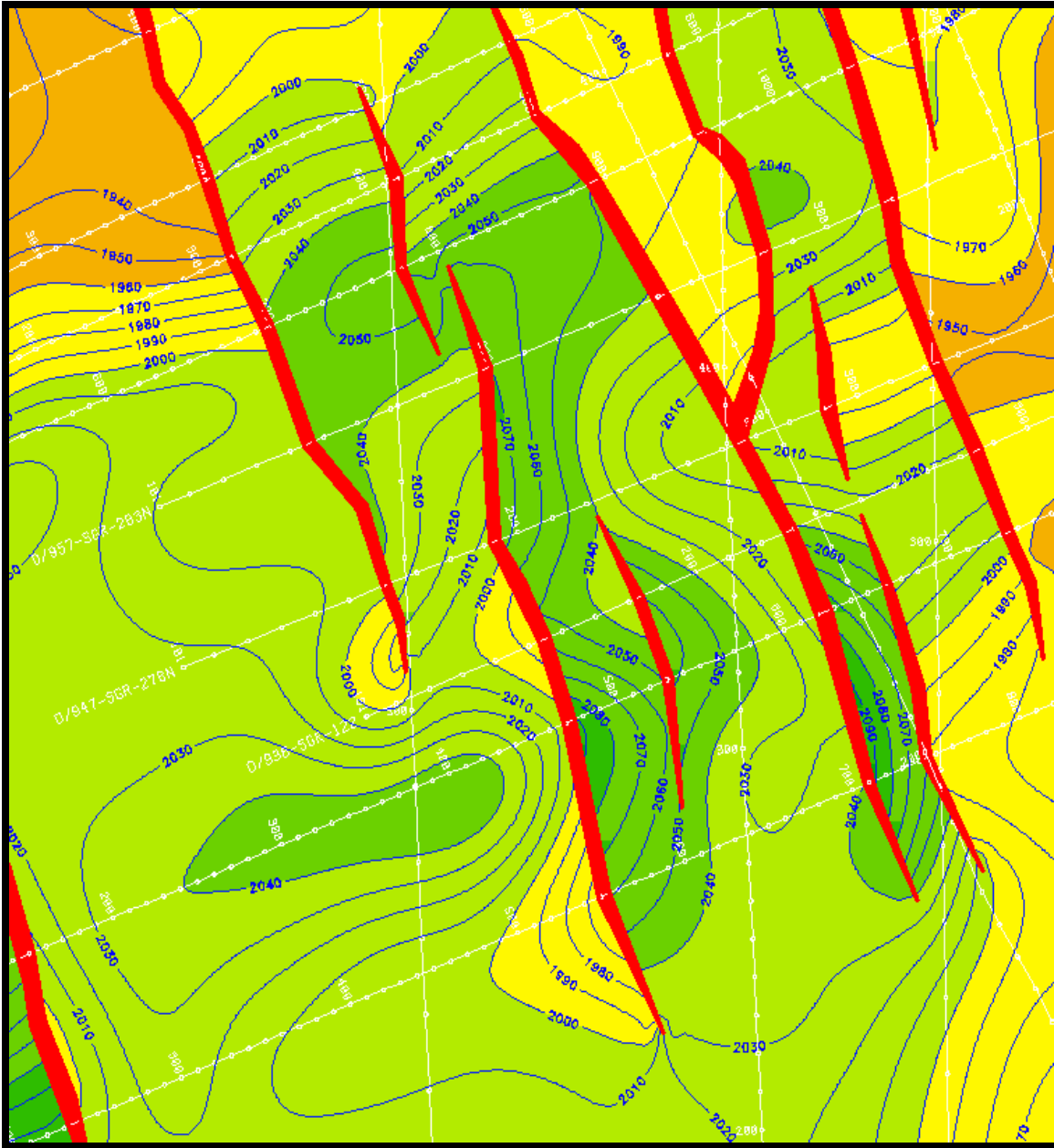


Figure 44: TWT contour map on Top Basal Sands (zoomed image)

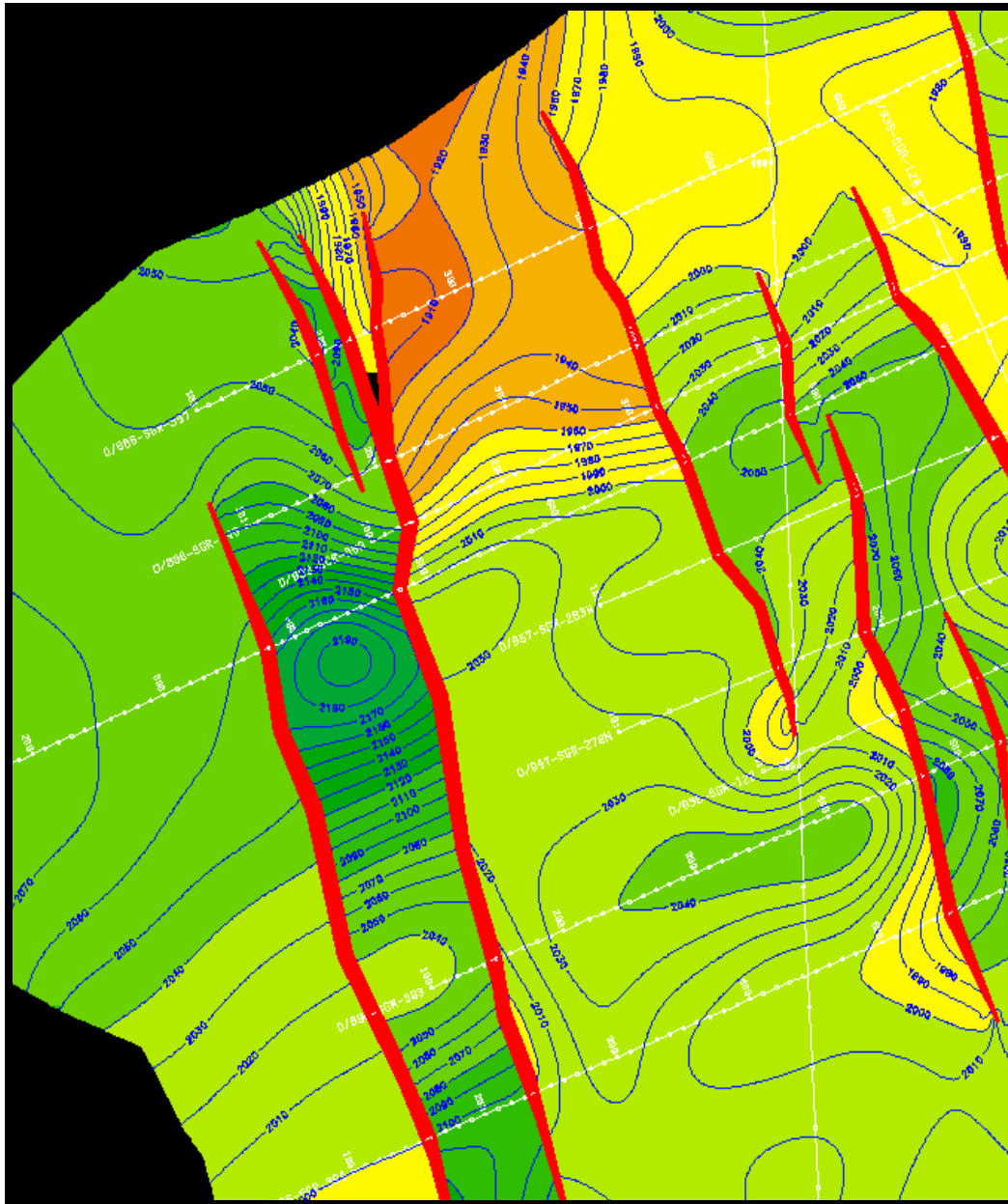


Figure 45: TWT contour map on Top Basal Sands (zoomed image)

Figure 42, 43, 44 & 45 show closures against faults. Figure 45 which is a zoomed version of Figure 42 shows the deepest portion on basal sands level. It is actually a graben, with highest contour value of about 2200 msec. All these images portray that area is extensively faulted. Faults and their associated splays could have been mapped in more detail if more seismic sections were available.

6.3.2.5 Depth Contour Map:

The depth contour maps are made by joining the points of equal depth values. The depth values are the calculated depth values in which a particular formation is present in the subsurface. In this dissertation, the depth values were calculated by firstly dividing the TWT by 2000 and then multiplying this by an average velocity. This average velocity is the velocity with which the seismic waves travel in that particular formation.

Again the same software was used for the construction of the depth maps. The depth maps are more reliable when giving the well position because it truly gives the position of a point in that formation. This is because the velocity factor is also involved.

Depth contour were generated on two horizons, Top Lower Goru (marked with yellow color on seismic sections) and Top Basal Sands (marked with red color on seismic sections). Depth conversion was done as follows:

$$\text{Depth} = \text{Velocity} \times (\text{Two way time}/2)$$

Depth is in meters, velocity in meters per second and time values in seconds.

Average velocity of Chak 7-A well was used in depth conversion. Velocities for different horizons are as under:

Parh Limestone = 2513 m/sec

Upper Goru = 2565 m/sec

Lower Goru = 2695 m/sec

Basal Sands = 2893 m/sec

Massive sands = 2920 m/sec

6.3.2.5.1 Depth Contour Map on TLG:

For depth contour map, grid was done in *Surfer 8.0* and contouring in *Field Pro* (Figure 46, 47a & 48). A cut polygon was also used as in TWT contouring of TLG and Basal Sands horizon.

Gridding method = Nearest neighbor

Contour Interval = 20 m

Minimum contour value = 1970 m

Maximum contour value = 2420 m

Faults direction = NW-SE

(Figure 46) shows the trend of TLG in project area. The color bar is indicating that red is the shallowest value, followed by orange, yellow, light green and finally the dark green which is the deepest value.

Green colored contours on the South eastern edge of the map can be regarded as pseudo because there is no data control in this region. The area is dominated by small horsts and grabens with 14 faults in the area. In the middle of (Figure 46), red to orange color is dominant, indicating that TLG is shallow in this region. A clear idea of this will be given by zoomed versions of Figure 46 (Figure 47 & 48) and 3D depth map of TLG.

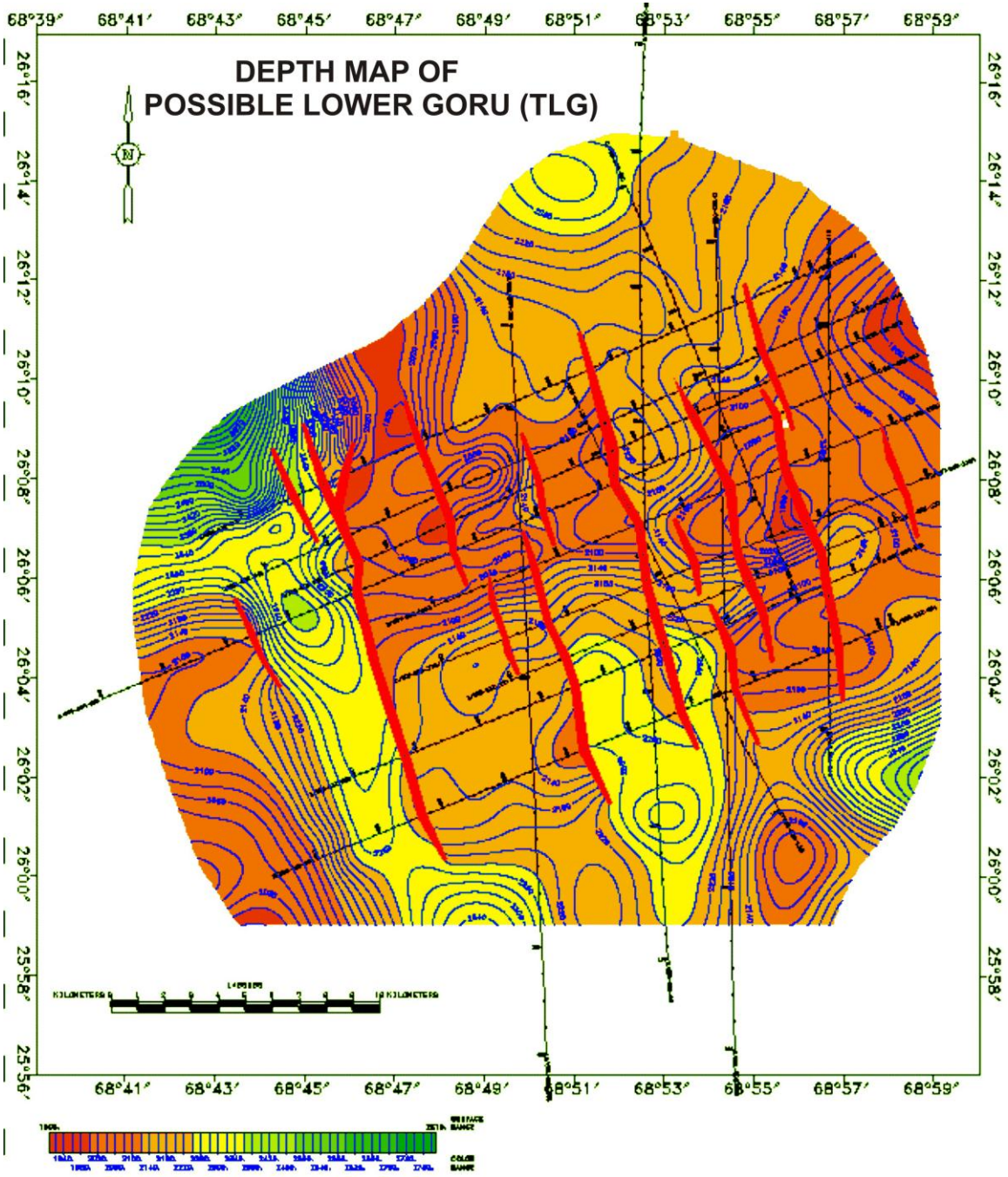


Figure 46: Depth contour map of Top Lower Goru

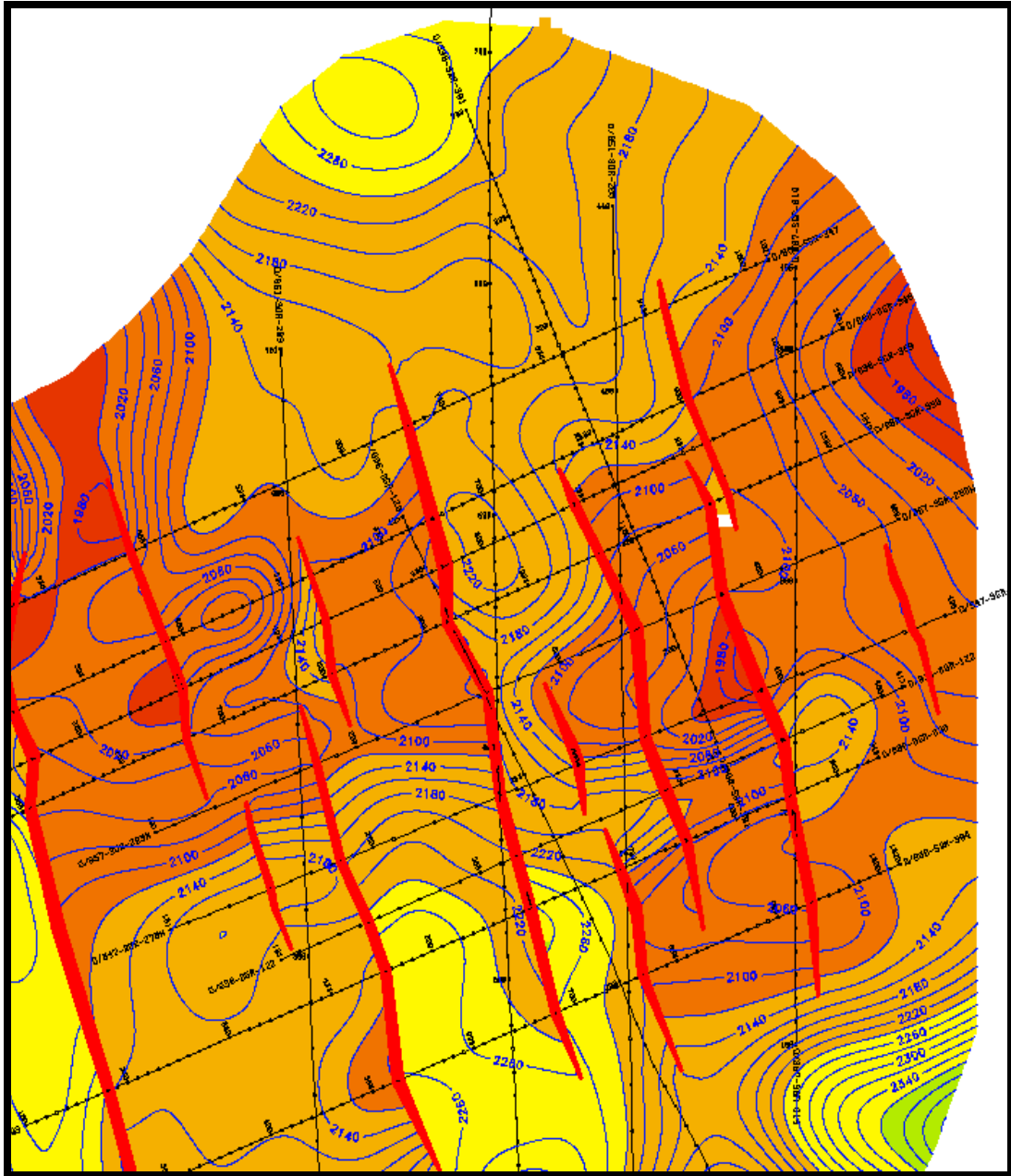


Figure 47: Depth contour map of Top Lower Goru (zoomed)

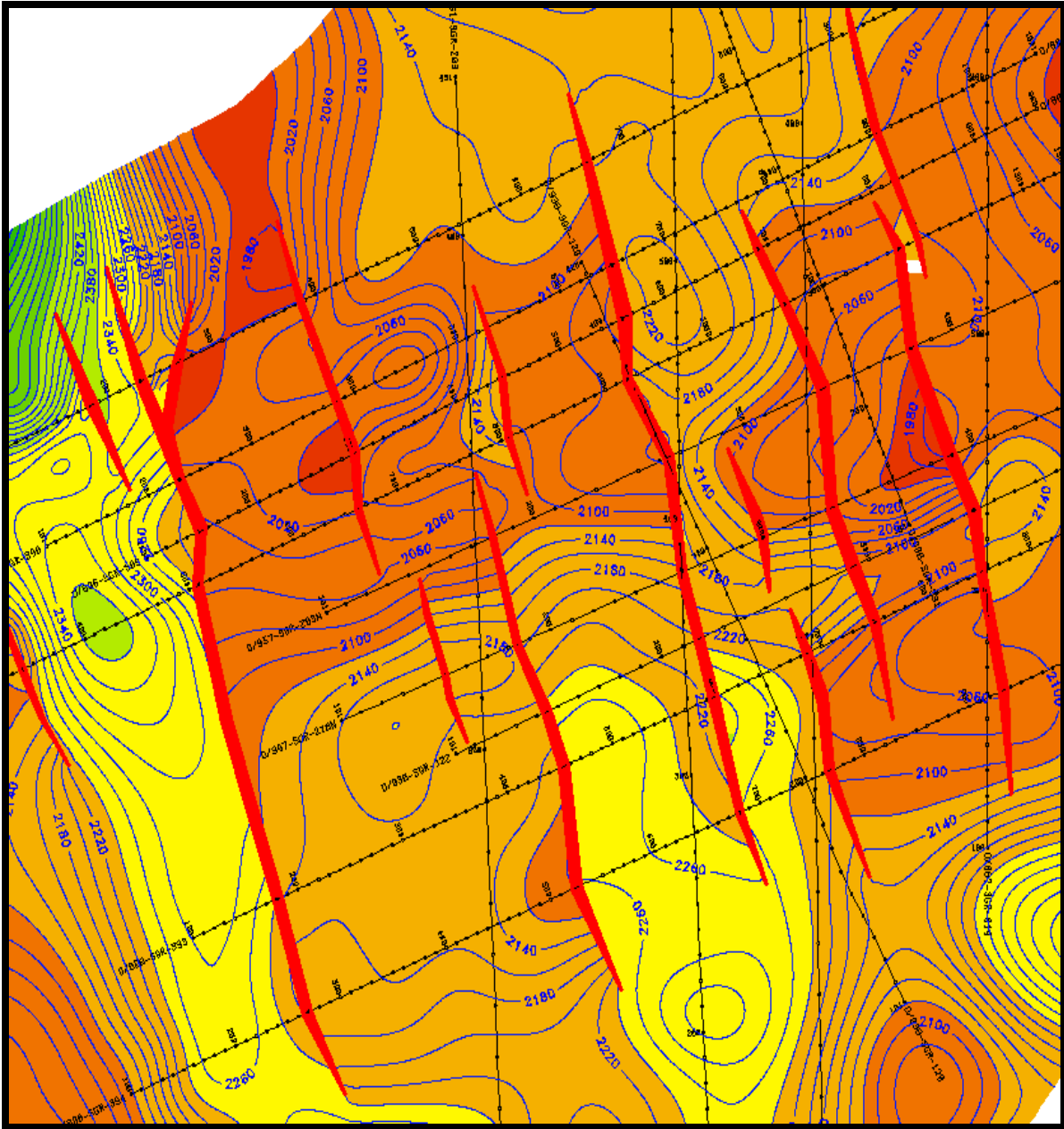


Figure 48: Depth contour map of Top Lower Goru (zoomed)

6.3.2.5.2 Depth Contour Map on Top Basal Sands:

Basal sands are the main target in the area.

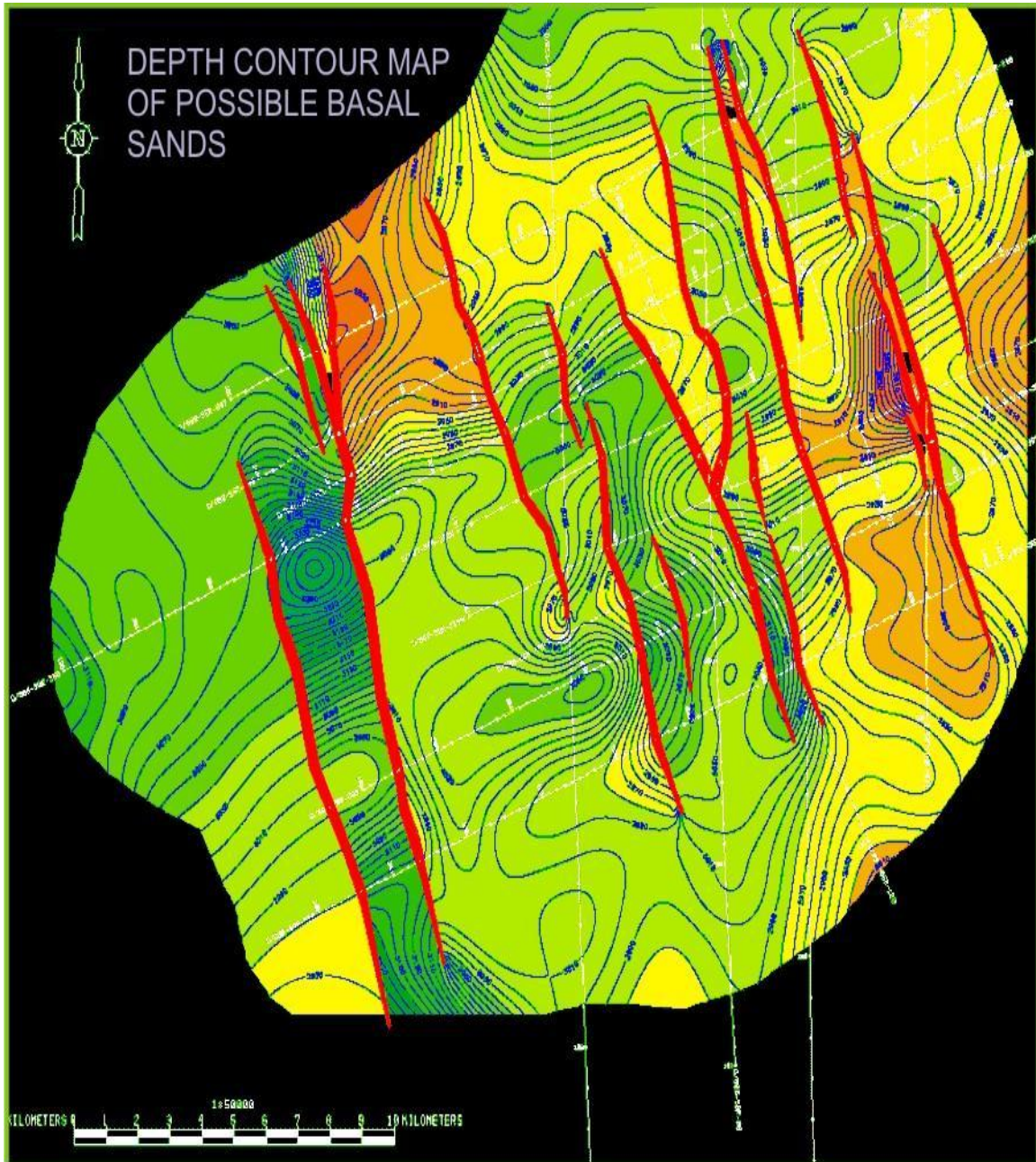


Figure 49: Depth Contour map of Basal Sands

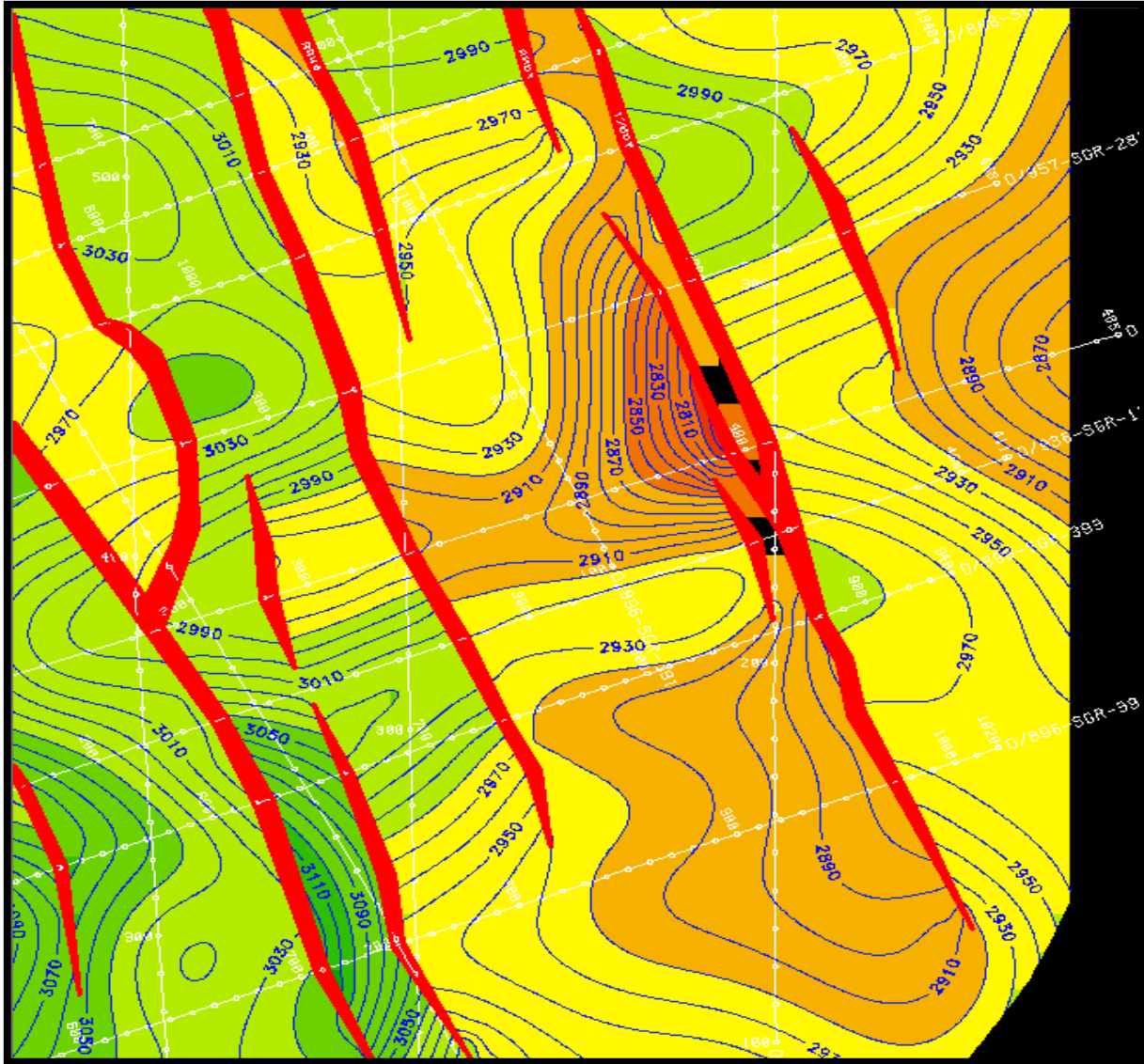
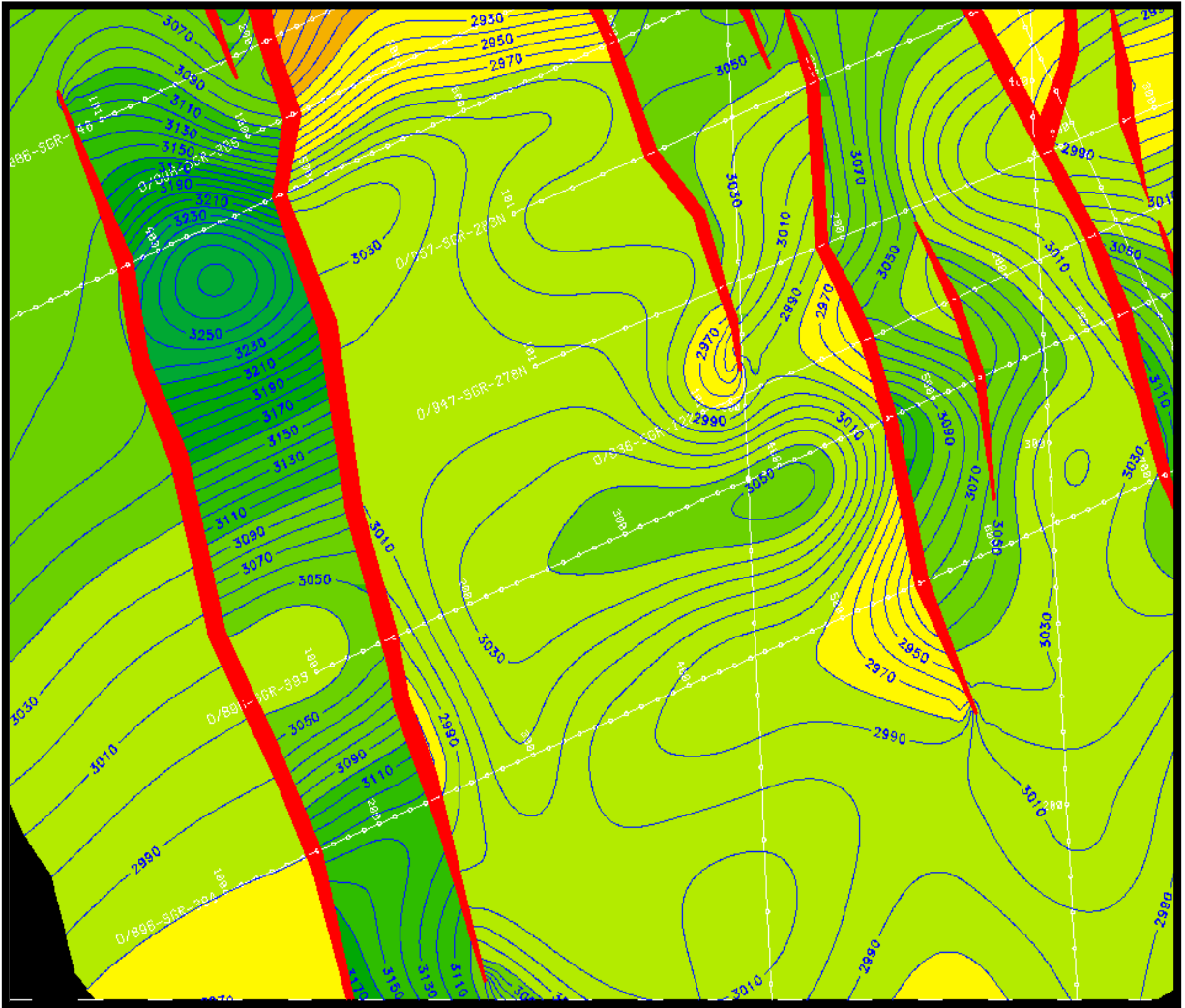


Figure 50: Depth Contour map of Basal Sands (zoomed)



6.3.2.6 3D Surface Models

Contour grid was made in the Surfer software using the navigation data and time of the reflectors, and then using the time grid and the fault trees, 3D time surface models of Basal Sands and TLG were made. Then using the time grid, the average velocity of seismic waves in the required formations, and math operator of SURFER software, the 3D Depth Surface Models of the same formations were made.

6.3.2.6.1 3D Time Model of Top Basal Sands:

A better idea of subsurface trend of Basal Sands and faults in the area is given by (Figure 39).

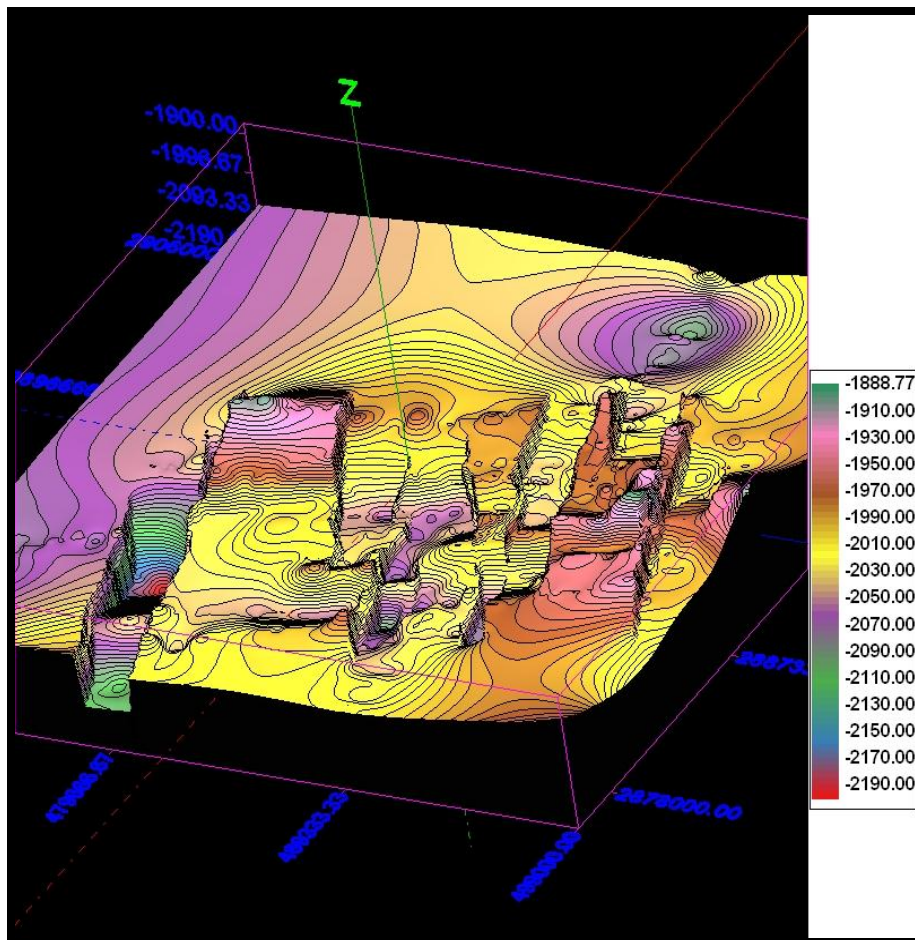


Figure 52: 3D Time Model of top Basal Sands

The red thin line in upper corner of (Figure 52) is indicating the North direction. As discussed earlier that Basal sands are the primary target in the area, all these closures are of great importance. These possible closures or leads are discussed in the next sections.

6.3.2.6.2 3D Time Model of Top Lower Goru (TLG):

TWT contour maps can be understood in a better way by looking at the 3D image. One can see the horst and grabens clearly on (Figure 37). The rising contours in north are not real; they are the result of extrapolation by the software.

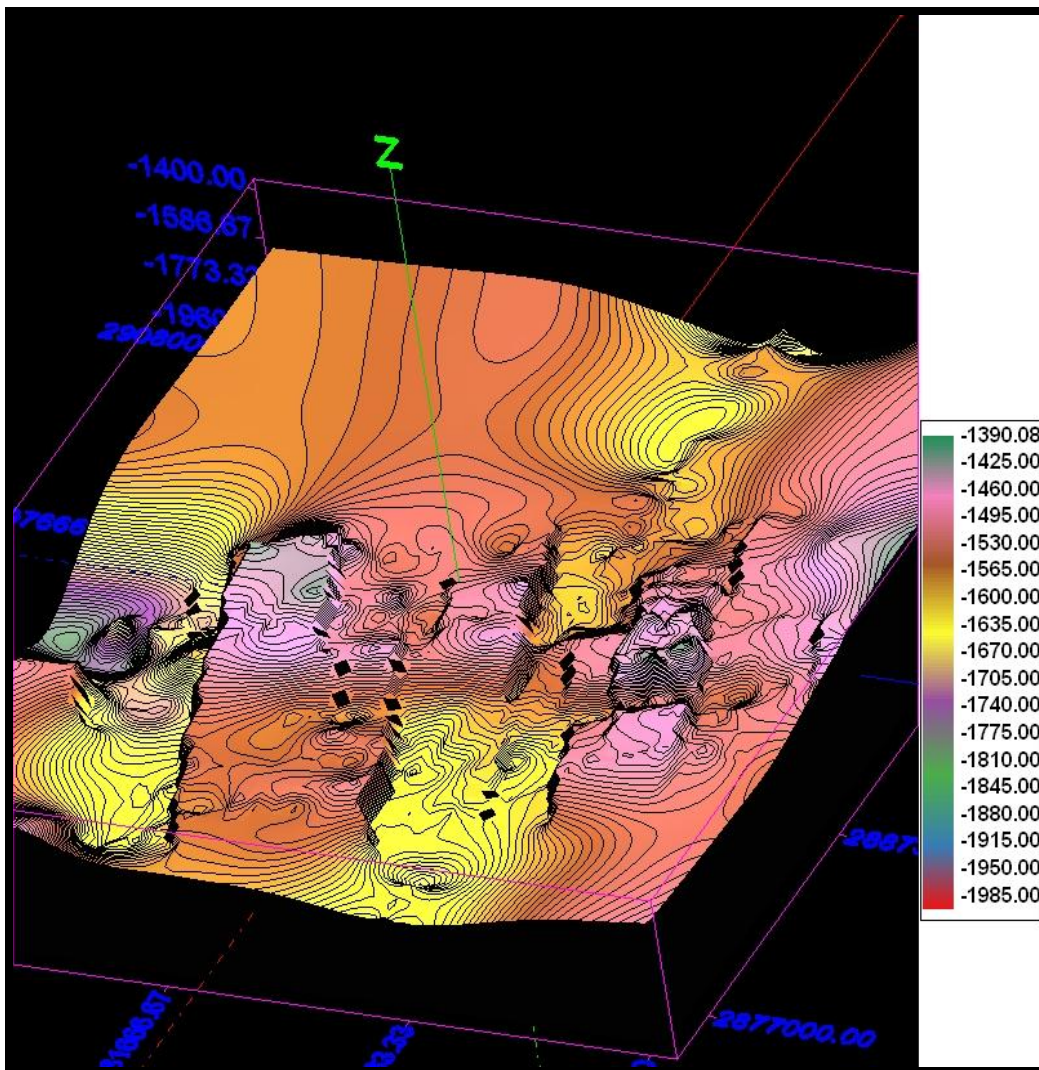


Figure 53: 3D Time Model of TLG

3D surface was generated by using *3DFieldPro*. Unfortunately there was no option in *3DFieldPro* to use a cut polygon to avoid extra contours. The red thin line in upper corner of (Figure 53) is indicating the North direction. The minus sign with the values is just because the software being used plots only 3D elevations rather than depths. So, the grid file generated in *Surfer 8.0* was multiplied with “-1” to generate 3D Model.

6.3.2.6.3 3D Depth Model of Top Lower Goru (TLG):

If Figure 48 (depth contour map of TLG) is compared with this 3D map, the depth variations in TLG can be understood in a better way. The minimum and maximum contour values shown by the vertical color bar might not be correct. The reason is the extrapolation by the software and its inability to draw a cut-polygon to limit the contours inside the data limits. The red thin line in upper portion of (Figure 54) is showing the North direction. Purple and yellow contours in the north are not real because they lie outside the data limits.

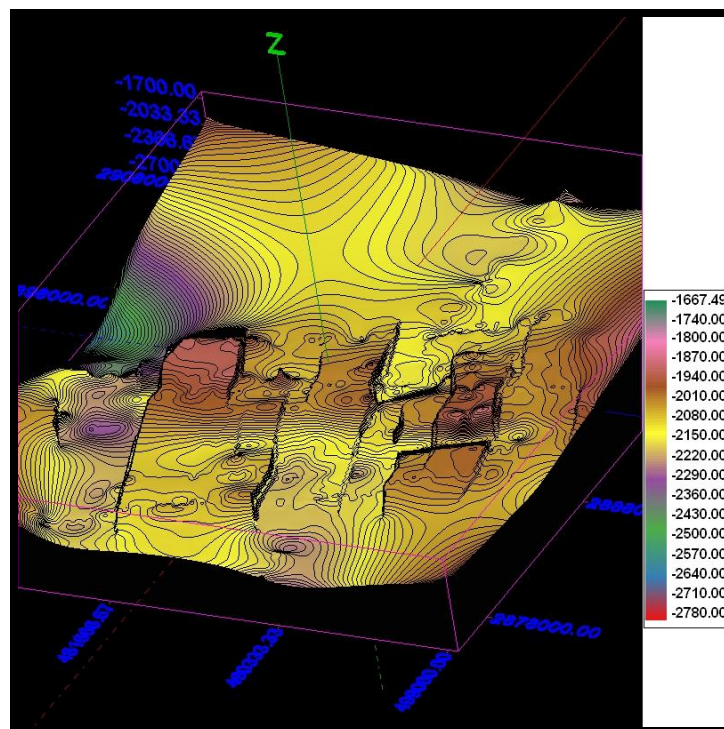


Figure 54: 3D Depth Model of Top Lower Goru

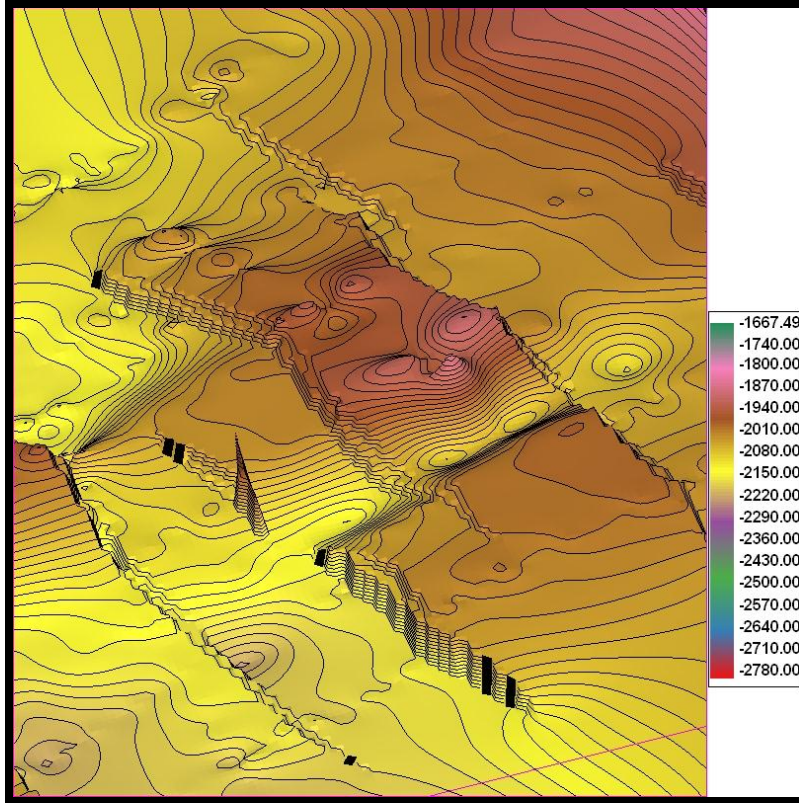


Figure 55: 3D Depth Model of Top Lower Goru (zoomed eastern portion of Figure 53).

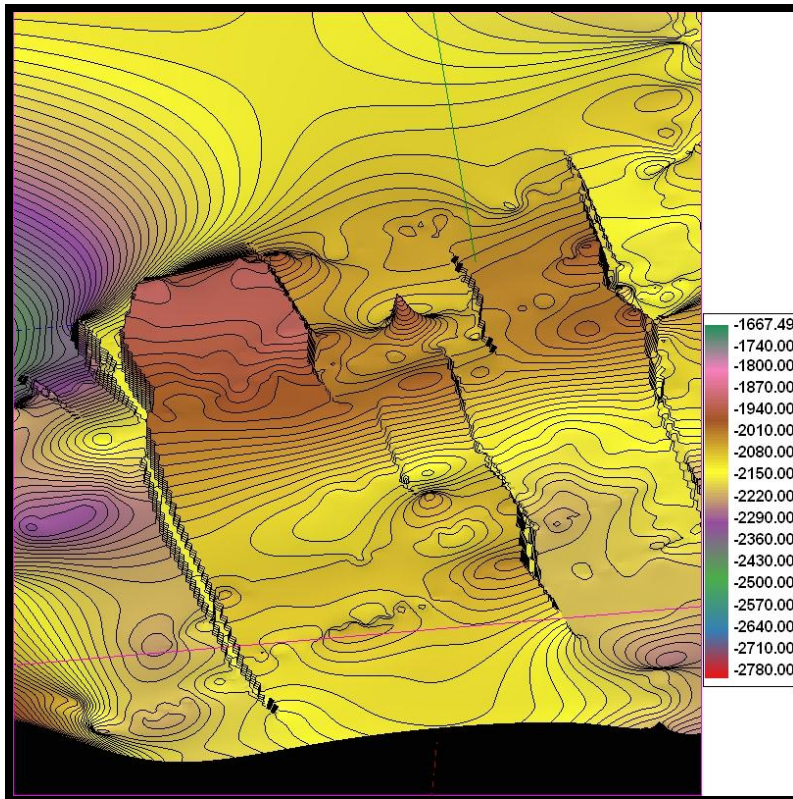


Figure 56: 3D Depth Model of Top Lower Goru (zoomed)

6.3.2.7 Leads formation and well proposals

The basic purpose of this tract was to locate the areas favorable for hydrocarbon accumulation. In the Sinlhoru E.L. the proven reservoir is the Basal Sands of Lower Goru, so in this dissertation, the aforementioned areas were only looked in the Basal Sands. Six leads are marked on the on the depth sections (Figure 49 – 51). The leads which are marked are also confirmed from the TWT map and also from the 3D Surface model of the formation. This area is very productive, and its productivity can be guessed from its exploration history.

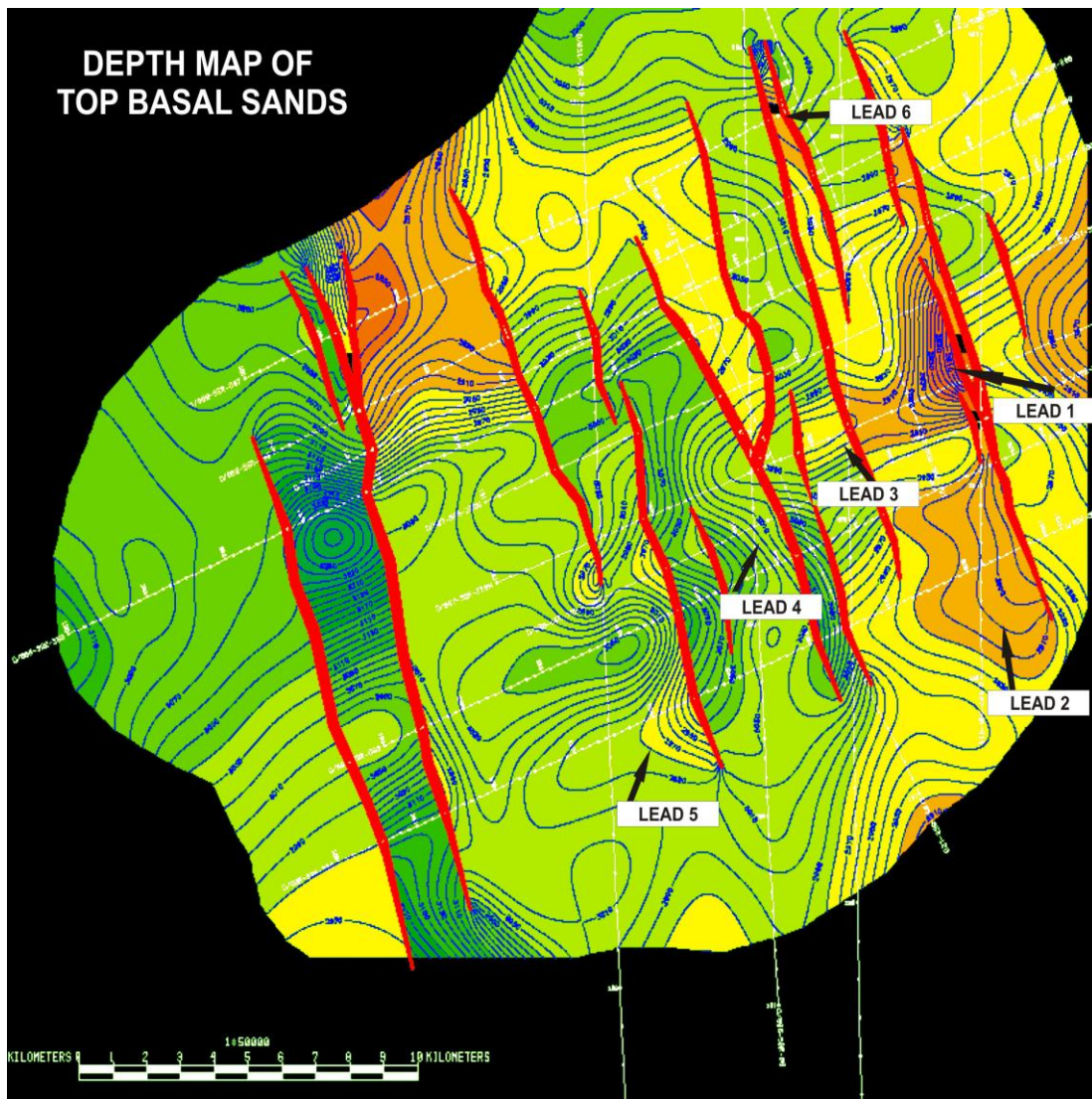


Figure 57: Depth Contour Map of Top Basal sands showing possible leads in the study area

1. Lead 1:

It is present on a horst block (Figure 58 and 59). As the major faults direction in Sanghar area is NW-SE, any feature of interest forming against the faults will have closure directions: *North Eastern, South Western, North Western and South Eastern*. North Eastern and South Western closure to the Lead1 is provided by faults; north eastern and South Western closures are provided by the dip. A better idea will be given by the following figure.

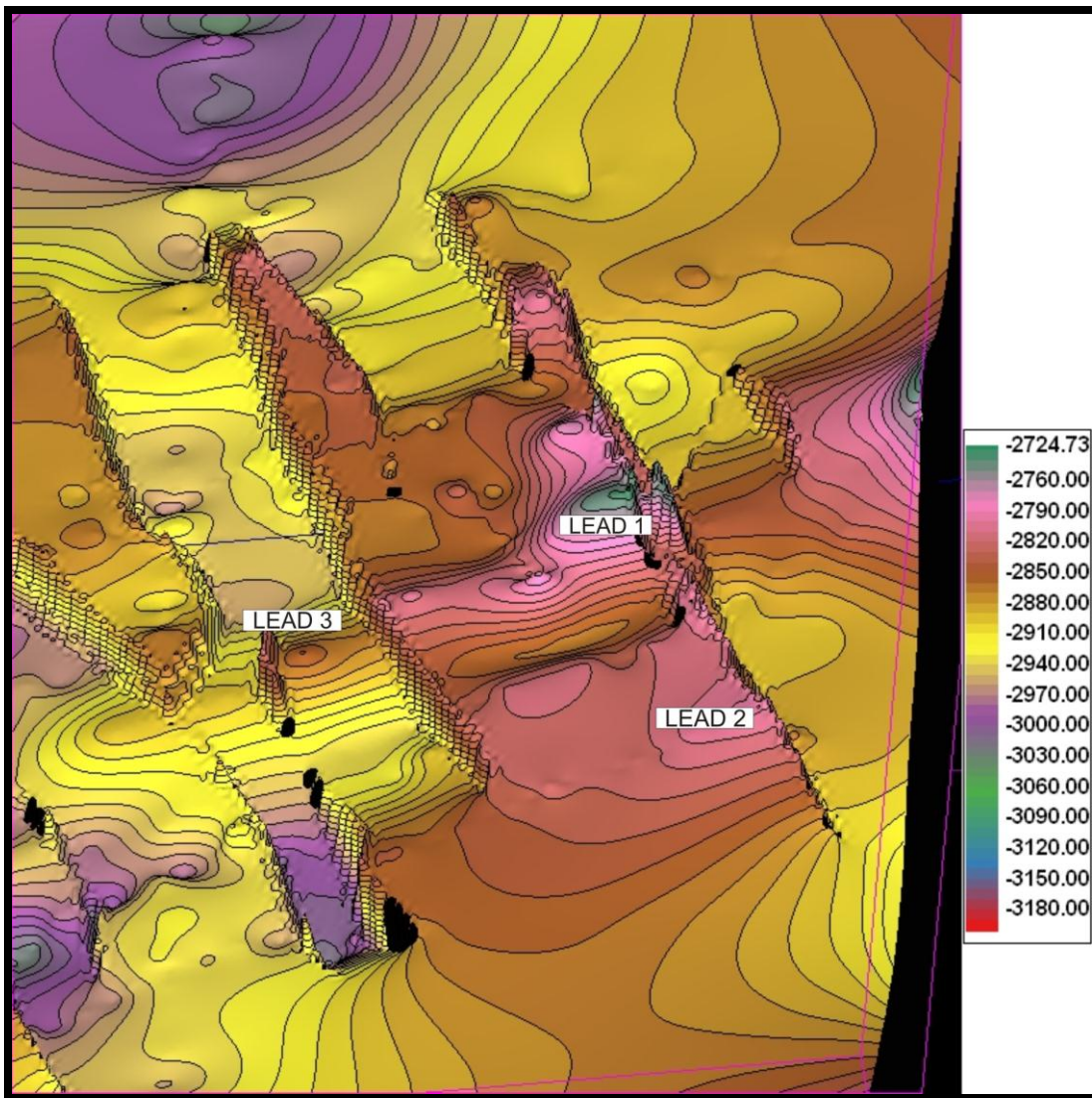


Figure 58: 3D Depth Model of Top Basal sands (zoomed) with possible leads (1, 2, and 3)

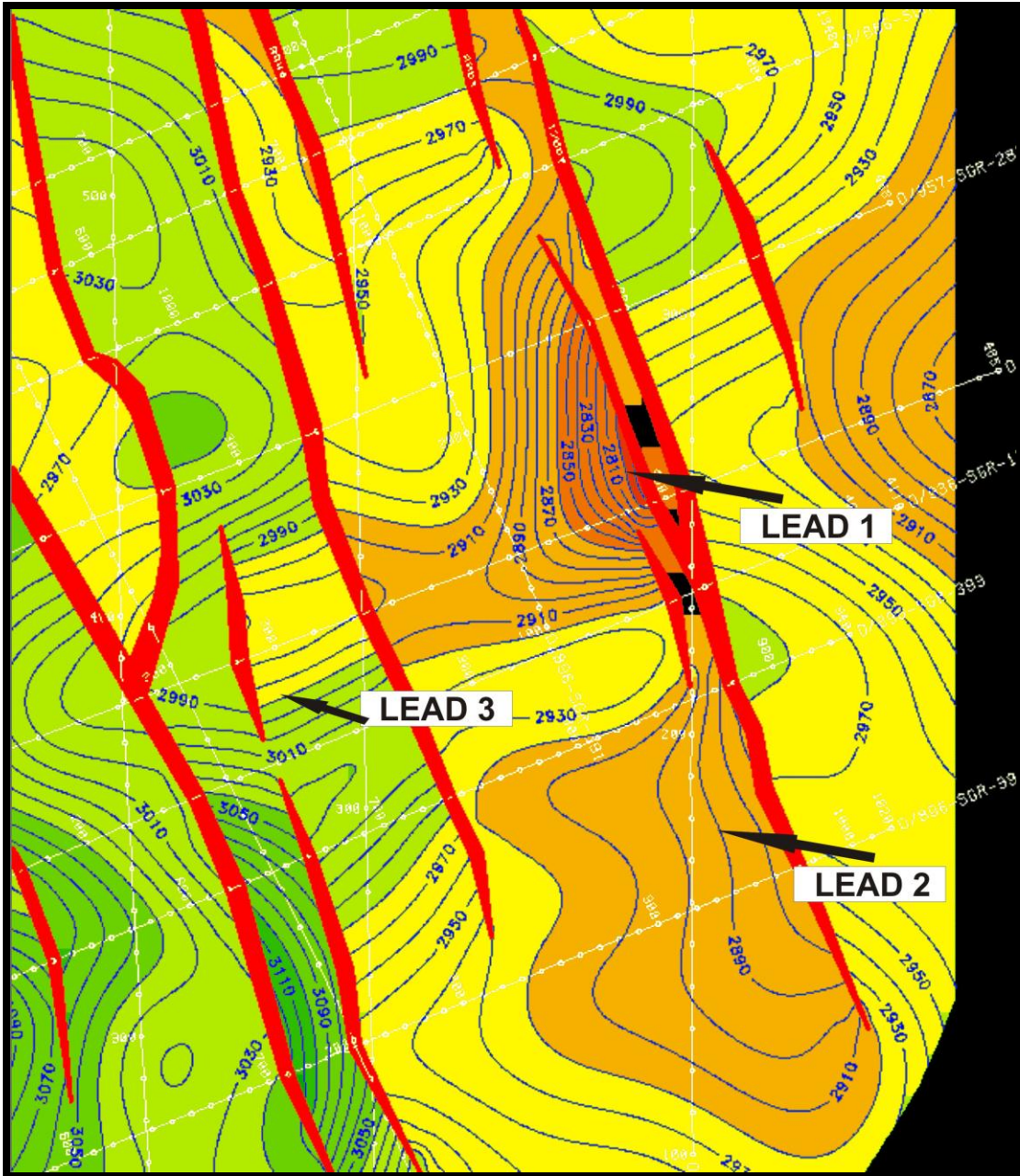


Figure 59: Depth contour map of Top Basal sands (zoomed) with possible leads (1, 2, and 3)

Minimum value in terms of time: 1890ms

Maximum value in terms of time: 1940ms

Minimum value in terms of depth: 2790m

Maximum value in terms of depth: 2900m

Vertical closure in terms of time: 50 ms

Vertical closure in terms of depth: 110 m & Total area: 11 km²

2. Lead 2:

It is present on the same horst block as lead 1. Closures in the NE and SW are provided by faults and the other two closures are provided by its dip.

Vertical closure in terms of time: 30 ms

Vertical closure in terms of depth: 50 m

Total area: 16 km²

Lead 2 is a gently dipping feature (Figures 58 and 59). Its south eastern dip is a bit doubtful because of sparse data.

3. Lead 3:

This lead is a step fault. It is present to the further west of the above discussed two leads (Figures 58 and 59). South western closure is provided by a small fault. In the north east, there is a big fault. The other two closures are provided by the dip of the feature.

Vertical closure in terms of time: 20 ms

Vertical closure in terms of depth: 40 m

Total area: 3 km²

4. Lead 4:

This lead is also a step fault. North eastern closure to this lead is provided by a major fault in the area (Figures 60 and 61). The other 3 side closures are provided by the dip of this feature.

Vertical closure in terms of depth: 30m

Vertical closure in terms of time: 20 ms

Total area of 4.6 km²

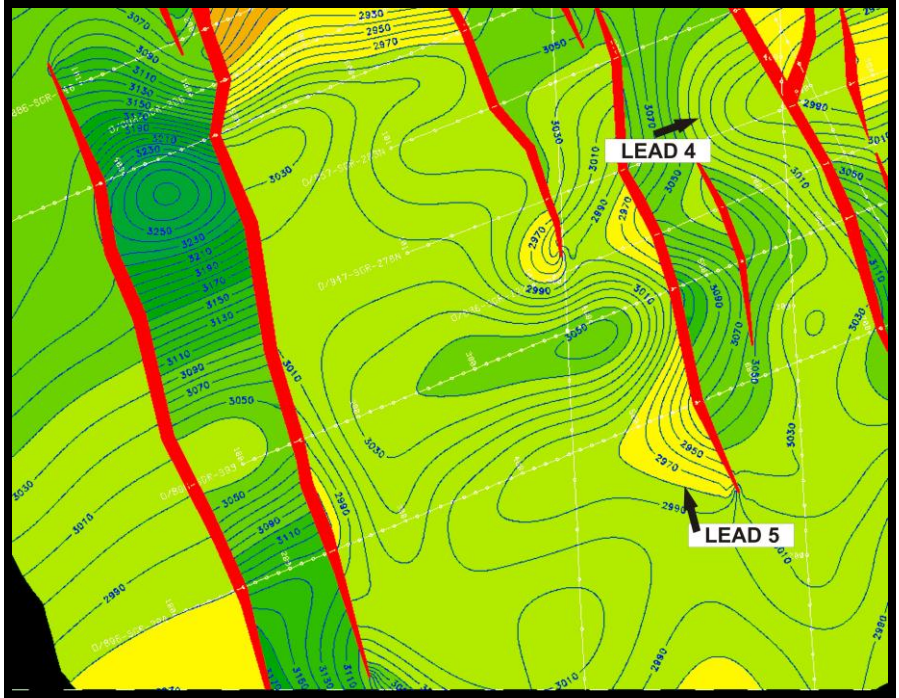


Figure 60: Depth contour map of Top Basal sands showing lead 4 & 5 (zoomed)

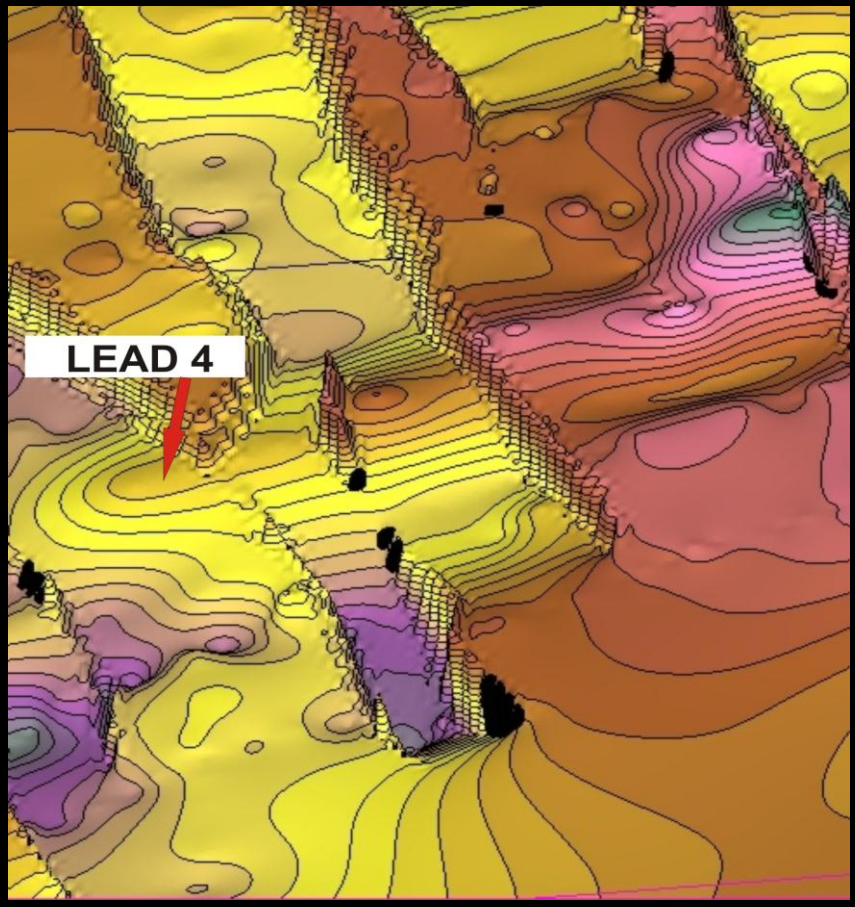


Figure 61: 3D Depth Model of Top Basal sands showing Lead 4 (zoomed)

5. Lead 5:

This lead comprises of a horst block. Like lead 4, this feature is also bounded by a major fault in north east. Closures from the other three sides are provided by its dip (Figures 60 and 62).

Vertical closure in terms of depth: 30m

Vertical closure in terms of time: 20 ms

Total area: 3.5 km²

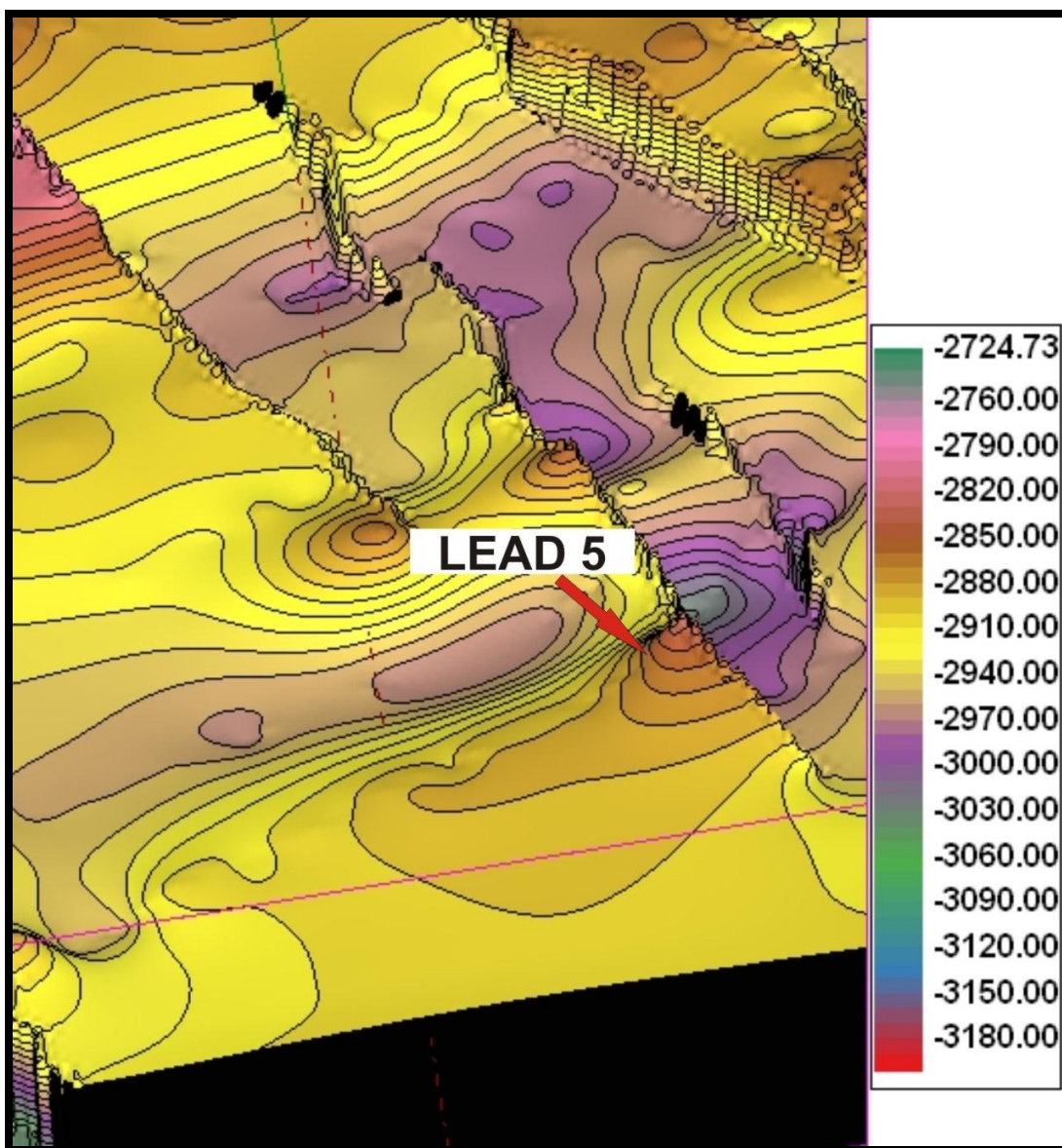


Figure 62: 3D Depth Model of Top Basal sands showing Lead 5 (zoomed)

Lead 6:

It is the smallest of all identified leads (about 1.9 km²) but it is important because it has Chak 7-A well drilled on it (Figure 63).

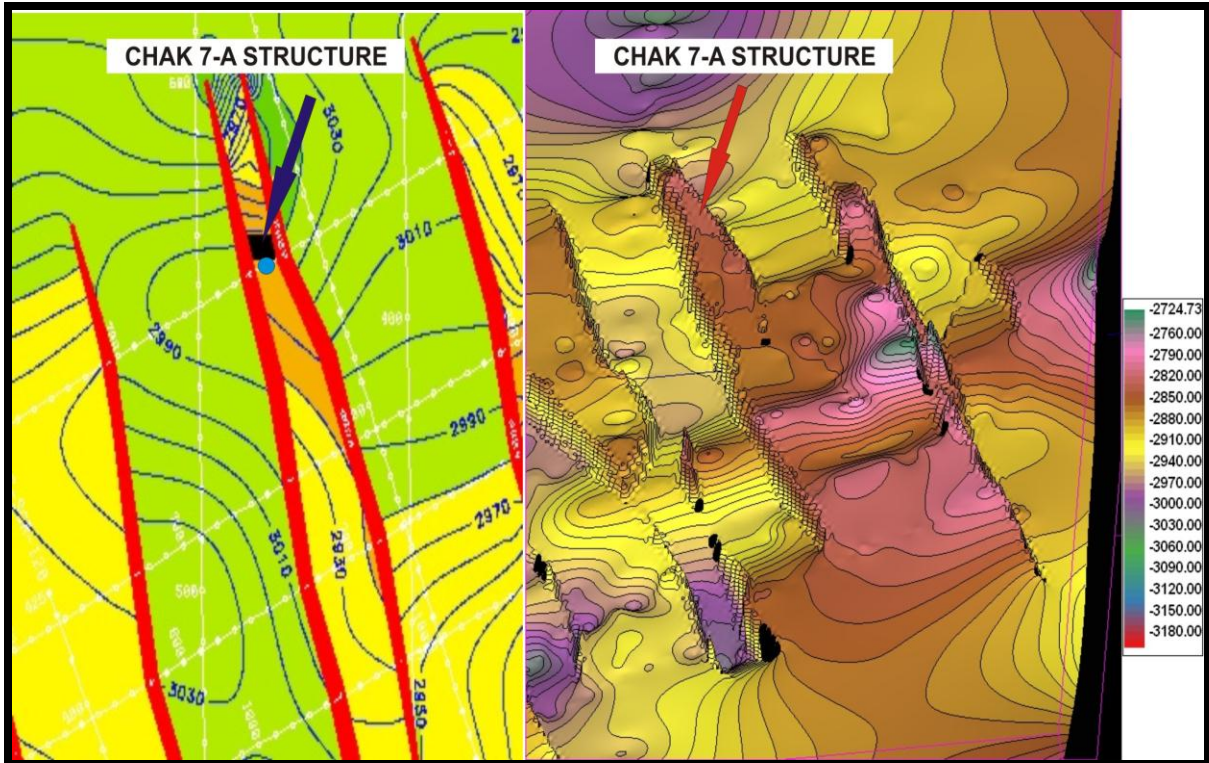


Figure 63: Lead 6 shown in 2D (left portion) and 3D (right portion)

It is clear from the figure 63 that north eastern and south western closures are provided by the faults while north western and south eastern by dip of the feature. Lead 6 is present on a small horst and it has an area of about 1.9 km².

6.3.2.8 Depth Models of Seismic Lines:

Based on the available well data and structural trend of the marked horizons, depth models have been generated along following two seismic lines:

886- SGR- 347 (Dip line)

886 - SGR- 391(Strike line)

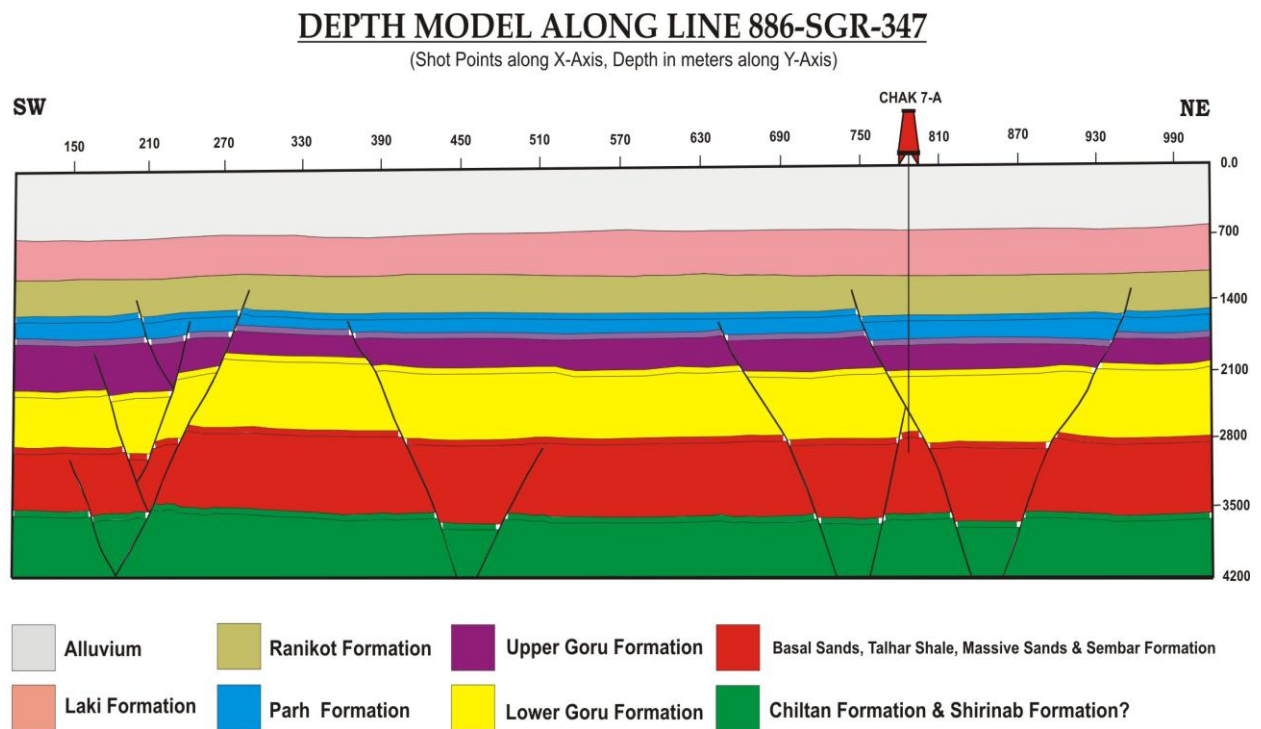


Figure 64: Depth model along dip line 886-SGR-347

All the formations in figure 66 have been marked on the basis of thicknesses encountered in Chak 7-A well. Since, Chiltan Limestone was not encountered in this well; it was marked on the basis of its character on seismic sections. The green colored portion in (Figure 66) is about 700 m thick, so it can also include the Shirinab formation of early Jurassic age.

DEPTH MODEL ALONG LINE 886-SGR-391

(Shot Points along X-Axis, Depth in meters along Y-Axis)

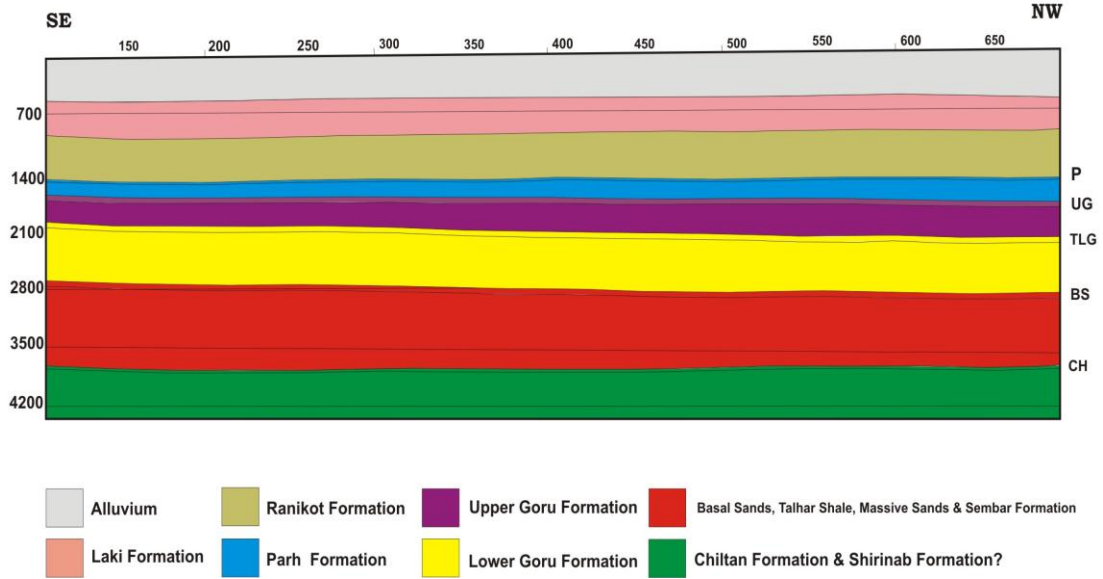


Figure 65: Depth model along strike line 886-SGR-391

This model was also generated on basis of well data of Chak 7-A well. This line is crossing the dip line 886-SGR-347 at shot point 818 and is located at a distance of 600 m East of Chak 7-A (Figure 50).

7 CONCLUSIONS

1. All the studies done in the area concludes that the area is a hydrocarbon proven area.
2. The project area falls in extensional regime and is dominated by faults; horst and grabens can be seen on all dip lines (oriented in NE-SW direction)
3. Petroleum system is well established in the area and horizon identification is not a problem since a lot of wells have been drilled in the area. Basal sands and massive sands are the main reservoirs
4. The time and depth contour maps that were made of the Basal Sands (primary target) show many possible locations having hydrocarbon potential.
5. Main play types in the area are Horst – Graben structures, step faults and tilted fault blocks.
6. 3D seismic surveys can also be done, and 3D seismic data can be acquired to improve the production in the area.
7. Incorporating previous studies and research work, and newly acquired 2D or 3D seismic data, Chiltan formation can also be tested for hydrocarbon reserves. It might act as a good reservoir, being extremely faulted and fractured.
8. Focus should also be given to stratigraphic traps, if any, by acquiring high resolution seismic data.
9. In order to have a more reliable picture of the subsurface, more and more seismic sections and well data can be used, for this dissertation, and for this area also. This can now be established easily because a lot of work has been done on this area.

REFERENCES

Al-Sadi, H.N., 1980. Seismic Exploration Technique and Processing, 1st Ed., Birkhauser Verlag publications, Basel, Switzerland, p. 215.

Badley, M.E., 1985. Practical Seismic Interpretation, IHRDC Publishers, Boston, p. 266.

Dobrin, M.B. and Savot, C.H., 1988. Introduction to Geophysical Prospecting, 4th Ed., McGraw-Hill, p. 867.

Earnest, S.S. Seismic Migration, unpublished PhD thesis, pp 1, 2.

Kearey, P. Brooks, M. and Hill, I., 2002. An Introduction to Geophysical Exploration, Blackwell Science Limited, oxford, p.262.

Quadri, V.N. and Shuaib, S.M., 1986, "Hydrocarbon Prospects of Southern Indus Basin, Pakistan", AAPG Bulletin, v.70. No. 6, p. 730-747.

Robinson, E.S. and Coruh, C., 1988. Basic Exploration Geophysics, John Wiley & Sons, New York, p. 562.

www.ppis.com

Yilmaz, O., 1987, Seismic Data Processing: Society of Exploration Geophysicists, Tulsa Oklahoma. pp 526.